

**Metabolic, Neurotoxic and Immunotoxic Effects of PFAAs and their
Mixtures on the Proteome of Plasma and Head Kidney from Rainbow
Trout**

by

Simon M. Pollard

A thesis submitted to the
School of Graduate and Postdoctoral Studies in partial
fulfillment of the requirements for the degree of

Master of Science in Applied Biosciences

Biology/ Ontario Tech University/ Science
University of Ontario Institute of Technology (Ontario Tech University)
Oshawa, Ontario, Canada

March 2023

© Simon Pollard, 2023

THESIS EXAMINATION INFORMATION

Submitted by: **Simon Pollard**

Master of Science in Applied Biosciences

Thesis title: Metabolic, Neurotoxic and Immunotoxic Effects of PFAAs and their Mixtures on the Proteome of Plasma and Head Kidney from Rainbow Trout
--

An oral defense of this thesis took place on May 02, 2023 in front of the following examining committee:

Examining Committee:

Chair of Examining Committee	Dr. Dario Bonetta
Research Supervisor	Dr. Denina Simmons
Examining Committee Member	Dr. Ève Gilroy
Examining Committee Member	Dr. Julia Green-Johnson
Thesis Examiner	Dr. Theresa Stotesbury, Faculty of Science, Ontario Tech University

The above committee determined that the thesis is acceptable in form and content and that a satisfactory knowledge of the field covered by the thesis was demonstrated by the candidate during an oral examination. A signed copy of the Certificate of Approval is available from the School of Graduate and Postdoctoral Studies.

ABSTRACT

PFAAs (Perfluoroalkyl acids) are a class of bioaccumulative, persistent and ubiquitous aquatic contaminants. A paucity of toxicological information exists for short chain PFAAs and PFAA mixtures. In order to address these knowledge gaps, we performed a 3-week, aqueous exposure of rainbow trout to 3 different concentrations of a PFAA mixture (50 - 500 ng/L) and individual PFAAs (25 nM of PFOS, PFOA, PFBS or PFBA). Untargeted proteomics and phosphorylated metabolomics were conducted on the blood plasma and head kidney tissue to evaluate differences in biological effect for congeners and mixtures. The mixture and PFOS exposures significantly altered the abundances of many plasma proteins involved in lipid metabolism and the nervous system. The PFOA and high mixture treatments altered many kidney proteins involved in oxidative stress and inflammation. The findings emphasize the need for more toxicological testing of PFAA mixtures and their potential to cause metabolic dysregulation and neurotoxicity in fish.

Keywords: Ecotoxicology; PFAS; Proteomics; Plasma; Kidney

AUTHOR'S DECLARATION

I hereby declare that this thesis consists of original work of which I have authored. This is a true copy of the thesis, including any required final revisions, as accepted by my examiners.

I authorize the University of Ontario Institute of Technology (Ontario Tech University) to lend this thesis to other institutions or individuals for the purpose of scholarly research. I further authorize University of Ontario Institute of Technology (Ontario Tech University) to reproduce this thesis by photocopying or by other means, in total or in part, at the request of other institutions or individuals for the purpose of scholarly research. I understand that my thesis will be made electronically available to the public.

The research work in this thesis that was performed in compliance with the regulations of Research Ethics Board/Animal care certificate file #15540.

Simon Pollard

ACKNOWLEDGEMENTS

I am grateful for the feedback and support provided by my supervisor Dr. Denina Simmons throughout the course of my thesis project. She provided me with the training, encouragement and expertise required to successfully plan and execute my thesis project in addition to the analysis and writeup of the results. I also want to acknowledge my committee members Dr. Ève Gilroy and Dr. Julia Green-Johnson for guidance during the planning and analysis stages of my thesis project. Finally, I am thankful to Ontario Tech University and our funding agencies including the Natural Sciences and Engineering Research Council of Canada (NSERC), Canadian Foundation for innovation (CFI) and the Canadian Research Chair Program for making this work possible.

STATEMENT OF CONTRIBUTIONS

The analysis of phosphorylated metabolites was conducted by our collaborators Dr. Vasile Furdui and Dr. Vlastimil Packa at the Ontario Ministry of Environment, Conservation and Parks (Toronto, ON). A summary of the raw data and methods were provided to me for statistical analysis and presentation.

The analysis of perfluoroalkyl acids (PFAAs) in the water and blood plasma was conducted by our collaborator Dr. Amila De Silva at Environment and Climate Change Canada (Burlington, ON). A summary of the raw data and methods were provided to me for data analysis and presentation.

I hereby certify that I was responsible for all other planning, execution, analysis and writeup of the thesis under the guidance of my supervisor and committee members. I confirm that no part of this thesis has been published or submitted for publication. I have used standard referencing practices to acknowledge ideas, research techniques and other materials.

TABLE OF CONTENTS

Thesis Examination Information	ii
Abstract	iii
Authors Declaration	iv
Acknowledgements	v
Statement of Contributions	vi
Table of Contents	vii
List of Tables	ix
List of Figures	x
List of Abbreviations and Symbols	xiv
Chapter 1 Introduction	1
1.1 General Overview	1
1.2 Perfluoroalkyl Acids	4
1.3 Uses of PFAS	4
1.4 Pathways into the Aquatic Environment	5
1.5 Occurrence of PFAAs in the Aqueous Environment.....	7
1.6 Bioaccumulation of PFAAs	8
1.7 Toxicokinetics	9
1.8 Impacts of PFAAs on Lipid Metabolism.....	10
1.9 PFAA Induced Mitochondrial Dysfunction.....	12
1.10 Impacts of PFAAs on the Nervous System.....	13
1.11 Immunotoxicity of PFAAs	14
1.12 Thesis Premise	15
1.13 Thesis Objectives	16
Chapter 2 Methods	17
2.1 Fish Housing Conditions	17
2.2 Chemical Exposures	18
2.3 Takedown and Dissection	21
2.4 Condition Factor and Hepatosomatic Index.....	21
2.5 Preparation of plasma samples for Proteomics.....	22
2.6 Preparation of Kidney samples for Proteomics.....	22
2.7 Proteomics Instrumental Analysis	23
2.8 Protein Identification and Relative Quantification.....	23
2.9 Analysis of Phosphorylated Metabolites.....	24

2.10 Analysis of PFAAs in Water and Plasma.....	25
2.11 Statistical Analysis.....	27
Chapter 3 Results	29
3.1 Hepatosomatic Index	29
3.2 Plasma Proteomics.....	30
3.3 Phosphorylated Metabolite Analysis.....	39
3.4 Head Kidney Proteomics.....	40
3.5 Analysis of PFAA Water and Plasma Chemistry.....	48
Chapter 4 Discussion	55
4.1 PFAA Mixtures	56
4.2 Individual PFAAs	60
4.3 PPARs and Lipid Metabolism.....	61
4.4 Oxidative Stress	62
4.5 Nervous System.....	64
4.6 PFAAs and Muscular Related Processes	68
4.7 Head Kidney Proteomics	70
4.8 Summary.....	74
Chapter 5 Conclusions	75
Bibliography	76

List of Tables

Chapter 1

Table 1.1: Chemical Structure Diagram of Perfluoroalkyl Acids Mentioned in this Thesis..... 2

Chapter 2

Table 2.1: Percent Composition and Concentrations of PFAAs Being Used in a 28-day, Aqueous exposure of Rainbow Trout. The relative compositions of PFAAs within the mixture groups (MIXLOW, MIXMED and MIXHI) are based on the composition of PFAAs detected in Lake Ontario by De Silva et al., 2011 (1)..... 20

Chapter 3

Table 3.1: Aqueous and Plasma Concentrations of PFAAs for the Single Exposure Groups. Bioconcentration factors (**BCF**) are calculated by dividing the plasma concentration by its respective aqueous concentration. Note, plasma concentrations were measured in ng/g..... 47

Table 3.2: PFAA Mixture Exposures Represented by Percent of Nominal Concentration. Percent of nominal was calculated by subtracting the actual concentration from control concentrations and then dividing by the nominal concentration..... 59

Table 3.3: Aqueous and Plasma Concentrations of PFAAs for the Mixture Exposure Groups. Brackets represent percent composition. Bioconcentration factors (**BCF**) are calculated by dividing the plasma concentration by its respective aqueous concentration. **Table 3.1.** Aqueous and Plasma Concentrations of PFAAs for the Single Exposure Groups. Bioconcentration factors (**BCF**) are calculated by dividing the plasma concentration by its respective aqueous concentration..... 51-52

List of Figures

Chapter 3

Figure 3.1: Violin Plot of the Hepatosomatic index of rainbow trout exposed to PFAAs and PFAA Mixtures. Hepatosomatic index was compared using a Kruskal-Wallis test followed by a Dunn's post-hoc. Error bars represent standard deviation..... 29

Figure 3.2: Overview of Untargeted Proteomics Results from the Blood Plasma of Rainbow Trout Chronically Exposed to PFAAs and PFAA Mixtures. The heatmap illustrates the top 800 proteins ranked by significance using a One-way ANOVA in addition to hierarchical clustering using Ward's method. Data is median normalized and log2 transformed..... 31

Figure 3.3: Venn Diagrams Illustrating the Commonality of Significant Plasma Proteins (p -adj<0.1) from Rainbow Trout Exposed to PFAAs and PFAA Mixtures. The top row (A, B) contains two charts comparing low and medium PFAA mixtures (MIXLOW and MIXMED) with PFOS; (A) includes only proteins with positive fold change (indicated by red) and (B) displays only those with negative fold change (blue). The bottom row (C, D) are representing the single compound exposure regimes also grouped by fold change..... 32

Figure 3.4: Venn Diagrams Illustrating the Commonality of Significant Plasma Proteins(p -adj<0.1) from Rainbow Trout Exposed to 3 Different Concentrations of a PFAA mixture. The top row (A, B) contains two charts comparing low, medium and high PFAA mixtures (MIXLOW, MIXMED and MIXHI) ;(A) includes only proteins with positive fold change (indicated by red) and (B) displays only those with negative fold change (blue)..... 33

Figure 3.5: Biological Processes Found to be Significantly Overrepresented ($p\text{-adj}<0.05$) in the Plasma of Rainbow Trout Exposed to PFAAs and PFAA Mixtures. Biological pathway analysis was conducted using Gene Ontology's overrepresentation analysis test which conducts a Fisher's exact test followed by a Benjamini-Hochberg correction for false discovery. The heatmaps have related biological pathways grouped by biological system and only contain noteworthy biological processes and only treatments with noteworthy significant results; numbers in the center of each panel represent FDR adjusted p-values. All the biological pathway results are available in supplementary..... 35

Figure 3.6: A heatmap Illustrating Significant Proteins ($p\text{-adj}<0.1$) from Rainbow Trout Plasma Belonging to Lipid Metabolic Processes. Protein levels are represented by the normalized average fold change of peak intensity..... 37

Figure 3.7: Box and Whisker of the Plasma Levels of Glucose-6-Phosphate Dehydrogenase (G6pd) and glucose-6-phosphate (G6P) in rainbow trout exposed to PFAAs and PFAA Mixtures. Boxplot divisions represent the interquartile range; error bars represent standard deviation and dots represent outliers. Asterisks indicate significance ($p\text{-adj}<0.05$)..... 38

Figure 3.8: Violin Plot Illustrating the Plasma Concentrations of Inorganic Phosphate of Rainbow Trout Exposed to PFAAs and PFAA Mixtures. The midline represents the median and asterisks represent significance ($p\text{-adj}<0.05$). Phosphate concentrations are \log_2 transformed and median normalized..... 39

Figure 3.9: Overview of Untargeted Proteomics Results from the Head Kidney of Rainbow Trout Exposed to PFAAs and PFAA Mixtures. The heatmap illustrates the top 400 proteins ranked by

significance using a One-way ANOVA in addition to hierarchical clustering using Ward's method. Data is median normalized and log₂ transformed..... 41

Figure 3.10: A Principle Component Analysis of Untargeted Proteomics Conducted on the Head Kidney of Rainbow Trout Exposed to PFAAs and PFAA Mixtures for 22 Days. The shaded ellipses represent 95% confidence intervals and are colored by treatment. Data is median normalized and log₂ transformed; axes titles indicate principle component number and proportion of raw data as a percentage..... 42

Figure 3.11: Venn Diagrams Illustrating the Commonality of Significant Kidney Proteins ($p_{adj}<0.1$) from Rainbow Trout Exposed to PFAAs and PFAA Mixtures. The top row (A, B) contains two charts comparing the high PFAA mixture (MIXHI) with PFOA; (A) includes only proteins with positive fold change (indicated by red) and (B) displays only those with negative fold change (blue). The bottom row contains two charts (C, D) displaying significant proteins in common between plasma and kidney tissues by exposure regime (MIXHI and PFOA respectively). Figures (C, D) have no color because they include proteins having both positive and negative fold change..... 43

Figure 3.12: Biological Pathways Found to be Significantly Overrepresented ($p_{adj}<0.1$) from the Head Kidney of Rainbow Trout Exposed to MIXHI and PFOA Exposure Regimes. Biological pathway analysis was conducted using Gene Ontology's overrepresentation analysis test which conducts a Fisher's exact test followed by a Benjamini-Hochberg correction for false discovery. The heatmaps have related biological pathways grouped by biological system and only contain noteworthy pathways and only treatments with noteworthy significant results; numbers in the center of each panel represent FDR adjusted p-values. All the biological pathway results are available in supplementary..... 44

Figure 3.13: A heatmap Displaying Significant Proteins ($p\text{-adj}<0.1$) from Rainbow Trout Head Kidney Involved in Lipid and Reactive Oxygen Species Metabolism. Protein levels are represented by average fold change of peak intensity..... 46

Figure 3.14: Aqueous Concentrations of PFAAs for the Mixture Exposure Regimes. Stacked bar charts represent the concentration of each PFAA comprising the mixture exposure water taken at the final timepoint (week2-3 pooled)..... 48

LIST OF ABBREVIATIONS AND SYMBOLS

Abcd ATP binding cassette subfamily

Abhd12 Abhydrolase domain containing 12, lysophospholipase

Acaca Acetyl-CoA carboxylase alpha

Acacb acetyl-CoA carboxylase 2

Acly ATP citrate lyase

Acot2 Acyl-CoA thioesterase 2

Acox3 Peroxisomal acyl-coenzyme A oxidase 3

Acs14 Acyl-CoA synthetase long chain family member 4

ADP Adenine diphosphate

AFFFs Aqueous firefighting foams

AKT ATK serine/threonine kinase

Aldh3a2 Aldehyde dehydrogenase 3 family member A2

ANOVA Analysis of Variance

ap1s1 Adaptor related protein complex 1, sigma subunit 1

Arid5b AT-rich interaction domain 5B

Arrdc3 Arrestin domain containing 3

ATK Protein Kinase B

ATP Adenine triphosphate

ATSDR U.S. agency for Toxic Substances and Disease Registry

BAF Bioaccumulation factor

BBB Blood-brain-barrier

Bbs4 Bardet-Biedel syndrome 4

BCF Bioconcentration factor

bdnf Brain derived neurotrophic factor
BSA Bovine serum albumin
CACN L-type calcium channel
CAMK2 Calmodulin kinase 2 subunit
CAMK4 Calmodulin kinase 4 subunit
Cat Catalase
CD36 Cluster of differentiation 36
CD4 Cluster of differentiation 4
CD8 Cluster of differentiation 8
Cgn Cingulin
Cgnl1 Cingulin like 1
CNS Central nervous system
COX1 Cyclooxygenase 1
COX2 Cyclooxygenase 2
Cpt1a Carnitine O-palmitoyl transferase
Creb cAMP-response element binding protein
Crebl in cAMP-response element binding protein-like
CTL Control
Cxadr Coxsackievirus and adenovirus receptor
Cyp51a1 Cytochrome P450 family 51 subfamily A member 1
Dgat Diacylglycerol O-acyltransferase
Dhcr7 7-Dehydrocholesterol reductase
Dlst Dihydrolipoamide S-succinyltransferase

DNA deoxyribonucleic acid
ECCC Environment and Climate Change Canada
ESI Electrospray ionization source
FABP Fatty acid binding protein
FADH Flavin adenine dinucleotide
Fads2 Fatty acid desaturase 2
Far1 Fatty acyl-CoA reductase 1
FDR False discovery rate
Fxr Farnesoid-X-receptor
G6P Glucose-6-phosphate
G6pd Glucose-6-phosphate dehydrogenase
Gls Glutaminase
Gpx4 Glutathione peroxidase subunit 4
Gss Glutathione synthase
Gstp1 Glutathione S-transferase
Hadha Trifunctional enzyme subunit alpha
Hmgcr 3-Hydroxyl-3-methylglutaryl-CoA reductase
HPLC high performance liquid chromatography
Hsd17b12 Hydroxysteroid 17-beta dehydrogenase 12
Hsd17b4 Hydroxysteroid 17-beta dehydrogenase 4
IFNA Interferon alpha
IGG Immunoglobulin gamma
IL1B Interleukin 1 beta

IL8 Interleukin 8
IP3R 1,4,5 triphosphate receptor
Lama Laminin
Lonp2 Lon protease subunit 2
LPS Lipopolysaccharide
Lss Lanosterol synthase
Lxr Liver-X-receptor
MIXHI High mixture
MIXLOW Low mixture
MIXMED Medium mixture
MS Mass spectrometry
MS/MS Tandem mass spectrometry
MYD88 Myeloid differentiation primary response 88
Myh Myosin heavy chain
Naca Nascent polypeptide-associated complex subunit alpha
NADH Nicotinamide adenine dinucleotide
NADPH Nicotinamide adenine dinucleotide phosphate
NFκB Nuclear factor-κB
Nnt Nicotinamide nucleotide transhydrogenase
Nox5 NADPH oxidase 5
NSCs Neural stem cells
OAT Organic anion transporter
OATP Organic anion transporting polypeptide

Oxr1 Oxidative resistance 1

p-adj Adjusted p-value

Pdha Pyruvate dehydrogenase E1 subunit alpha 1

Pdk2 Pyruvate dehydrogenase kinase 2

PFAAs Perfluoroalkyl acids

PFAE Perfluoroalkyl ethers

PFAS Per- and polyfluoroalkyl substances

PFBA Perfluorobutanoate

PFBS Perfluorobutane sulfonate

PFCA Perfluoroalkylcarboxylate

PFDA Perfluorodecanoate

PFDS Perfluorodecane sulfonate

PFHpA Perfluoroheptanoate

PFHpS Perfluoroheptane sulfonate

PFHxA Perfluorohexanoate

PFHxS Perfluorohexane sulfonate

PFNA Perfluorononanoate

PFNS Perfluorononanoate sulfonate

PFOA Perfluorooctanoate

PFOS Perfluorooctane sulfonate

PFSA Perfluoroalkylsulfonate

PFUnDA Perfluoroundecanoate

PI3K Phosphoinositide 3-kinase

Pla2g4a Phospholipase A2 group IVA

Plec Plectin

PPAR Peroxisome proliferator activated receptor

PPARA Peroxisome proliferator activated receptor alpha

PPARD Peroxisome proliferator activated receptor beta/delta

PPARG Peroxisome proliferator activated receptor gamma

RAD52 RAD52 homologue, DNA repair protein

RNA ribonucleic acid

ROS Reactive oxygen species

RXR Retinoid X receptor

Rxrb Retinoid-X-receptor beta

RYR Ryanodine receptor

Sdha Succinate dehydrogenase complex flavoprotein subunit A

SEM Scanning electron microscopy

Slc22A Solute carrier family 22 member

slco2b1 Solute carrier organic anion transporting polypeptide 2b1

Slco5a1 Solute carrier organic anion transporter family member 5A1

SPE Solid-phase extraction

Srebf2 Sterol regulatory element binding transcription factor 2

Stard10 StAR related lipid transfer domain containing 10

Suclg1 Succinate-CoA ligase GDP/ADP-forming subunit alpha

TECP Tris(2-chloroethyl) phosphate

tgf1a Transforming growth factor beta 1a

Tjp Tight junction protein

TLR Toll-like receptor

TNFA Tumor necrosis factor alpha

Tysnd1 Peroxisomal leader peptide-processing protease

UPLC Ultra-high performance liquid chromatography

VLDL Very low-density lipoprotein

WWTP Wastewater treatment plant

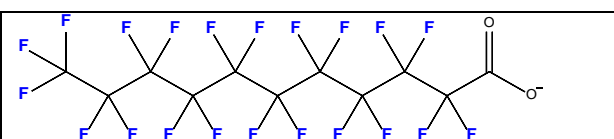
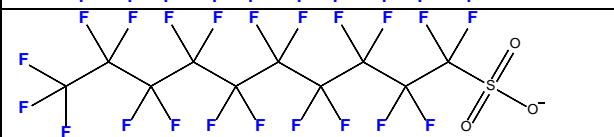
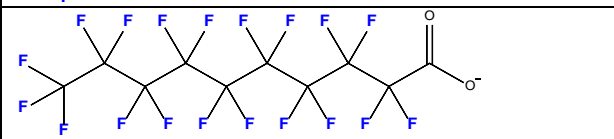
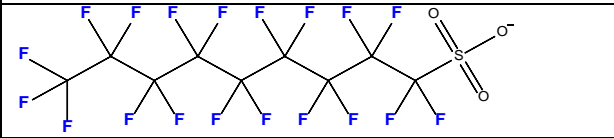
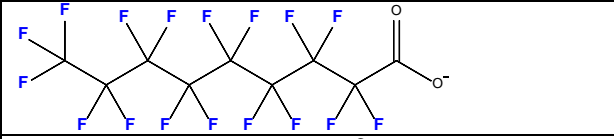
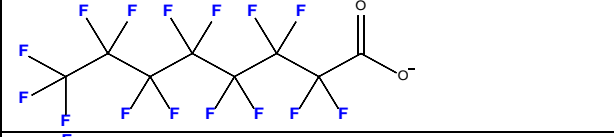
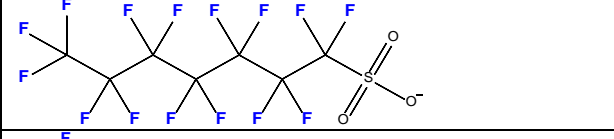
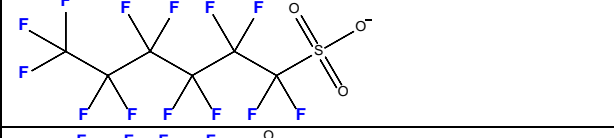
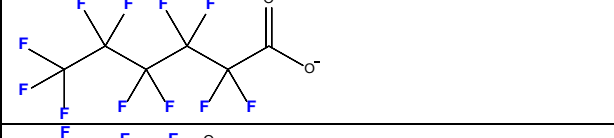
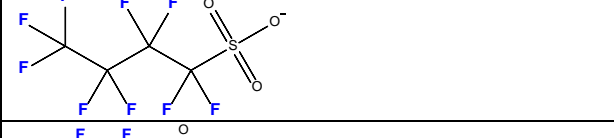

Chapter 1. Introduction

1.1 General Overview

Per- and polyfluoroalkyl substances (PFAS) are a class of persistent and bioaccumulative pollutants which are characterized by alkane moieties which have two or more fully fluorinated carbons (1, 2). PFAS have been used in a variety of products including non-stick cookware, aqueous firefighting foams, disposable food packaging and surface protective coatings for carpets, apparel, furniture and other fabrics (3, 4). PFAS are valued due to several physical and chemical properties including their hydrophobic and oleophobic properties which provide a non-stick, stain repellency in surface coatings. The perfluorinated alkane moiety within PFAS is quite chemically inert, being robust against many forms of chemical attack (i.e. acid/base, oxidation, thermal, radiation etc.) (3, 4). It is due to these unique physicochemical properties that PFAS is highly valued in a large variety of industrial processes. However, it is the same chemical inertness which makes these compounds highly persistent environmental pollutants, as it is believed that they persist in the environment indefinitely. PFAS are a major environmental pollutant, being frequently detected in biota and environmental matrices around the world (5-7).

In particular, perfluoroalkyl acids (PFAAs) are deemed the final degradation products of larger forms of PFAS (5). PFAAs comprise the vast majority of PFAS which exist in surface waters and biota, being comprised of perfluorinated alkane groups and an anionic moiety typically being either a carboxylate or sulfonate group (Table 1.1).

Table 1.1. Chemical Structure Diagram of Perfluoroalkyl Acids Mentioned in this Thesis.

PFUnDA: Perfluoroundecanoate (C11)	
PFDS: Perfluorodecane sulfonate (C10)	
PFDA: Perfluorodecanoate (C10)	
PFNS: Perfluorononoate sulfonate (C9)	
PFNA: Perfluorononanoate (C9)	
PFOA: Perfluorooctanoate (C8)	
PFHpS: Perfluoroheptane sulfonate (C7)	
PFHxS: Perfluorohexane sulfonate (C6)	
PFHxA: Perfluorohexanoate (C6)	
PFBS: Perfluorobutane sulfonate (C4)	
PFBA: Perfluorobutanoate (C4)	

PFAAs have been widely detected in human blood and always exist as mixtures of structurally similar congeners in surface waters (Table S1) (5-8). PFAAs are being investigated as potential carcinogens and adversely affect many biological systems including development, metabolism and immune function in vertebrates (9-12). Currently, there is a large paucity of data evaluating the toxicology of PFAA mixtures and compounds which are considered short chain (being < C8 for perfluoroalkyl carboxylates (PFCAs) and < C7 for perfluoroalkyl sulfonates (PFSAs) (13). Reports from Environment and Climate Change Canada (ECCC) have acknowledged the lack of information available for PFAAs other than PFOA and PFOS; including addressing mixture toxicity (14, 15). Currently, only two national regulatory agencies have established a framework for addressing potential risks associated with complex mixtures of PFAAs in drinking water which is due to lack of data to support such a framework. Health Canada and The National Institute for Public Health and the Environment within the Netherlands have both established a hazard index type framework for quantifying relative toxicity of various PFAAs based on dose response with an established health criterion (13, 15). Establishment of environmental guidelines for PFAAs other than PFOA and PFOS in Canada and the world are absent due to the lack of information regarding toxicity of short chain PFAAs and PFAA mixtures (15-17). Regulatory bodies such as the U.S. Agency for Toxic Substances and Disease Registry (ATSDR) acknowledges similarity of adverse health outcomes of some PFAAs but states that there is evidence of mechanistic differences and insufficient information on interactions between diverse PFAA mixtures (13, 14, 18). Clearly, there is a great need to better establish the toxicology of short chain PFAAs and PFAA mixtures for informed risk assessment.

1.2 Perfluoroalkyl Acids

PFAAs are a subgroup of PFAS which are the most abundant form in the environment and are the final degradation products from the diverse number of chemical species extant in consumer and industrial products (3, 4, 19). The forms of PFAS which degrade into PFAAs are commonly termed as ‘precursors’ within the literature (5, 20). Perfluorooctanoate sulfonic acid (PFOS) and perfluorooctanoic acid (PFOA) are examples of the most infamous and well-studied forms of PFAAs initially garnering attention from the American public and the U.S Environmental Protection Agency following their ubiquitous detection in the blood of American citizens as well as being detected in biota around the world (6, 8). PFOS in particular was phased out from 2000 - 2002 by its major manufacturer 3M due to concerns regarding its widespread occurrence in American surface waters and high bioaccumulative potential (5). Currently, PFASs of > 7 carbons and PFCAs of > 6 carbons are not permitted to be manufactured or imported into most developed nations which has resulted in a shift to production of PFAAs of shorter chain length and other alternative chemistries (21). Regardless of the restrictions, legacy PFAAs remain in the environment while short chain PFAAs levels are increasingly entering the aqueous environment through both point sources (industrial wastes, wastewater treatment plants, aqueous firefighting foams, landfills etc.) and non-point sources (surface runoff and atmospheric discharges) (5, 7, 22, 23).

1.3 Uses of PFAS

PFAS have invaluable physical and chemical properties making them very useful in an extensive number of applications (19, 24, 25). A recently published review by Glüge et al., 2020

found over 200 use categories for over 1400 PFAS which is the most comprehensive and up to date publication on PFAS use (24). Some examples of the most frequent industrial use categories include: photographic industry, semiconductor industry, stain and grease repellent coatings, paints, varnishes, fluorinated polymers, lubricants, fire-fighting formulations (AFFF), medical utensils, personal care products, and printing (24). The most frequently used forms of PFAS are the fluorotelomer based-products which consist of a perfluorinated alkyl group conjugated to a methyl or ethyl alcohol and are known to readily degrade into PFAAs in the environment (24). Unfortunately, the voluntary phase outs of long chain PFASs and PFCAs by major US manufacturers have not completely eliminated illegal import of products containing long chain PFAAs into developed nations i.e. electronics, cars and others (26). Thus, long chain or legacy PFAAs continue to enter the environment via the degradation of legacy products in landfills and current products which may unknowingly contain restricted PFAAs.

1.4 Pathways into the Aquatic Environment

Sources of PFAS into the environment are caused by a contribution of point and non-point sources (5). Point sources of PFAAs include industrial and municipal wastewater treatment plants (WWTPs), landfill leachates, and aqueous firefighting foams (AFFF) (5). Non-point sources include sewage sludge application to crops, wet and dry atmospheric deposition, soil and street surface runoff (5). Generally, wastewater treatment of PFAS is not effective because they are not designed to remove PFAS from waste flows. It is common to observe increased concentrations of PFAAs in wastewater effluent because of the degradation of PFAS precursors (5, 27-31). For example, the fate of several PFAAs were monitored in six WWTPs in New York State and the

mass flows of PFOS, PFOA, PFNA, PFDA and PFUnDA were all found to significantly increase following secondary treatment (29). Concentrations of PFAAs in have been determined to be 5-10 times higher in effluent than surface waters along the river Elbe, Germany (32). Industrial influenced WWTPs are another important point source sometimes resulting in highly elevated levels of PFAS in the environment (29, 33, 34). A study conducted in Taiwan found the semiconductor and electronics industry to have a large influence on concentrations of PFAAs in receiving waterways (33). Although conventional wastewater treatment processes are poor at removing PFAS, technologies do exist that have been found to be effective in lowering PFAS concentrations to safe standards such as granular activated carbon, reverse osmosis and anion-exchange resins (35). All of these technologies fall under the category of tertiary treatment for WWTPs and are costly to implement and maintain (35). Landfill leachates are another important point source, where various products containing PFAS degrade, contaminating underlying groundwater or undergo municipal wastewater treatment (36, 37). Landfill leachates in Germany contained 199-1537 ng/L PFASs but due to the relatively slow rate of flow for leachates, contribution of PFAS to the environment through this method may be quite slow (38). Finally, aqueous firefighting foams are another major point source of PFAAs (3, 4, 19). AFFFs contain various compositions of PFAS and were widely utilized by the American military (aircraft bases etc.), oil and gas production, refining industries, and at airports worldwide (19). A spill that occurred at Toronto Pearson Airport, Ontario Canada in 2002 resulted in 22000 L of AFFF being spilled into Etobicoke Creek. Total PFSA concentrations in the creek ranged from 0.017 to 2260 µg/L and total PFOA concentrations ranged from 0.009 - 11.3 µg/L (39).

1.5 Occurrence of PFAAs in the Aqueous Environment

PFAS is ubiquitously present in the global environment, tending to be in the hydrosphere due to its high-water solubility (4, 19, 40, 41). A recent review of the environmental occurrence of PFAS in surface waters was summarized herein (Table S1) where over 80 different locations from 68 different academic studies report many forms of PFAAs at large ranges of concentrations. The median summative concentration of PFAS was found to be 38.4 ng/L with a minimum of non-detect to a maximum of almost 67 µg/L (Table S1). Studies included within Table S1 are all chosen based on having an environmental sampling time by the year 2009 in order to get a more recent overview of PFAA levels in surface waters. From the review, it is clear that PFAAs always exist in surface waters as mixtures, containing a suite of PFCAs and PFSA of different carbon chain length (Table S1). According to a search conducted in Web of Science as of February, 2023, over 7000 scientific articles have been published using keywords 'PFOA' or 'PFOS'. Clearly, a great degree of research has been done regarding the two most important forms of PFAAs but there is much to understand regarding the many other forms that exist (42). New forms of structurally similar PFAS are being manufactured at locations around the world, including classes such as the short chain congeners and perfluoroalkyl ethers (PFAEs) (24, 43). The burden of PFAAs in the environment is gradually shifting as these newer alternatives are increasingly entering the environment (i.e. PFOA and PFOS). For example, a shift in PFAA composition was observed in the sediment profile in lake Michigan from long chain PFAAs to short chain alternatives (4 carbon PFBA and PFBS) (64). The Cape Fear River basin in North Carolina, a site historically influenced by perfluorochemical production, has seen shifts in PFAS composition over the years from predominantly long chain PFCAs (C7-C9) in 2006 to short chain PFCAs (C5 - C6) in 2013 (65, 66). In addition, appearance of a novel form of PFAAs known as hexafluoropropylene oxide-dimer

acid or GenX is being detected in the environment. GenX is an alternative to PFOA developed by Chemours, a sister company of Dupont in anticipation of American production phase outs of PFOA from 2010 - 2015 (65-67). Unfortunately, GenX is still believed to be highly persistent and as toxic as PFOA, the compound it was designed to replace.

1.6 Bioaccumulation of PFAAs

PFAAs do not tend to bioaccumulate in fatty tissues like the majority of persistent environmental pollutants, likely being due to the oleophobic character of the perfluorinated alkane moieties (44-51). Non-covalent binding of PFOA and other PFAAs have been observed in human and rat serum albumins along with human liver fatty acid binding protein (23, 46, 47, 49, 51-55). Thus, it is not surprising that highest levels of PFAAs are in blood, kidneys, and liver where select classes of proteins are at their highest (55). Elimination half-lives of PFOA and PFOS in humans are exceptionally high when compared to other biota being 5.3 years, 3.4 years and 2.7 years for PFHxS, PFOS and PFOA respectively (56-60). Stark differences exist in the elimination rates across species, age, and sex in vertebrates where serum half lives in non-human vertebrates are drastically less (on the order of days and hours) (56, 60). Bioaccumulation of PFAAs in fish tissues have a very wide range of values (Table S2) between 10^0 – 10^4 orders of magnitude. Bioaccumulative potential tends to be a function of chain length and functional group. In general, every perfluorinated carbon added can increase the bioaccumulative factor (BAF) by an order of magnitude with the PFSAs generally having BAFs that are 1-2 orders of magnitude higher than PFCAs with equal chain length (61). Longer chain PFAAs tend to be approximately 1-2 orders of magnitude more acutely toxic and have higher affinity towards a key mode of action: peroxisome

proliferator activated receptor alpha (PPARA) (62). Biomagnification is another important variable which is observed to occur in the Great Lakes in higher trophic level birds, fish and mammals having significantly higher levels of PFAAs (63-66). Several studies in fish have also found significantly higher rates of elimination in females for PFOA and PFOS than in males (67-69).

1.7 Toxicokinetics

Urinary and fecal elimination are deemed the primary routes of PFAS elimination in rodent studies with metabolism not occurring due to the chemical inertness of PFAAs (70). Urinary elimination is highly dependent on carbon chain length while fecal elimination is relatively constant regardless of chain length (2-5% (71)). Urinary rates of elimination are also influenced by circulating sex hormones which affect expression of organic anion transporters (OATs) and organic anion transporting polypeptides (OATPs) in the renal tubules of the kidney (72). A rodent study co-treating rats with PFOA and an OAT inhibitor (probenecid) almost completely eliminated urinary excretion of PFOA (73). Further gene expression analysis of the renal tubules found distinct differences in expression of *Oat1*, *Oat2* and *Oatp2* across males and females as well as between castrated males, testosterone, estradiol and ovariectomy cohorts (72, 74). Renal resorption was determined to be another important factor for determining renal elimination rates of PFAS with the location and density of OAT and OTAP proteins on the apical and basal membrane of renal tubules being an important determinant (75, 76). Although there are less toxicokinetic studies conducted on fish, many of the same observations occur as with mammals, with body burdens of PFAAs differing by sex, chain length, and functional group (77). One study

dosing rainbow trout with PFOA and PFOS in respirometer-metabolism chambers measured half-lives of 16 days and 86.8 days, respectively. Route of elimination was confirmed to be primarily via urine, as is observed in mammals. Branchial elimination was another factor but was occurring at approximately 10-fold lower rates when compared to the renal route (78, 79).

1.8 Impacts of PFAAs on Lipid Metabolism

Some of the most well documented effects of PFAAs are on lipid and carbohydrate metabolism across many model organisms including fish species (12, 68, 80-88). A high dose exposure of PFOS or PFOA to rodents caused weight loss, hepatocellular hypertrophy, hepatic steatosis, reduced serum triglycerides, glucose, and cholesterol as well as an induction of enzymes involved in fatty acid β -oxidation (12, 85, 86, 89-96). Several studies in mammals and fish have found decreased hepatic excretion of very low-density lipoprotein (VLDL) particles along with increased liver uptake of lipids through upregulation of Cluster of Differentiation 36 (CD36) (12, 68, 87, 88, 97-99).

The primary mode by which PFAAs are believed to affect lipid and carbohydrate metabolism is from ligand mediated activation of peroxisome proliferator activated receptor alpha (PPARA) (80, 81, 95, 96, 100-102). The peroxisome proliferator activated receptors (PPARs) are a class of nuclear hormone receptors which belong to the NR1C subgroup of the nuclear receptor superfamily (103, 104). Three PPAR isotypes have been identified in vertebrates (PPARA, PPARD, PPARG) which are encoded by separate genes. PPARs play an important role in lipid and carbohydrate metabolism being activated by a variety of endogenous lipids including fatty acids (primarily unsaturated), fatty acid derivatives, phospholipids, eicosanoids and prostaglandins

(103, 104). There is some degree of overlap between PPAR ligand recognition across isotypes with some ligands transactivating multiple isotypes at once, however with varying affinities (104). PPARA is primarily involved in fatty acid catabolism and is expressed in tissues which undergo higher rates of mitochondrial and peroxisomal β -oxidation which include brown adipose tissue, hepatocytes, cardiomyocytes, enterocytes, proximal tubules of the kidney and skeletal muscle (103, 105, 106). PPARs mediate control on the expression of target genes through heterodimerization with the retinoid X receptor (RXR) which binds to peroxisome proliferator response elements on the genome. In the event that the PPAR:RXR heterodimer binds a specific PPAR agonist, binding leads to the release of the co-repressor complex and subsequent recruitment of several coactivators culminating in the binding of peroxisome proliferator response elements in the genome and transcription of target genes (104). The affinity of C4 - C7 PFAAs for human PPARA have been evaluated *in vitro* and a clear positive relationship is observed with increasing chain length, and PFCAs bind more strongly than PFSAs (45, 62, 100, 101).

One abnormal effect of PFOA and PFOS on lipid homeostasis in livers was micro vesicular accumulation of fatty acids which is not an outcome which occurs from PPAR activation (95, 96). Tan et al., 2013 observed significant accumulation of long chain fatty acid and long chain acyl-carnitines such as linoleic acid and linoleoyl carnitines in mice fed high fat diets while also being exposed to 5 mg/kg bw of PFOA for 3-weeks (12). The accumulation of long chain fatty acids and acyl carnitines suggested a dysfunction in downstream oxidation of long chain fatty acids. In addition to this, carbohydrate metabolism within the liver appeared to be impacted following PFOA exposure with fructose, mannitol, galactose, fumaric acid, malic acid and citric acid were all significantly reduced along with transcript levels of various glucose metabolism enzymes (12). In particular, a reduction in hepatic citric acid levels along with a downregulation of several genes

involved in the citric acid cycle (*Acly*, *Dlst*, *Pdha*, *Sdha* and *Suclg1*) suggested a dysfunction occurring in oxidative phosphorylation may explain the accumulation of long chain fatty acid metabolites and reduction in carbohydrate metabolites (12).

1.9 PFAS Induced Mitochondrial Dysfunction

Dysregulation of lipid and carbohydrate metabolism can occur when mitochondrial function is impaired. Lipids in particular can only generate ATP efficiently through generation of NADH and FADH₂ which are subsequently used as reducing equivalents in the electron transport chain. However, as seen in many disease states, when oxidative phosphorylation is impaired, it serves as a bottleneck for the generation of ATP from lipids (107). An adverse outcome pathway which explains this phenomenon describes mitochondrial dysfunction as a cause of hepatic steatosis through impaired catabolism of lipids within the liver leading to the buildup of lipids (108). A plethora of studies report some form of mitochondrial dysfunction occurring following exposure to PFAAs such as PFDA, PFNA, PFOA (109-112). For example, an ex vivo study exposed isolated rat brain and liver mitochondria to 1.5 mM PFOA exhibited mitochondrial membrane potential collapse, mitochondrial swelling, cytochrome C release and a dose dependent reduction in ATP production, up to 83% at 1.5 mM (111) Hagenaaers et al., 2013 mitochondrial uncoupling occurring in zebrafish exposed to PFOA, finding a 55% reduction in electron transport chain activity in fish exposed to 1 mg/L PFOA (68). Another study exposing Crucian Carp to 25 mg/L of PFOA found a decrease in expression of genes coding for adenine nucleotide translocase and voltage dependent anion channel proteins at the 4-day exposure but not the 7-day exposure concentrations (87).

1.10 Effects of PFAAs on the Nervous System

PFAAs are deemed to cause behavioral deficits in developmentally exposed human children, mice and fish (113). Zebrafish embryos exposed to 0.5 µg/L of PFOS found effects on thigmotaxis, light:dark preference, increased embryonic mortality, swim bladder inflation and spinal curvature (113). Many behavioral studies exist on the effects of PFOS and some other PFAAs on important cognitive and neuromuscular responses in mammals and fish (114). Several prominent examples of impacts of PFAAs on behavioral phenotypes include impaired spatial learning, memory, and swimming velocity in mice exposed to a high dose of PFOS for 1 month (114). Several studies have found altered locomotion in fish exposed to PFAAs (113, 115-117).

Assessing PFOS exposure at multiple time points reveals that the length of PFOS exposure was a variable in predicting morphological effects (113). Exposure of zebrafish for 5 days post-fertilization to 2 µg/L PFNA or PFOS caused sex specific differences in lighting preferences and decreased aggression in the males (118). A small panel of mRNA transcripts involved in early zebrafish development were found to be changed including brain derived neurotrophic factor (*bdnf*), adaptor related protein complex 1, sigma subunit 1 (*ap1s1*) transforming growth factor beta 1a (*tgf1a*) and solute carrier organic anion transporting polypeptide 2b1 (*slco2b1*) (118, 119). Several potential modes of action for PFAA induced neurotoxicity exist; PFOA and PFOS affect multiple aspects of calcium homeostasis in neurons including L-type calcium channels, inositol 1,4,5-triphosphate receptors and ryanodine receptors (120-123). *In utero* exposure of rats exhibited apoptosis of hippocampal neurons at 5 and 15 mg/L of PFOS in drinking water with a dose dependent increase in calcium levels in the hippocampus (124). Calcium acts as an important secondary messenger in neurons regulating many functions including apoptosis, synaptic transmission and plasticity (113).

1.11 Immunotoxicity of PFAAs

Adverse effects on immune function may be one of the more sensitive endpoints affected by PFAS (11, 41). An epidemiological study investigating antibody production in infants vaccinated for tetanus and diphtheria found significant negative correlations for PFOS and PFOA levels and anti-diphtheria antibody concentrations being -38.6% and -16.2% respectively for 5-year-old children (125). Similar associations exist with serum concentrations of various PFAAs and antibody concentrations specific towards rubella, mumps and *Hemophilus influenzae* vaccinations in children and adults (126-130). Similar effects have been found in rodents exposed to PFOA and PFOS which resulted in reductions of antibody responses following immune challenges (11, 131-133). Rodent exposures to high doses of PFOA (40 mg/kg/day for 7 days) have also resulted in lowered spleen and thymus weights and reduced immature CD4+ and CD8+ T cells in the thymus and spleen (134). In a study conducted by Qazi et al., 2012 exposure of mice to a 10-day dietary exposure to PFOA and PFOS caused reductions in the cellularity of the spleen, thymus and bone marrow (135).

The primary mode by which PFAAs are believed to exert their immunotoxic effects is via PPAR-mediated modulation of the immune system. PPARs generally exert an anti-inflammatory effect via multiple mechanisms which depend on the isoform involved. The primary mode is from the negative cross-talk that exists between PPARs and the proinflammatory transcription factor nuclear factor Kappa B (NFκB). PPARs also have relatively high expression levels in key immune effector cells including macrophages, neutrophils and lymphocytes (136, 137). Previous studies exposing mice to peroxisome proliferators have caused similar immunological effects including thymus and splenic atrophy along with reductions in CD4+ and CD8 + cell populations within the thymus (138-140). Interestingly, the effects of Wy14-643 and PFOA were not found to cause

splenic and thymic atrophy in *Ppara* null mice while causing a less significant change in the T cell populations of the thymus and no change in leukocyte numbers within the spleen (138).

Relatively less information is available on the immunotoxicity of PFAAs in fish however there are some studies which tend to have similar findings as those in mammals. Embryonic exposures of marine medaka to 1 mg/L of PFOS caused an impaired immune response following a lipopolysaccharide (LPS) challenge at 27 days post hatch. The transcript levels of several key genes involved in the inflammatory response to LPS including *Il8*, *Cox1*, *Cox2*, *Tnfa* and *Il1b* were found to be significantly lowered in the PFOS treatment. Another study exposing zebrafish to PFOA (0.05, 0.1, 0.5, and 1 mg/L) for 21 days found increased expression of proinflammatory cytokines *il1b* and *il21* in the spleen at the low dose but its suppression at higher doses (141). Additionally, a clear trend was observed between immunoglobulin gamma levels (Igg) and cytokine secretion suggesting the antibody responses of fish may be affected by PFAAs just like those in mammalian studies (141). Thus, it is likely for PFAAs to cause immunotoxicity in fish via conserved mechanisms.

1.12 Thesis Premise

PFAAs are a major global aqueous contaminant and exist as chemical mixtures of a number of structurally similar congeners. Current toxicological information is lacking when it comes to addressing the effects of PFAA mixtures at concentrations and compositions typically found in surface waters. Additionally, relatively little information is available on the toxicity of short chain PFSA and PFCA congeners. PFAAs have a pleotropic mode of action on many biological systems emphasizing the importance of using an untargeted, multi ‘Omics approach on different organs

will allow for a thorough analysis of any toxicological effect. Structural and toxicological similarity of PFAAs could allow for these compounds to be grouped as a class for more efficient risk assessment. However, much more research into the toxicological dose response to short chain PFAA congeners and PFAA mixtures needs to be conducted. Within this thesis, we will address these knowledge gaps by conducting two types of chemical exposure: (1) PFAA mixture exposures at environmentally relevant concentrations and (2) Single component exposures to different PFAA congeners. Specifically, we conducted a 3-week aqueous exposure of rainbow trout and performed untargeted proteome analyses on the blood plasma and head kidney tissue. An additional set of single component exposures was also conducted at higher, equimolar concentrations to elucidate the potential for differences in proteomic response across chain length (C4 and C8) and functional groups (carboxylate or sulfonate) of PFAA congeners. Overall, the proposed research project hopes to generate toxicity data for PFAAs and their mixtures that will aid in risk assessment, and protein profiles that could be used for monitoring the effects of PFAS in wild fish populations.

1.13 Objectives

The objectives of the study were to: (1) Analyze and compare changes in the plasma and head kidney proteome of rainbow trout following waterborne exposures to different PFAA congeners and their mixtures (2) Establish biological processes likely to be affected using pathway analysis software on protein information (3) Analyze changes in phosphorylated carbohydrates in the plasma and link them to changes observed in the proteome (4) Measure the concentrations of PFAAs in the exposure water and blood plasma of rainbow trout to investigate toxicokinetics of low concentration PFAA mixture exposures.

Chapter 2. Methods

2.1 Fish Housing Conditions

Juvenile Rainbow trout (*Oncorhynchus mykiss*) approximately 70 – 100 grams, 6 – 8 months of age were acquired from Linwood Acres Trout Farms LTD, Campbellcroft Ontario. All animal experimentation was done in compliance with the Canadian Council on Animal Care Guidelines. Fish were allowed to acclimate for 4 weeks in 4000 L fiberglass tanks, receiving flow-through, de-chlorinated water at 12 C°, 16:8 light:dark photoperiod. During the acclimation period, fish were fed a maintenance diet of 0.4 % body weight every 3 days to minimize growth. Uneaten food and feces were cleared every two days. Fish were randomly transferred to 70 L glass aquaria and allowed to acclimate for an additional 1 week prior to commencing chemical exposures. There were four replicate tanks per treatment with 5 fish per tank and an approximate stocking density of 1.2 g/L. It must be noted that due to feasibility constraints, 1 replicate tank per treatment was 60 L instead of 70 L and had an approximate stocking density of 1.4 g/L. Any potential effects caused by the differences in tank size were predicted to be controlled due to every treatment having one 60 L tank. All fish within the glass aquaria received the same water, temperature and photoperiod as within the fiberglass tanks. Water quality was maintained via flow-through, with 5, 95% tank turnovers every 24 hours. The chosen flow rate has previously been determined to ensure high molecular mixing and optimal water quality parameters for rainbow trout (142). Oxygen readings of several of the tanks prior to beginning the chemical exposures were determined to be saturated. Water quality parameters were not specifically taken within the glass aquaria because water quality is deemed not to be an issue for flow through systems at high

turnover rates (142). General water quality parameters for the system water are also taken daily within the laboratory i.e. temperature, PH, nitrite and ammonia.

2.2 Chemical Exposures

Following the acclimation period, fish were exposed to different compositions of waterborne PFAAs for 22 days (Table 2.1). Originally, the duration of exposures was been planned to be 28 days but was shortened due to a university shutdown in the wake of the COVID-19 outbreak in Ontario, Canada, mid-March 2020.

The first set of chemical exposures were considered environmentally relevant consisting of a mixture of 8 different PFAAs at summative concentrations of 50, 100, and 500 ng/L (Table 2.1). The composition of the mixture exposures was modeled after the species of PFAAs quantified in Lake Ontario after 2009 by Amila et al., 2011 (61). The second set of chemical exposures consisted of 4 different aqueous exposures to a single PFAA compound at substantially higher concentrations (25 nM PFOS, PFOA, PFBS or PFBA; Table 2.1). Each treatment group had n = 20 and consisted of 4 replicate tanks. The purpose of conducting single compound exposures at non-environmentally relevant concentrations was to induce clear protein and metabolite responses for comparison between treatments.

All of the PFAA chemicals were purchased from Sigma Aldrich except the C6 congeners (PFHxA and PFHxS) which were purchased from Toronto Research Chemicals Inc. PFAA compounds were purchased as either the purified anionic form for the PFCAs (97% PFNA; 95% PFOA, 99% PFHpA and 98% PFBA) or the potassium salt for the PFSAs (98% PFOS). All nominal concentrations represented the concentration of the free anion. A carrier was not used within the

study and all compounds were solubilized in distilled water with stirring and mild heating. Less soluble PFAAs (mainly PFOA and PFOS) had limits of solubility in the several hundreds of mg/L which were not required for conducting the current study. Bottles of stock solution (1 L) were replaced once a week, for a total of 3 times throughout the course of the experiment. Water samples were taken for later analysis of PFAAs at 3 timepoints throughout the experiment; always being 24 hours following a change in the 1 L bottles of stock. Approximately 3 ml of water was taken from each tank and pooled by treatment. Water was stored in 15 ml, polypropylene falcon tubes and stored at room temperature, in the dark.

Table 2.1. Percent Composition and Concentrations of PFAAs Being Used in a 28-day, Aqueous Exposure of Rainbow Trout. The relative compositions of PFAAs within the mixture groups (MIXLOW, MIXMED and MIXHI) are based on the composition of PFAAs detected in Lake Ontario by De Silva et al., 2011 (1).

Treatment Group	PFNA (ng/L)	PFOS (ng/L)	PFOA (ng/L)	PFHpA (ng/L)	PFHxS (ng/L)	PFHxA (ng/L)	PFBS (ng/L)	PFBA (ng/L)	Σ PFAAs (ng/L)
Mixture composition	5%	35%	30%	10%	5%	5%	5%	5%	100%
MIXLOW	2.5	17.5	15	5	2.5	2.5	2.5	2.5	50
MIXMED	5	35	30	10	5	5	5	5	100
MIXHI	25	175	150	50	25	25	25	25	500
Control	--	--	--	--	--	--	--	--	--
PFOS	--	12,500	--	--	--	--	--	--	12,500
PFOA	--	--	10,300	--	--	--	--	--	10,300
PFBS	--	--	--	--	--	--	7,500	--	7,500
PFBA	--	--	--	--	--	--	--	5,300	5,300

2.3 Takedown and Dissection

Upon completion of the 23-day exposures, fish were anesthetized by immersion in 100 mg/L tricaine methane sulfonate and fish weight and fork length were measured. Blood was drawn from the caudal vein (22 and ½ gauge needle, 1” length) and collected in 4 ml heparinized vacutainers and stored on ice. All fish were euthanized via exsanguination and the spinal cord was severed with a knife prior to dissection. Within 1-2 minutes of sampling, blood samples were transferred to 1.5 ml microcentrifuge tubes and stored on ice for a maximum of 20 minutes prior to centrifugation. Samples were centrifuged at 10,000 rpm for 4 minutes under refrigeration (4 C°) and the plasma was subsequently transferred to 1.5 ml cryovials and flash frozen in liquid nitrogen. Plasma samples were then transferred to a -80 C° freezer for long term storage.

Liver and kidney samples were also collected by dissection. Liver masses were recorded for determination of hepatosomatic index and divided into two sections using a scalpel and stored separately for future analysis. In order to ensure consistency of protein and metabolite contents of liver cross sections amongst samples, cross sections were always made at the same anatomical division. Tissues were transferred to cryovials and flash frozen in liquid nitrogen for storage at – 80 C°.

2.4 Condition Factor and Hepatosomatic Index

Condition factor was measured based on the ratio of fork length to body weight and calculated according to a widely used mathematical formula: $K = (10^5 * W) / L^3$ (W = body mass in g, L = fork length in cm) (143). Hepatosomatic index was simply calculated as the ratio of liver mass to body mass and multiplied by 100.

2.5 Preparation of plasma samples for Proteomics

The method used has been described elsewhere (144) and will be summarized herein with some minor modifications. Plasma samples were thawed on ice (approximately 2 hrs) and 15 μ l was transferred into low retention microcentrifuge tubes containing 50 mM tris-HCL. Samples were then reduced using tris(2-chloroethyl) phosphate (TECP) followed by an alkylation step using iodoacetamide for prevention of reformation of disulfide bonds. Proteins were then digested using formic acid at a temperature of 115 C°. Following digestion, samples were evaporated to near dryness using a Thermo Scientific Savant SpeedVac and then resuspended in 20 μ l of 95% milli-q water and 5% acetonitrile and centrifuged for a final time (14,000 x g for 15 minutes). 20 μ l of supernatant was transferred to high performance liquid chromatography (HPLC) vials with 200- μ l polypropylene spring-bottom conical inserts for subsequent analysis using HPLC tandem mass spectrometry (HPLC-MS/MS).

2.6 Preparation of Kidney samples for Proteomics

Kidney samples were prepared in a similar manner to the plasma samples with some additional steps conducted prior to the previously described plasma proteomics workflow. Due to limitations in sample amount, a total of 10 kidney samples were prepared for each treatment by pooling 2 samples together out of a total of n=20. Samples were subsequently weighed for 50-100 mg of tissue depending on the amount available and then added to 2 ml microcentrifuge tubes (on ice) along with an ammonium bicarbonate buffer equaling a mass to volume ratio of 1:2. Samples were homogenized using a ball mill homogenizer at 20 Hz for 2 minutes and centrifuged for 15 minutes at 14000 x g. Following centrifugation, 50 μ l of supernatant was transferred to low

retention microcentrifuge tubes and the remaining sample preparation was conducted using the exact same method as for the plasma proteomics workflow.

2.7 Proteomics Instrumental Analysis

Samples analysis was done on an Agilent 1260 Infinity Binary pump high performance liquid chromatography (HPLC) with a Quadrupole tandem Time of Flight mass spectrometer as the detector. The method for untargeted proteomic analysis has been previously published (144). In brief, peptides are separated using an Agilent 1260 Infinity Binary HPLC, with a C18 column at a controlled temperature of 40 C°. Solvent A consisted of 5% acetonitrile, 0.1% formic acid, and Solvent B consisted of 95% acetonitrile, and 0.1% formic acid. In order to ensure quality control, a blank, a peptide standard and Bovine Serum Albumin (BSA) digest standard was injected every 10 runs.

2.8 Protein Identification and Relative Quantification

Mass spectral data files were collected using Mass Hunter Data acquisition. Spectrum Mill Software (Version A.03.03 SR4) was used to extract good quality spectra. Peptide identifications were carried out using Spectrum Mill and searching against the UniProt Rainbow Trout reference proteome (UP000193380, downloaded 2019) using a custom formic acid digest enzyme script (C- and N- terminus at cleavage sites DSLP). Peptide identifications were validated if they had a score higher than 6, minimum of one peptide match with a %SPI greater than 70%. Spectral intensity values were calculated in Spectrum Mill using the mean intensity of all peptides assigned to a

given protein. Skyline was subsequently used for MS1 filtering (145) to find missing values. The chromatographic area of the precursor ion intensity was used for relative quantification.

2.9 Analysis of Phosphorylated Metabolites

In collaboration with Dr. Vasile Furdui and Vlastamil Packa at the Ontario Ministry of the Environment and Parks, the analysis of phosphate and phosphorylated carbohydrates was conducted on the plasma. A total of 20 plasma samples per treatment were analyzed for a suite of analytes including phosphate, fructose-phosphate, galactose-phosphate, ribulose-phosphate and glucose-6-phosphate and were quantified using isotopically labeled standards.

A publication which describes the methods used for this procedure are described in detail elsewhere and will only be summarized herein (146). Sample preparation consisted of a 1:500 dilution of 10 μ l of plasma in HPLC grade water.

Instrumental analysis was performed on an ICS 5000⁺ ion chromatograph, HESI-II electrospray ionization source (ESI), coupled to a QExactive Mass Spectrometer (MS). The MS was operated in negative mode, full scan (m/z 50-700) at 70 000 resolution. Ion chromatograph eluent was always combined with 0.2 ml/min acetonitrile prior to entering the ESI.

Chromatographic separation was achieved using method A (mentioned in the publication) at a flow rate of 0.3 ml/min, 100 μ l injection volume, AG24 Dionex guard column and AS24 Dionex separation column. A 30-minute gradient was used beginning with 20 mM OH⁻ increased incrementally to 60 mM for 24 minutes of runtime and then decreased back to 20 mM OH⁻ for the final 5 minutes. Quantification of analytes was achieved by preparation of a set of calibration

standards comprised of each analyte at 0 nM, 10 nM, 100 nM and 1000 nM followed by spiking samples with a cocktail of isotopically labeled standards.

2.10 Analysis of PFAAs in Water and Plasma

In collaboration with Dr. Amila De Silva at Environment and Climate Change Canada (ECCC), water and plasma samples were shipped to Dr. De Silva's lab at ECCC Burlington to be analyzed for a suite of PFAAs using UHPLC (Ultra-high performance liquid chromatography) MS/MS (tandem mass spectrometry). Prior to shipping, water samples of the exposure water were taken at week 1 (50 ml), 2 (25 ml) and 3 (25 ml) and stored in polypropylene conical vials. Water samples taken at the respective timepoints were pooled evenly from each of the 4 tank replicates used for each treatment.

Due to the extremely low concentrations of PFAAs present in the 3 PFAA mixtures, a larger volume of water was required which involved the pooling of water taken at week 2 and week 3 for analysis of the mixtures. Thus, the water used for analysis of PFAA mixtures involved 50 ml from week 1 and another 50 ml which was pooled from week 2 and 3. In contrast, samples taken at week 1 and 3 were chosen for analysis of the single PFAA mixtures because sample volume was not limiting for analysis of PFAAs at these higher concentrations ($\mu\text{g/L}$ range). With respect to the plasma samples, a total of five samples were analyzed from each treatment which were pooled evenly from the 18-20 samples available for each respective treatment. A total of 30 μl of plasma was weighed and shipped for analysis.

A more detailed report on the methods and results of PFAA analysis is available in the supplementary materials but will be summarized herein. For individual PFAA exposure water, 0.5

ml of water was transferred to a pre-cleaned polypropylene conical tube and weighed (± 0.0001 g). 0.5 ml of methanol was added along with 30 μ l of methanolic isotopically labeled surrogate standards (20 ng/L). Samples were then analyzed using HPLC MS/MS monitoring for a full suite of C4-C15 PFCAs and C4-C12 PFSAAs. Chromatographic separation was achieved using a Waters Acuity UPLC chromatograph and a Waters BEH C18 column with a gradient of water and methanol solvents along with 2mM of ammonium acetate (full pump timetable available in supplementary). Method blanks consisted of 0.5 ml HPLC-grade water added to 0.5 ml methanol. Limit of detection was calculated based on a concentration of analyte which would yield an instrumental signal with a signal to noise ratio of 3. The method detection limit was a metric used to consider the limit of detection in combination with the % recovery found from extraction of each PFAA. Measurement of the PFAA mixture water was a little different due to the low concentration ranges used (2.5-175 ng/L for individuals in the mixture). Firstly, samples were concentrated using a weak anion exchange solid phase extraction where 10-25 ml of sample was concentrated to 1.0 ml. Analyte recovery of the extraction was accounted for by using 20 ml of HPLC-grade water spiked with a PFAA mixture which indicated good recovery at 93-95% for the PFAAs in the mixture. Extracts were analyzed using the same instrumental conditions as for the single compound PFAA exposure water. However, it was observed that a PFOS contamination issue occurred in the mixture water because of the low-level calibration standards having much higher levels of PFOS than expected. Additionally, there was a mixture of branched and linear isomers present in the contaminated samples which would not have been from the original PFOS used in the exposure water which was composed of only linear isomers.

Analysis of the fish plasma involved spiking of 30 μ l of plasma with 30 μ l of methanolic isotopically labeled surrogate standards (1.0 ng/ml final concentration for each surrogate).

Following spiking, PFAAs were extracted using two sequential additions of 5 ml of acetonitrile followed by centrifugal evaporation of the extracts to a final concentration of 1.0 ml. A clean up step was used by adding 50 mg of graphitized carbon and further centrifugation which resulted in sample concentration to 0.5 ml. 0.5 ml of SPE-polished HPLC-grade water was then added and then analyzed on the instrument using the same method as for the water. Preliminary analysis indicated PFOS concentrations exceeded the calibration range and therefore, extracts were diluted using 1:1 methanol/water by a factor of 100. Further, PFOA exceeded the calibration curve and therefore these extracts were diluted further by a factor of 10.

2.11 Statistical Analysis

Statistical analysis on the phosphorylated metabolites and the hepatosomatic index (HSI) were conducted using GraphPad Prism 9. All checks for normality were done using the Shapiro-Wilk test along with manual observation of histograms and QQ-plots. The assumption of equal variances was also assessed using Levene's test. Due to all of the phosphorylated metabolites and HSI failing assumptions of normality, a Kruskal-Wallis test followed by a Dunn's post hoc were employed at a p-value cutoff of <0.05.

Plasma protein levels were represented by peak intensity values of each respective protein. The proteomics data were analyzed using an R software package known as Normalyzer DE which is designed for normalization and statistical analysis of large proteomics datasets (147, 148). Proteomics data were normalized using a logarithm base 2 transformation along with a median normalization of samples. Following normalization, a One-way ANOVA with Tukey's HSD post

hoc test was conducted; the raw p-values were then corrected for a false discovery rate (Benjamini-Hochberg method) ($p\text{-adj} < 0.1$). Significant proteins were not filtered by fold change.

Biological pathway analysis was conducted using Gene Ontology Resource's gene overrepresentation analysis (biological process selection) which employs an FDR corrected Fisher's Exact Test comparing the number of gene's which would be expected to be in a dataset of a given size to the actual number.

Figures/graphs were generated using either Metaboanalyst 5.0, Graphpad Prism 9 or the Ggplot2 package available in R statistical programming language (version 4.1.2). Namely, figure 3.2 and 3.9 are heatmaps and figure 3.10 is a principal component analysis generated using Metaboanalyst 5.0. Figure 3.7 is a boxplot generated in Graphpad Prism 9. The remaining figures were all generated using the Ggplot2 package in R; the scripts used are available in supplementary.

Chapter 3. Results

3.1 Hepatosomatic Index

Hepatosomatic index was a higher-level endpoint chosen due to its relative sensitivity in response to PFOA and PFOS exposure in the literature. No significant differences ($p\text{-adj}<0.05$) were found in any of the treatment groups tested (Figure 3.1).

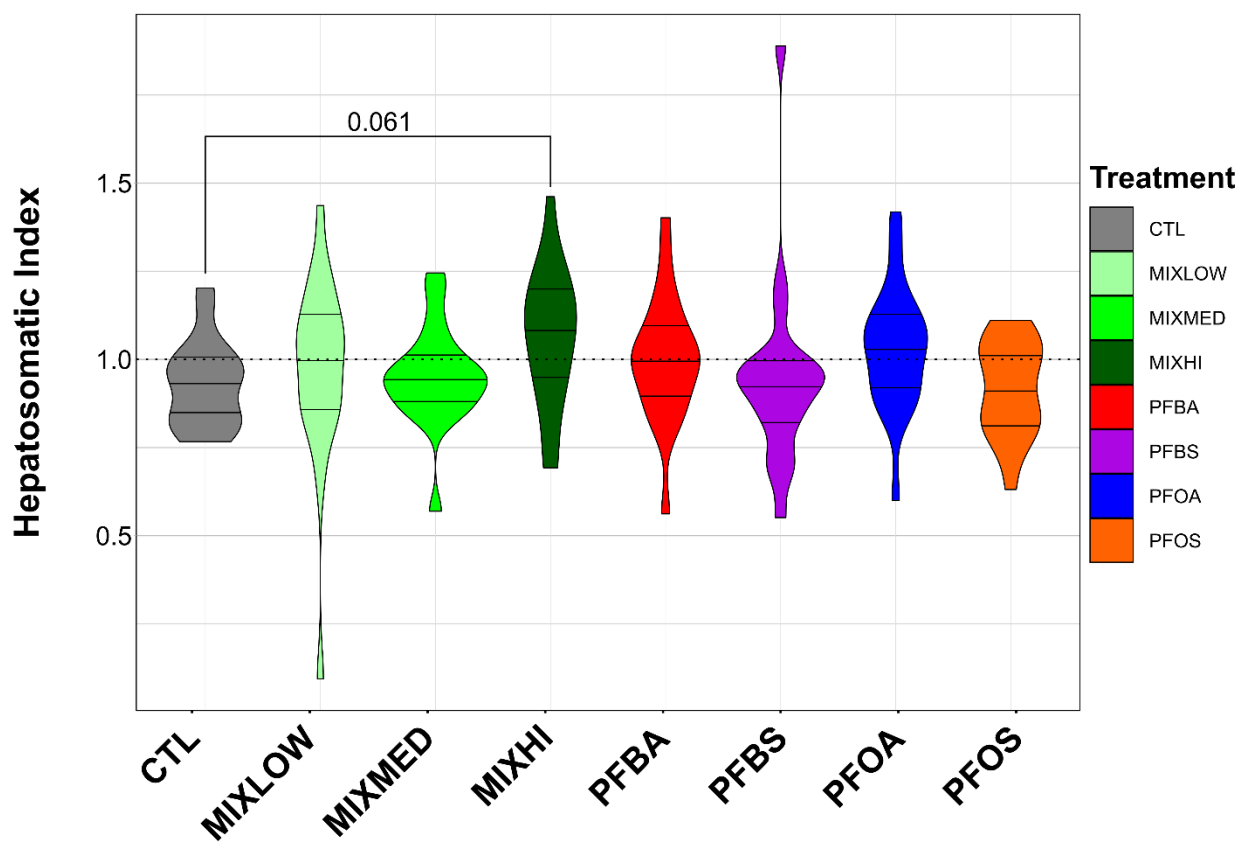


Figure 3.1. Violin Plot of the Hepatosomatic index of rainbow trout exposed to PFAAs and PFAA Mixtures. Hepatosomatic index was compared using a Kruskal-Wallis test followed by a Dunn's post-hoc.

3.2 Plasma Proteomics

Exposure to the PFAA mixtures caused the greatest number of plasma proteins to be significantly altered ($p\text{-adj}<0.1$) at 1956, 1509 and 254 for the low, medium and high mixture exposures respectively. The single PFAA exposure regimes generally caused significant changes to a lower number of proteins being 483, 78, 190 and 1579 for the PFBA, PFBS, PFOA and PFOS exposures respectively. A heatmap of the top 800 plasma proteins (ranked by ANOVA) across all treatments, reveals the low mixture, medium mixtures and PFOS groups to cluster most closely together, sharing similar proteomic profiles (Ward's method; figure 3.2). The PFBA, PFBS, PFOA and high mixture treatments clustered more closely with control and did not exhibit clear differences in proteomic profiles.

Comparing the number of significant proteins altered in the same direction ($p\text{-adj}<0.1$) among the low mixture, medium mixture and PFOS exposures indicated that they shared a large number in common where 468 proteins (33%) are increased in abundance and 299 proteins (22%) are decreased (Figure 3.3 a, b). Plasma from the low and medium mixtures shared an additional 236 proteins (17%) increased and 245 proteins (18%) decreased. However, the single PFAA exposure regimes exhibited a low proportion of proteins in common across all 4 groups with 99 proteins (11%) increased and 104 proteins (12%) decreased. Plasma from the PFOS exposure regime contained the highest number of significantly altered proteins exclusive to its set compared to the other single PFAA exposures at 70% (646 proteins) increased and 65% (543 proteins) decreased (Figure 3.3, c and d).

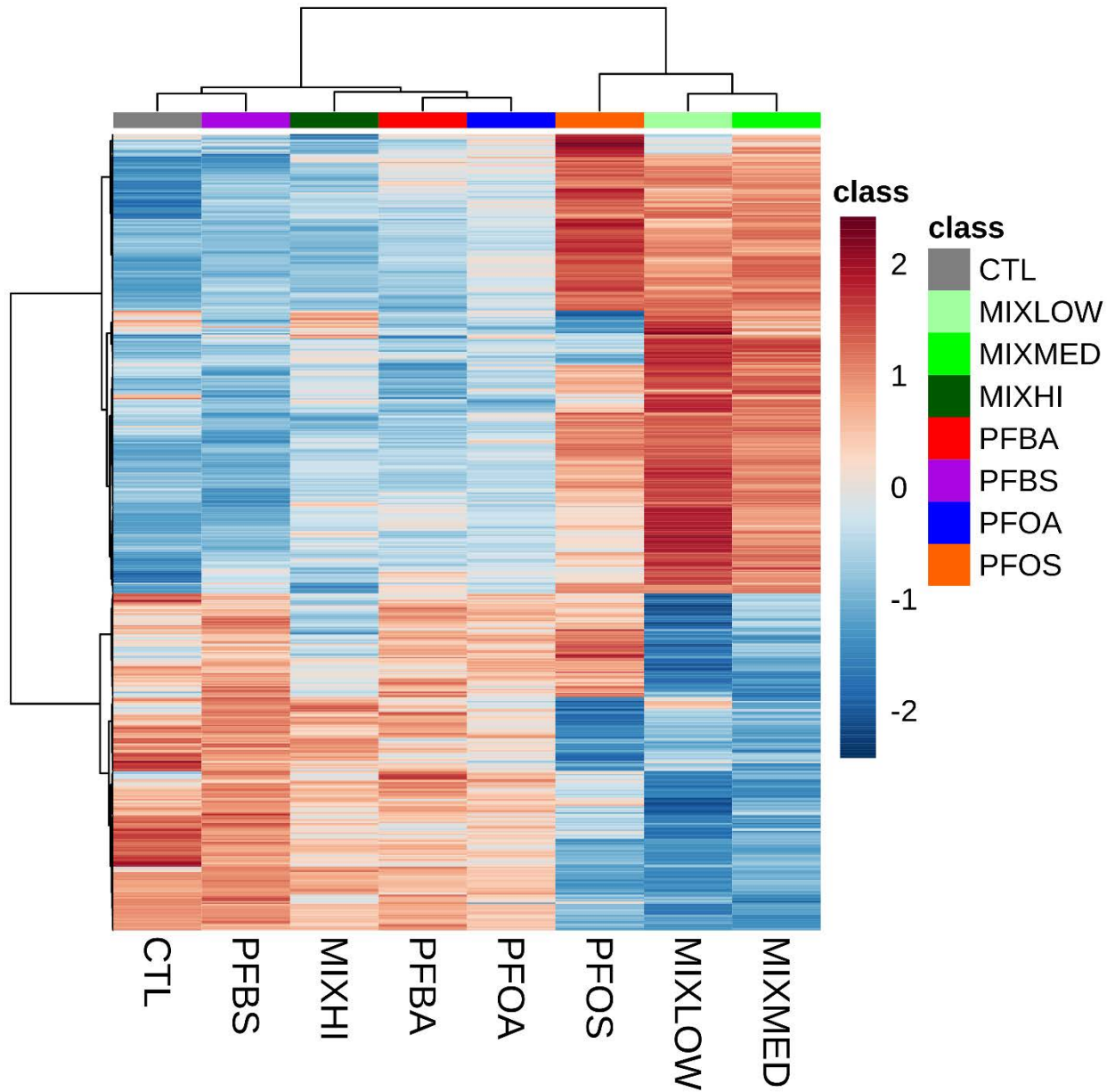


Figure 3.2. Overview of Untargeted Proteomics Results from the Blood Plasma of Rainbow Trout Chronically Exposed to PFAAs and PFAA Mixtures. The heatmap illustrates the top 800 proteins ranked by significance using a One-way ANOVA in addition to hierarchical clustering using Ward's method. Data is median normalized and log₂ transformed.

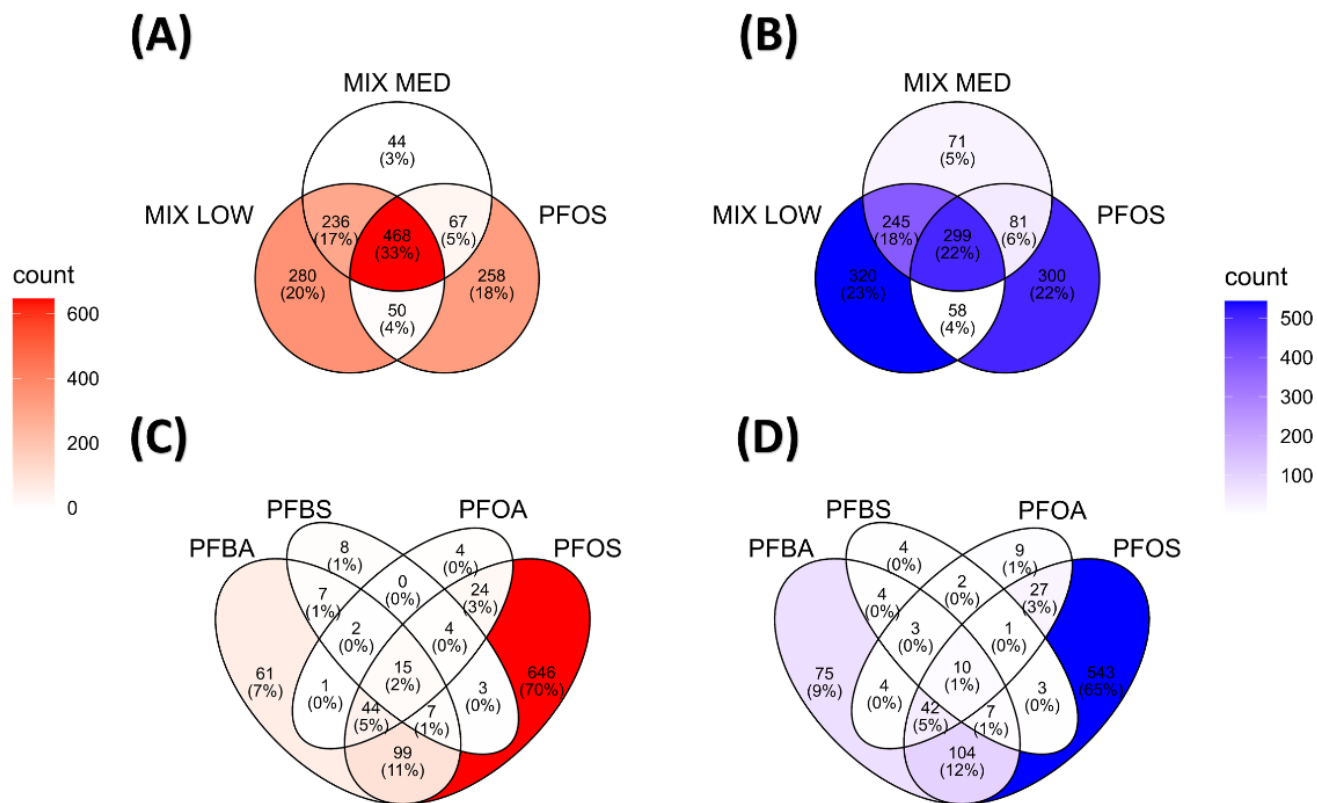


Figure 3.3. Venn Diagrams Illustrating the Commonality of Significant Plasma Proteins (p-adj<0.1) from Rainbow Trout Exposed to PFAAs and PFAA Mixtures. The top row (**A**, **B**) contains two charts comparing low and medium PFAA mixtures (MIXLOW and MIXMED) with PFOS; (**A**) includes only proteins with positive fold change (indicated by red) and (**B**) displays only those with negative fold change (blue). The bottom row (**C**, **D**) are representing the single compound exposure regimes also grouped by fold change.

Plasma from the high mixture exposure regime shared a relatively low number of significant proteins with the low and medium mixtures with 79 proteins (7%) increased and 93 proteins (8%) decreased whereas the low and medium mixtures shared an additional 625 proteins (54%) increased and 451 proteins (41%) decreased (Figure 3.4, a and b).

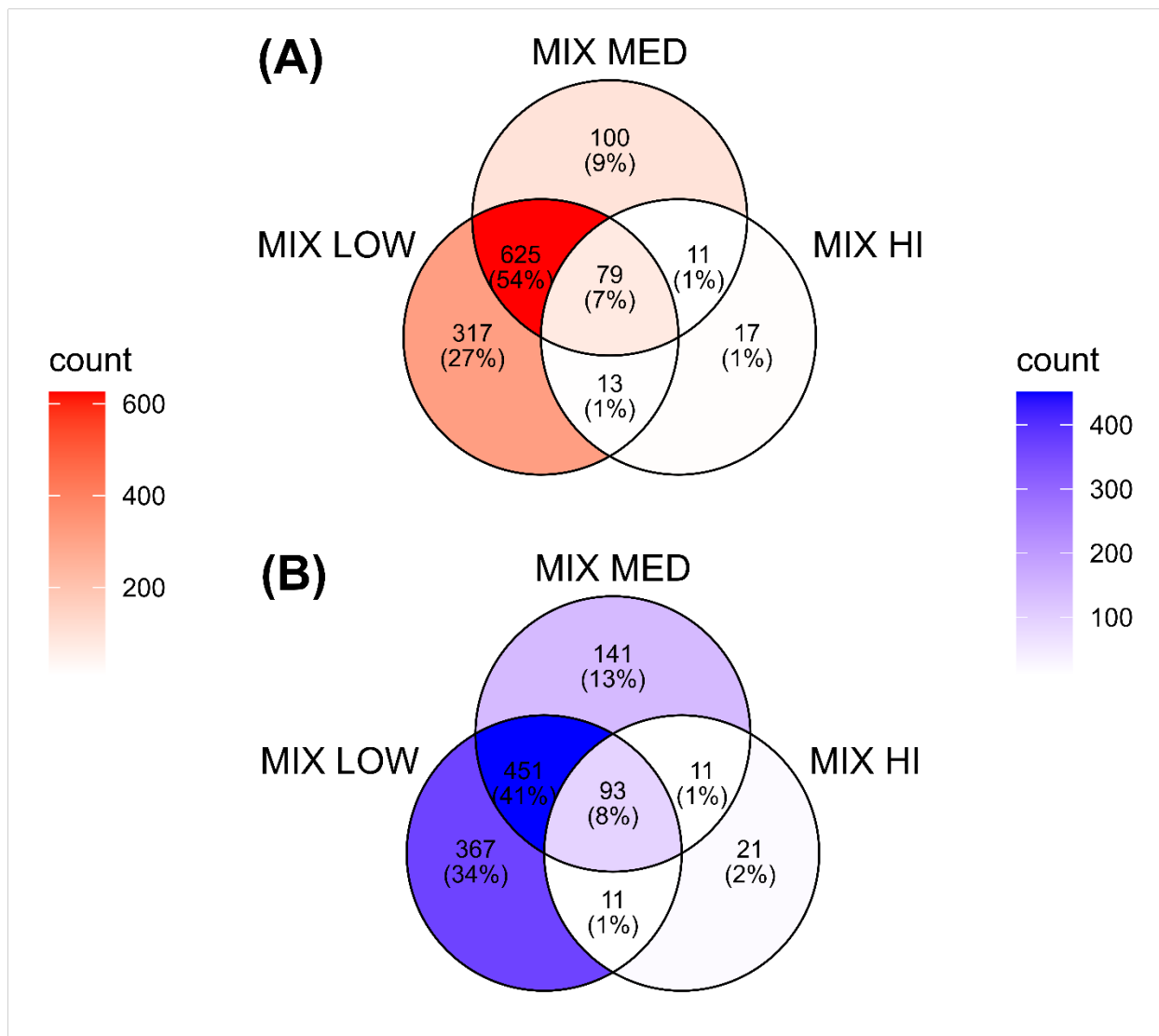


Figure 3.4. Venn Diagrams Illustrating the Commonality of Significant Plasma Proteins ($p\text{-adj} < 0.1$) from Rainbow Trout Exposed to 3 Different Concentrations of a PFAA mixture. The top row (**A**, **B**) contains two charts comparing low, medium and high PFAA mixtures (MIXLOW, MIXMED and MIXHI); (**A**) includes only proteins with positive fold change (indicated by red) and (**B**) displays only those with negative fold change (blue).

Gene Ontology Resource's Overrepresentation Analysis revealed many biological processes to be significantly altered ($p\text{-adj} < 0.05$) in the low mixture, medium mixture and PFOS exposures (291, 251 and 284 respectively) whereas a relatively low number of biological processes were found to be significantly altered for the high mixture, PFBA, PFBS and PFOA exposures (6, 65, 0 and 0)

(full results available in supplementary). With many of the significant biological processes being redundant or too general, a summary of the biological pathway results from the low mixture, medium mixture and PFOS exposure are the only results addressed herein (Figure 3.5). Generally, the 3 exposure regimes elicited changes in many of the same biological processes which were primarily associated with the nervous system, circulatory and muscle systems, metabolism and pathways related to DNA repair mechanisms, apoptosis and cellular proliferation included (Figure 3.5). One of the few distinctions in biological pathway results between the 2 mixture treatments and PFOS was the significant effect PFOS had on phosphatidyl 3-kinase signaling while the mixtures did not. Some other distinctions are that PFOS had a more significant effects on processes related to carbohydrate metabolism while the mixtures had a greater effect on glutamine family catabolism.

GO Biological Process

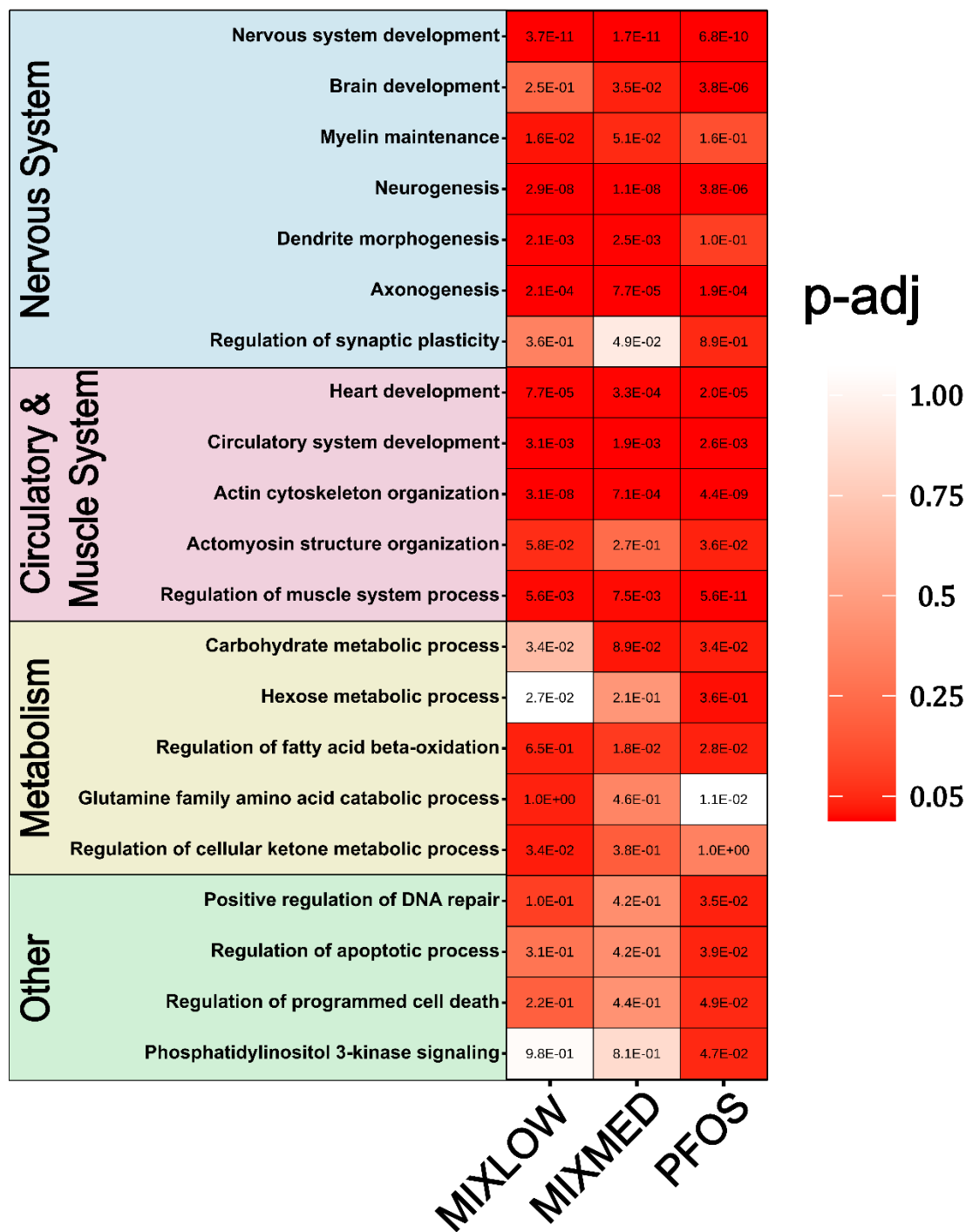


Figure 3.5. Biological Processes Found to be Significantly Overrepresented ($p\text{-adj} < 0.05$) in the Plasma of Rainbow Trout Exposed to PFAAs and PFAA Mixtures. Biological pathway analysis was conducted using Gene Ontology’s overrepresentation analysis test which conducts a Fisher’s exact test followed by a Benjamini-Hochberg correction for false discovery. The heatmaps have related biological pathways grouped by biological system and only contain

noteworthy biological processes and only treatments with noteworthy significant results; numbers in the center of each panel represent FDR adjusted p-values. All the biological pathway results are available in supplementary.

The low mixture, medium mixture and PFOS exposures caused significant increases ($p\text{-adj}<0.1$) in nuclear receptors known as peroxisome proliferator receptor delta and gamma (Ppard and Pparg) along with their heterodimerization partner, the retinoid-X-receptor b (Rxb; Figure 3.6). All 3 PFAA exposures caused changes in these receptors in addition to a number of markers of their activation including pyruvate dehydrogenase kinase 2 (Pdk2) and lipoprotein lipase (Lpl) while carnitine O-palmitoyl transferase (Cpt1a) is included in the heatmap due to its relevance but was not found to be significantly different in any of the treatments. Several markers of peroxisomal and mitochondrial fatty acid β -oxidation were found to be significantly altered including the significant increase in peroxisomal leader peptide-processing protease (Tysnd1), ATP binding cassette subfamily D member 1 and 2 (Abcd1 and Abcd2), trifunctional enzyme subunit alpha (Hadha) and StAR related lipid transfer domain containing 10 (Stard10) while a significant decrease was observed for the peroxisomal acyl-coenzyme A oxidase 3 (Acox3) and lon protease subunit 2 (Lonp2). Generally, all the proteins involved in fatty acid β -oxidation changed either dose dependently (MIXLOW<MIXMED<PFOS) or at a similar magnitude for the 3 exposure regimes except for Abcd1, Abcd2 and Hahda which appeared to be highest in the mixtures. It should also be noted that Tysnd1 and Stard10 exhibited the greatest magnitude of change relative to the others at a $-\log_2$ fold change of -2.3, -2.6 and -3.1 respectively for Tysnd1 and a $-\log_2$ fold change of -1.0, -1.5 and -1.48 respectively for Stard10. Several proteins involved in fatty acid synthesis were also significantly altered ($p\text{-adj}<0.1$) including increases in acetyl-CoA carboxylase 2 (Acacb) and acyl-CoA synthetase long chain family member 4 (Acsl4) and a decrease in fatty

acid desaturase 2 (Fads2). Finally, several proteins involved in cholesterol metabolism were also altered which included sterol regulatory element binding transcription factor 2 (Srebf2), lanosterol synthase (Lss), 7-dehydrocholesterol reductase (Dhcr7), 3-Hydroxyl-3-methylglutaryl-CoA reductase (Hmgcr) and cytochrome P450 family 51 subfamily A member 1 (Cyp51a1). Cholesterol metabolism exhibited the clearest differences in protein level changes between the mixtures and PFOS exposures. Namely, the mixtures appeared to cause greater changes in Srebf2, Hmgcr and Cyp51a1 compared to the PFOS treatment.

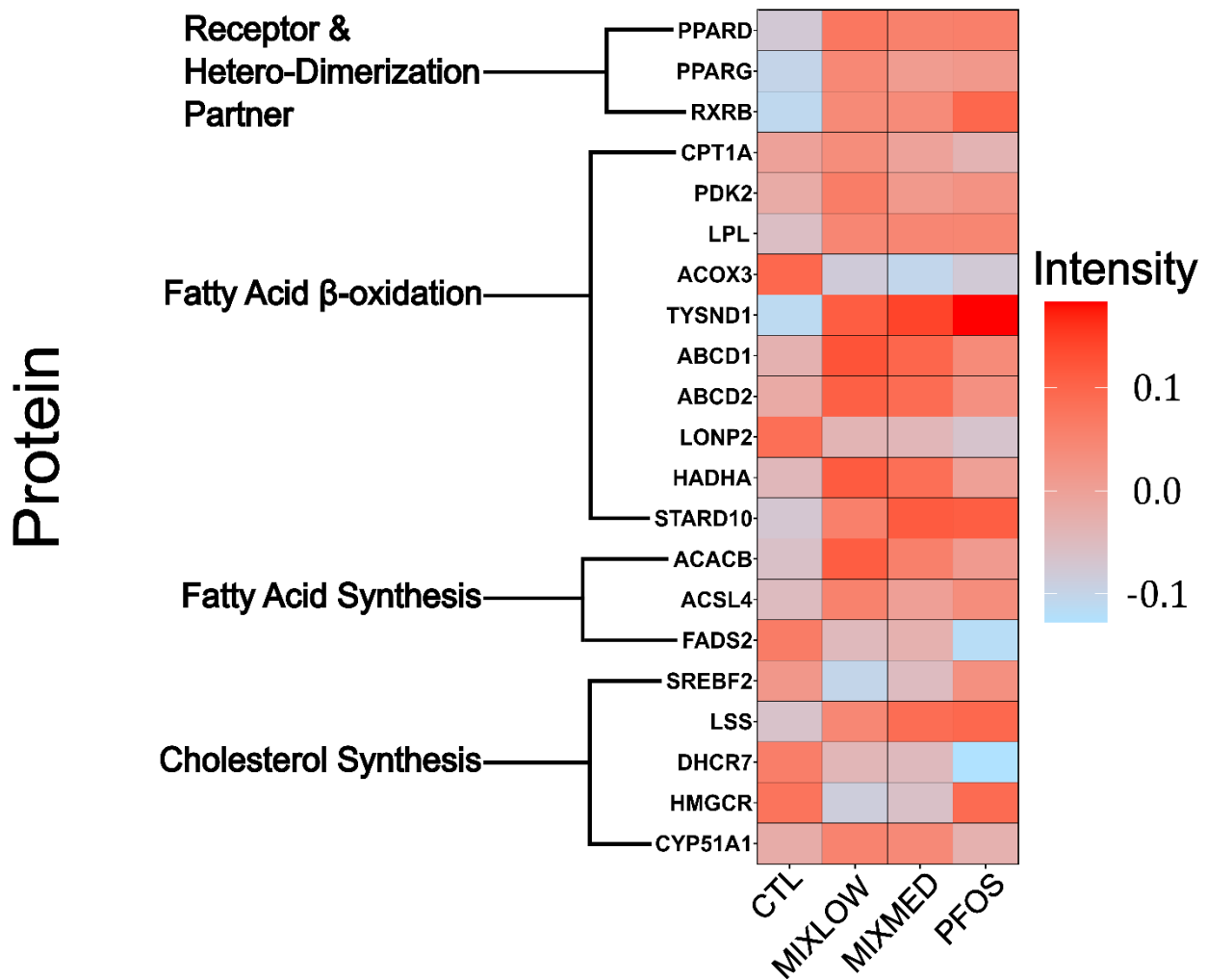


Figure 3.6. A heatmap illustrating significant proteins ($p\text{-adj} < 0.1$) from Rainbow Trout Plasma belonging to lipid metabolic processes. Protein levels are represented by the normalized average fold change of peak intensity.

3.3 Phosphorylated Metabolite Analysis

Phosphorylated metabolite analysis conducted on the plasma revealed the PFOS exposure regime caused a significant increase ($p\text{-adj}<0.05$) in glucose-6-phosphate levels along with a coordinate significant decrease ($p\text{-adj}<0.1$) in the plasma protein levels of glucose-6-phosphate dehydrogenase (G6pd) (Figure 3.7).

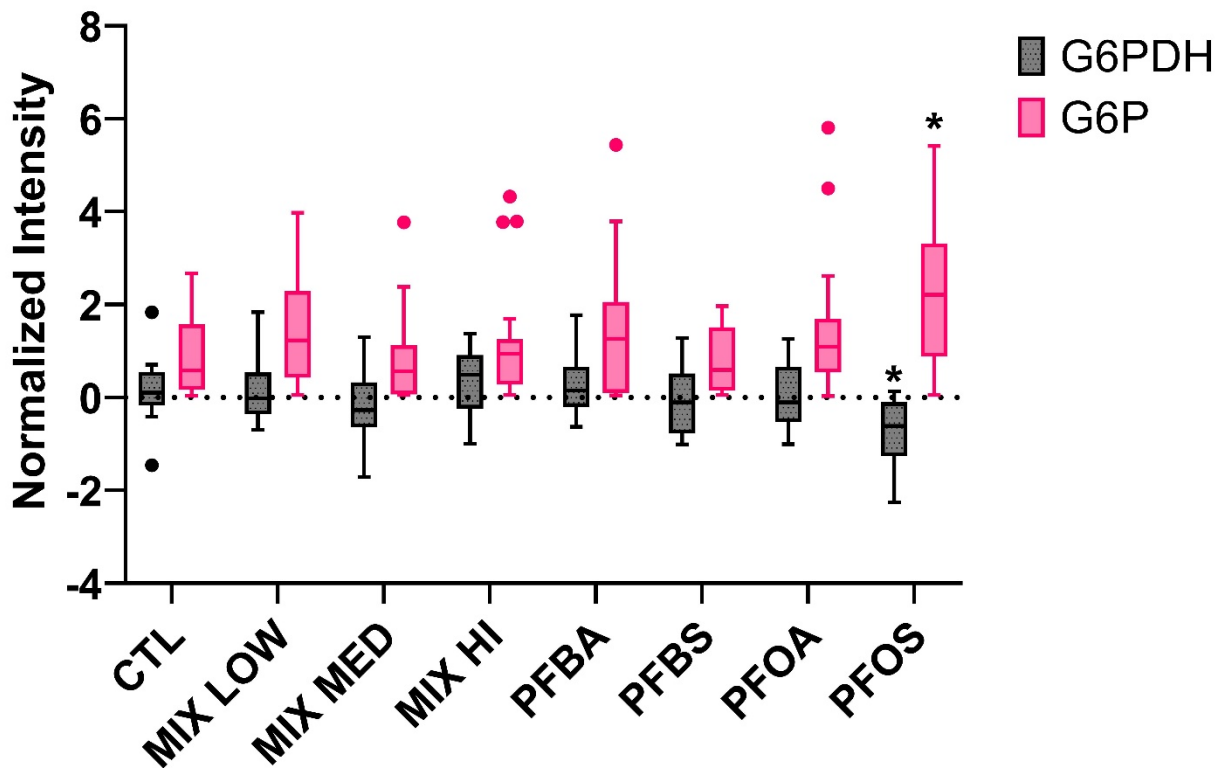


Figure 3.7. Box and Whisker of the Plasma Levels of Glucose-6-Phosphate Dehydrogenase (G6pd) and glucose-6-phosphate (G6P) in rainbow trout exposed to PFAAs and PFAA Mixtures. Boxplot divisions represent the interquartile range; error bars represent standard deviation and dots represent outliers. Asterisks indicate significance ($p\text{-adj}<0.05$).

Analysis of inorganic phosphate levels in the plasma found a significant decrease in the PFOA exposure regime (Figure 3.8).

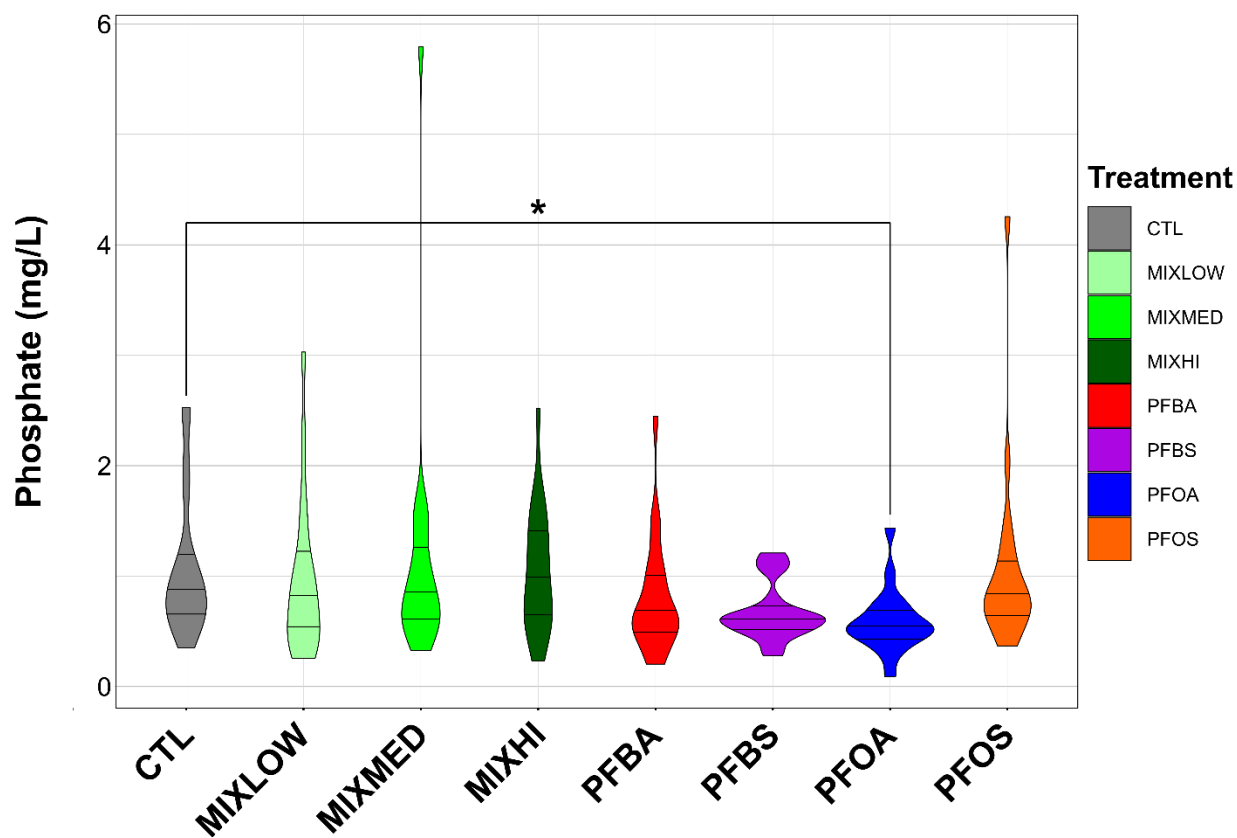


Figure 3.8. Violin Plot Illustrating the Plasma Concentrations of Inorganic Phosphate of Rainbow Trout Exposed to PFAAs and PFAA Mixtures. The midline represents the median and asterisks represent significance ($p\text{-adj} < 0.05$). Phosphate concentrations are log₂ transformed and median normalized.

3.4 Head Kidney Proteomics

Statistical analysis of protein levels in the head kidney tissue of rainbow trout revealed only the high mixture and PFOA exposure regimes to have significant effects ($p\text{-adj} < 0.1$) on

protein abundance (158 and 332 respectively). It is possible that PFOA as a PFAA has particularly high toxicity to the kidney of rainbow trout considering that the 2 treatments contain the highest levels of PFOA with the high mixture being 30% PFOA by composition.

Hierarchical clustering (Ward's method) of the top 400 kidney proteins ranked by significance (ANOVA raw-p-values) reveal high similarity between the proteomic profiles of the high mixture and PFOA treatments indicating the two likely caused similar biological effects on the head kidney of rainbow trout (Figure 3.9).

Principal component analysis conducted on all PFAA treatments visually illustrates that PFOA and the high mixture were the most distinct from controls, changing primarily along principal component 1 (Figure 3.10). Unexpectedly, PFOA appears to have much lower variation when compared to the other treatments, even the controls. Another unexpected result is the grouping of most data points from the other treatments into two separate areas on the distal ends of the ellipses. Cross referencing the sample numbers with the batch in which they were run on the mass spectrometer indicates that this is likely due to a batch effect. Such an effect is not ideal because it decreased statistical power from increased statistical variation. However, the results are still valid because samples were randomly assigned from each treatment into the 2 batches prior to being run on the instrument which allowed for an even distribution of the batch effect across all treatment groups. The batch effect was likely due to differences in instrument sensitivity between the two runtimes because the average total ion intensity counts were observed to be lower in the first batch than in the second; as such we compensated for this by adjusting protein total intensity counts by the average difference in total ion intensities between bovine serum albumin standards run across the 2 batches.

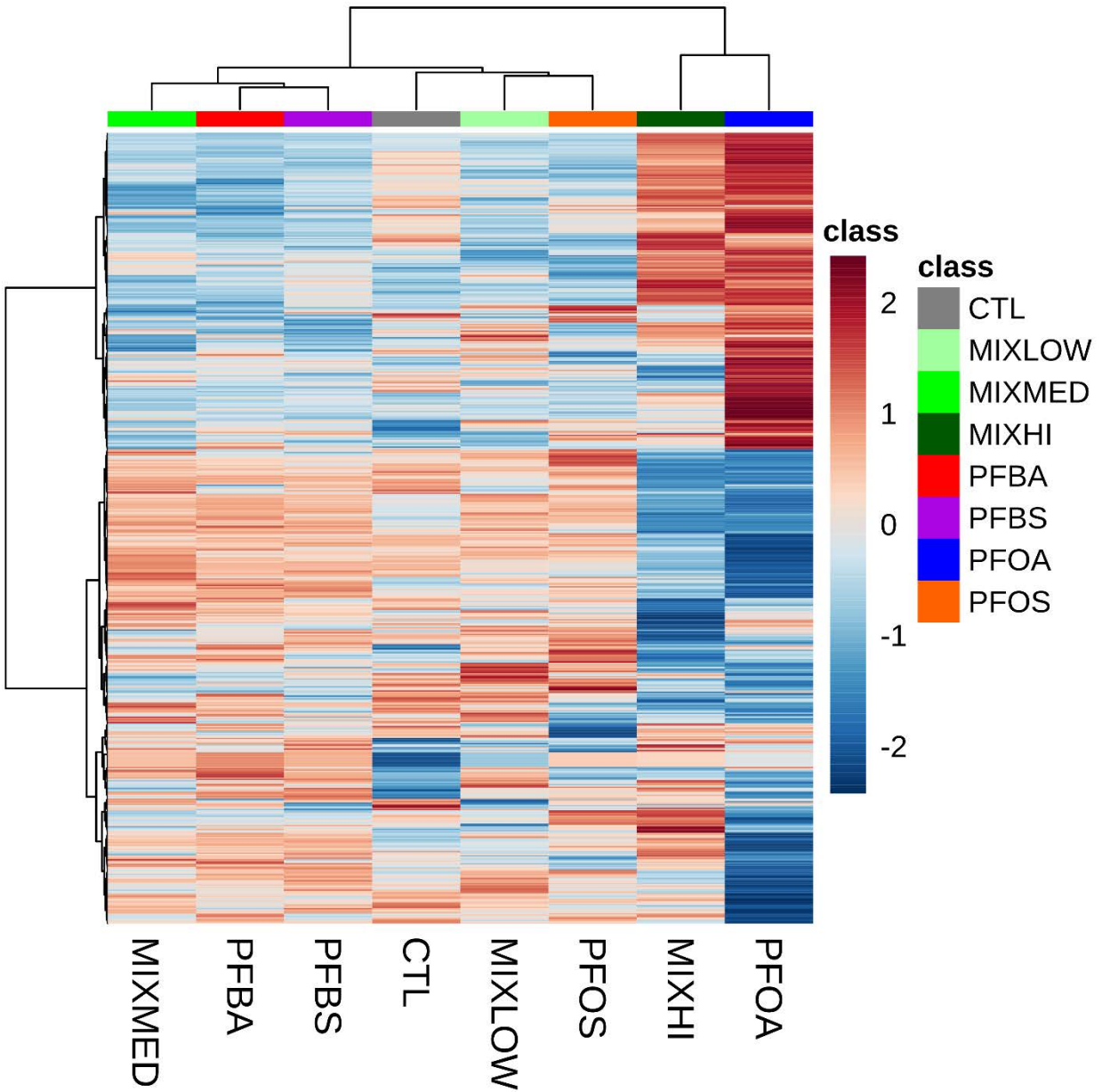


Figure 3.9. Overview of Untargeted Proteomics Results from the Head Kidney of Rainbow Trout Exposed to PFAAs and PFAA Mixtures. The heatmap illustrates the top 400 proteins ranked by significance using a One-way ANOVA in addition to hierarchical clustering using Ward's method. Data are median normalized and log2 transformed.

A comparison of the proteins found to be significantly altered ($p\text{-adj} < 0.1$), in the same direction between the high mixture and PFOA treatments found 32 (18%) proteins to be increased and 40 (21%) proteins decreased (Figure 3.11 a, b). There was also some overlap between plasma and

kidney proteomics results for the respective treatments with MIXHI sharing 32 (18%) significant proteins and PFOA sharing 10 (2%) (Figure 3.11, c and d).

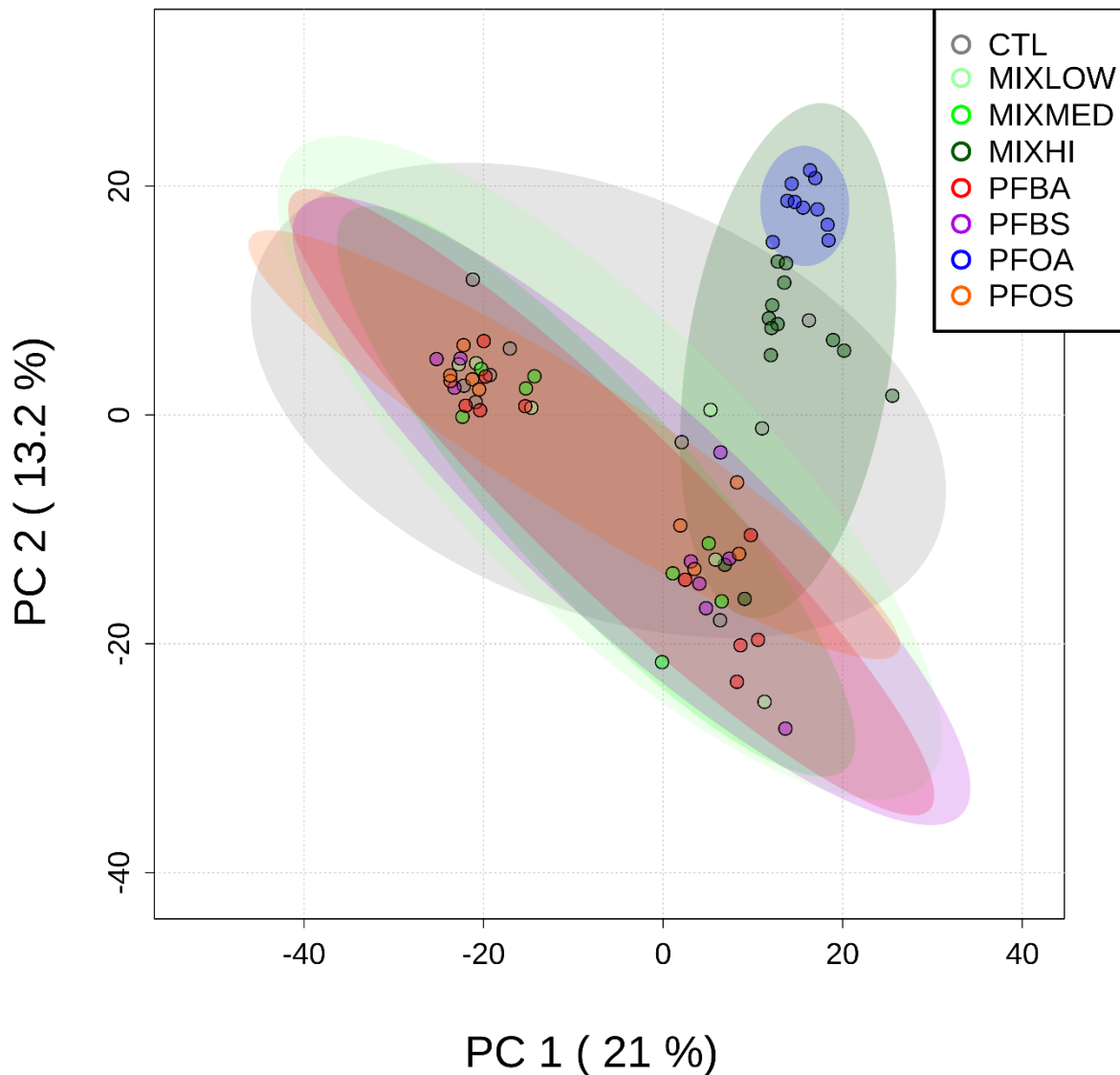


Figure 3.10. A Principal Component Analysis of Untargeted Proteomics Conducted on the Head Kidney of Rainbow Trout Exposed to PFAAs and PFAA Mixtures for 22 Days. The shaded ellipses represent 95% confidence intervals and are colored by treatment. Data is median normalized and log₂ transformed; axes titles indicate principle component number and proportion of raw data as a percentage.

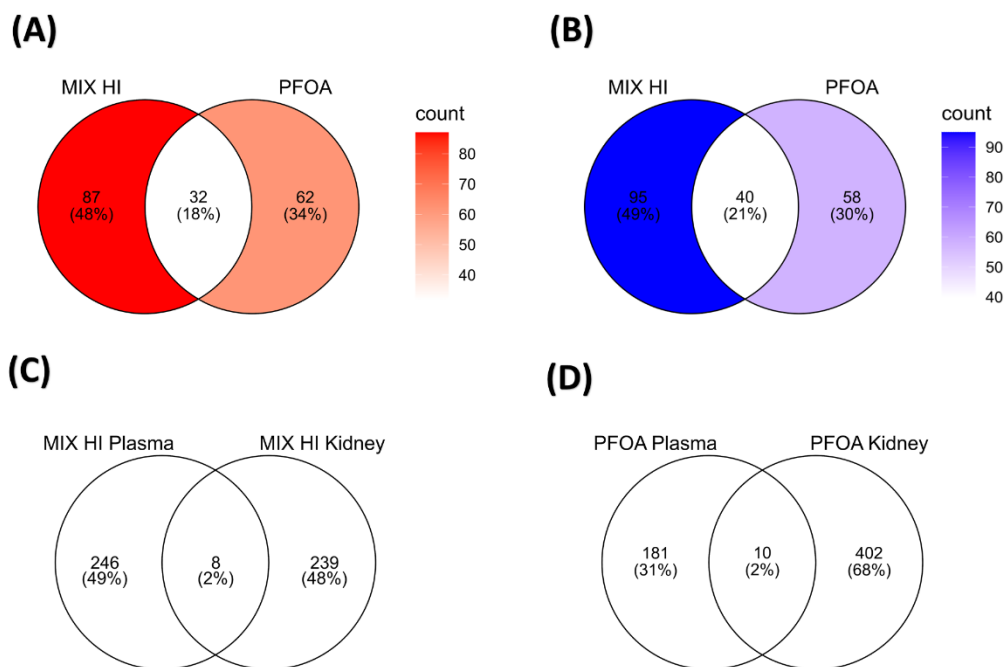


Figure 3.11. Venn Diagrams Illustrating the Commonality of Significant Kidney Proteins ($p\text{-adj}<0.1$) from Rainbow Trout Exposed to PFAAs and PFAA Mixtures. The top row (**A**, **B**) contains two charts comparing the high PFAA mixture (MIXHI) with PFOA; (**A**) includes only proteins with positive fold change (indicated by red) and (**B**) displays only those with negative fold change (blue). The bottom row contains two charts (**C**, **D**) displaying significant proteins in common between plasma and kidney tissues by exposure regime (MIXHI and PFOA respectively). Figures (**C**, **D**) have no color because they include proteins having both positive and negative fold change.

Biological pathway analysis of significant proteins ($p\text{-adj}<0.1$) from the head kidney for the high mixture and PFOA exposures found many significantly altered biological processes to be in common between the two treatments suggesting a similar biological effect. Biological processes were primarily related to lipid metabolism, reactive oxygen species metabolism and interferon-alpha signaling (Figure 3.12). More specifically, several processes related to lipid metabolism were significantly altered for the high mixture treatment while PFOA did not affect as many lipid

metabolic processes (only fat pad development) but did cause significant changes ($p\text{-adj}<0.05$) in the regulation of interferon alpha (Ifna) production.

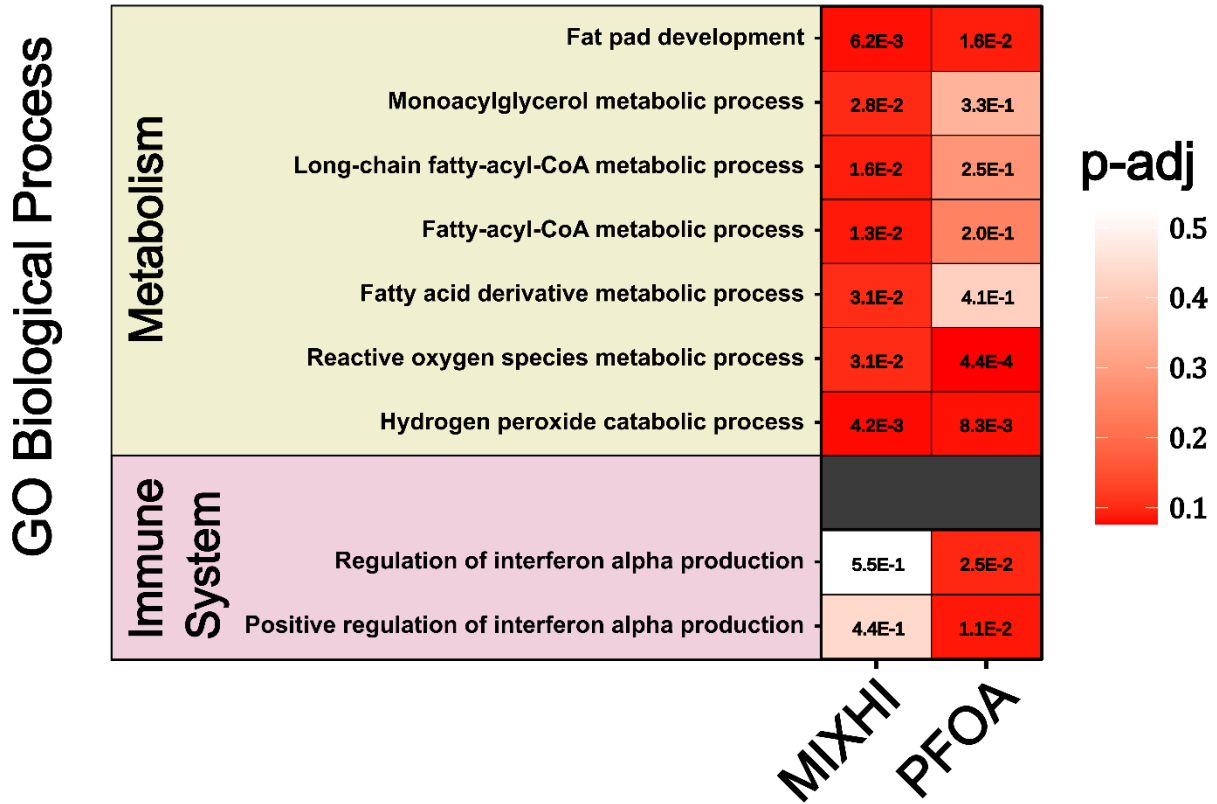


Figure 3.12. Biological Pathways Found to be Significantly Overrepresented ($p\text{-adj}<0.1$) from the Head Kidney of Rainbow Trout Exposed to MIXHI and PFOA Exposure Regimes. Biological pathway analysis was conducted using Gene Ontology's overrepresentation analysis test which conducts a Fisher's exact test followed by a Benjamini-Hochberg correction for false discovery. The heatmaps have related biological pathways grouped by biological system and only contain noteworthy pathways and only treatments with noteworthy significant results; numbers in the center of each panel represent FDR adjusted p-values. All the biological pathway results are available in supplementary.

A more specific examination of the proteins involved in lipid and ROS metabolism found both PFOA and the high mixture to significantly alter many of the same proteins (Figure 3.13). Those exclusively related to lipid metabolism included the significant ($p\text{-adj}<0.1$) increase in diacylglycerol O-acyltransferase 1 and 2 (Dgat1 and Dgat2), arrestin domain containing 3 (Arrdc3), abhydrolase domain containing 12, lysophospholipase (Abhd12), Bardet-Biedel syndrome 4 (Bbs4), phospholipase A2 group IVA (Pla2g4a), acetyl-CoA carboxylase alpha (Acaca), hydroxysteroid 17-beta dehydrogenase 4 (Hsd17b4) and significant decrease in acyl-CoA thioesterase 2 (Acot2), fatty acyl-CoA reductase 1 (Far1), AT-rich interaction domain 5B (Arid5b) and hydroxysteroid 17-beta dehydrogenase 12 (Hsd17b12). Finally, there were several proteins exclusively related to reactive oxygen species metabolism including glutaminase (Gls), catalase (Cat), NADPH oxidase 5 (Nox5), aldehyde dehydrogenase 3 family member A2 (Aldh3a2) and nicotinamide nucleotide transhydrogenase (Nnt). Generally, Cat, Nox5 and Nnt were seen to decrease for both the high mixture and PFOA exposures except for Gls which significantly increased for both exposures and Aldh3a2 which was significantly higher for the high mixture but significantly lower for the PFOA exposure regime.

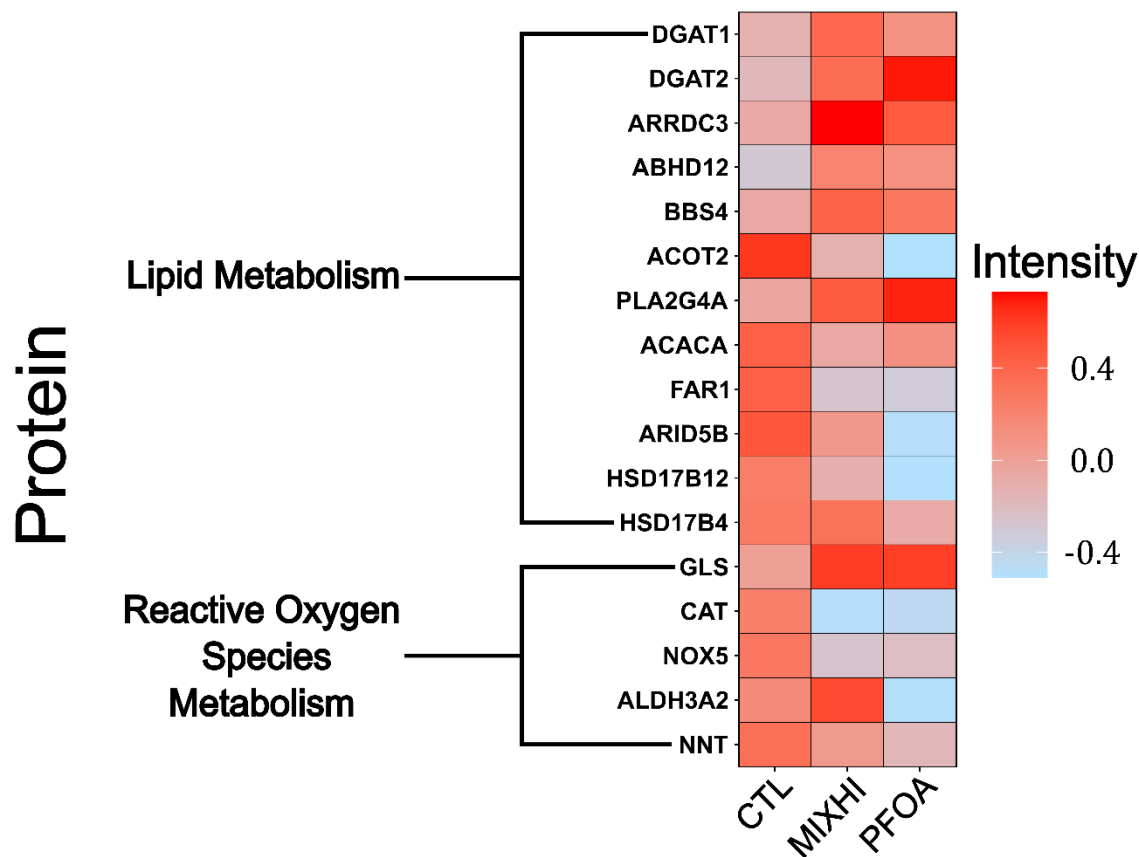


Figure 3.13. A heatmap Displaying Significant Proteins ($p\text{-adj} < 0.1$) from Rainbow Trout Head Kidney Involved in Lipid and Reactive Oxygen Species Metabolism. Protein levels are represented by average fold change of peak intensity.

3.5 Analysis of PFAA Water and Plasma Chemistry

An analysis of the water concentrations of PFAAs from exposure water taken at week 1 and a pooled sample from weeks 2 and 3 found water concentrations of the single compound exposure regimes to be 20-30% lower than nominal except for the PFOS treatment which was only 34% of nominal (Table 3.1). Some possibilities for this difference could be loss from adsorption to surfaces during stock solution preparation and potential error from pipettes and analytical scales.

Analysis of the PFAA concentrations in the plasma reveals only the long chain PFAAs to bioaccumulate compared to their short chain congeners. Bioconcentration factors (BCFs) were calculated for each PFAA being 0.3 kg/L, 0.09 kg/L and 18 kg/L for PFBA, PFBS and PFOA respectively while PFOS was found to be the most bioaccumulative with a BCF of 1.8E+03 and 2.3E+03 for total and linear PFOS respectively.

Table 3.1. Aqueous and Plasma Concentrations of PFAAs for the Single Exposure Groups. Bioconcentration factors (BCF) are calculated by dividing the plasma concentration by its respective aqueous concentration. Note, plasma concentrations were measured in ng/g.

	PFBA	PFBS	PFOA	Total PFOS	Linear PFOS
Week 1	4.2E+03	5.8E+03	7.9E+03	7.4E+03	4.6E+03
Week 2-3	4.4E+03	5.6E+03	7.5E+03	5.3E+03	3.4E+03
Percent of Nominal	81%	76%	75%	34%	32%
Mean Water (ng/L)	4.3E+03	5.7E+03	7.7E+03	6.3E+03	4.0E+03
Mean Plasma (ng/kg)	1.3E+03	5.1E+02	1.4E+05	1.1E+07	9.1E+06
BCF (kg/L)	3.0E-01	9.0E-02	1.8E+01	1.8E+03	2.3E+03

Instrumental analysis of the control water revealed unexpectedly high levels of PFAAs at a summative concentration of approximately 60 ng/L which inflated the concentrations of the mixture exposure regimes (Figure 3.14). Some of the burden of PFAAs in the control can be attributed to the contamination of water samples with additional PFOS during instrumental analysis, which makes the reporting of PFOS concentrations in these water samples inflated and only rough estimates (described in methods section 2.10).

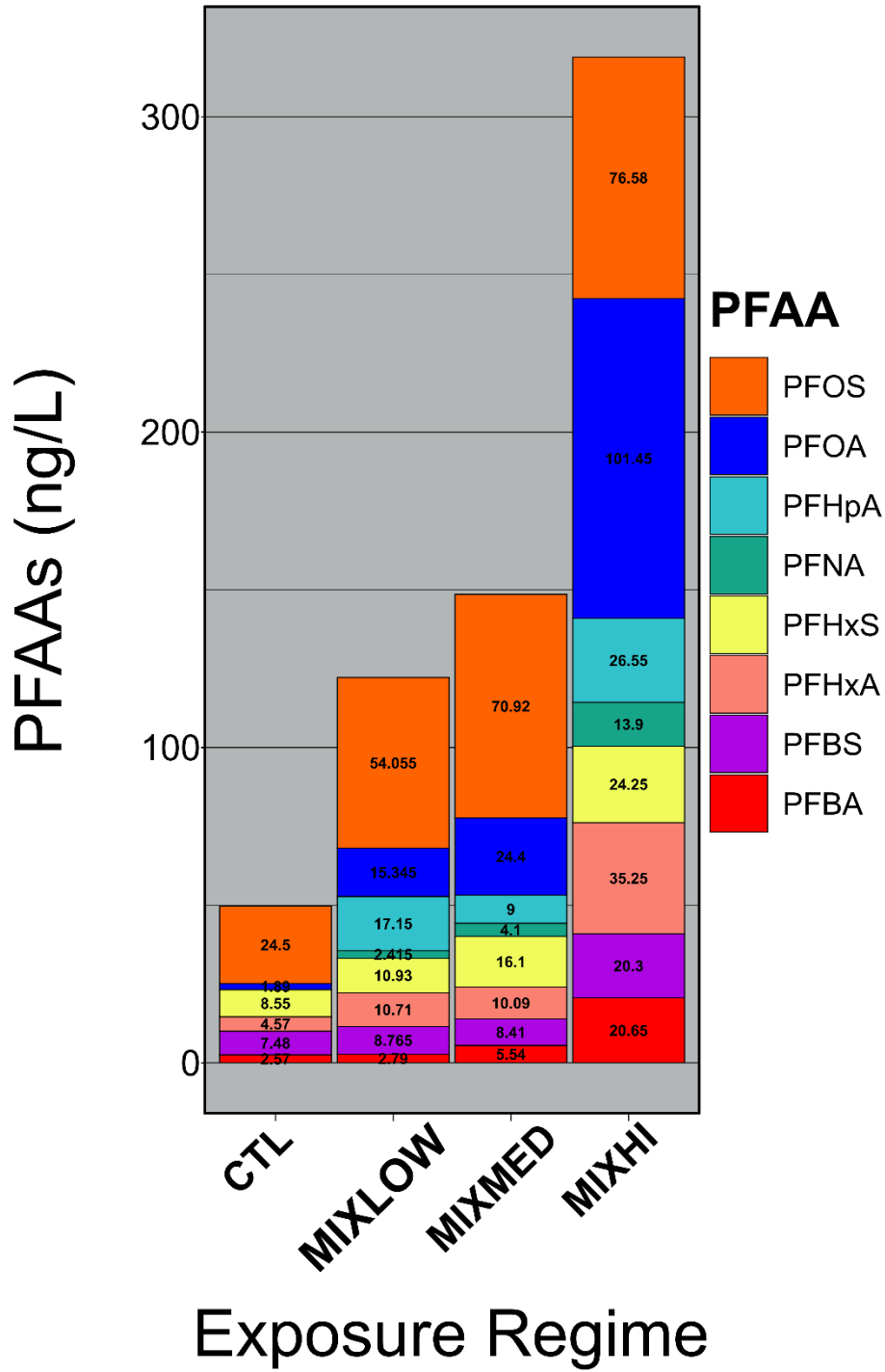


Figure 3.14. Aqueous Concentrations of PFAAs for the Mixture Exposure Regimes. Stacked bar charts represent the concentration of each PFAA comprising the mixture exposure water taken at the final timepoint (week2-3 pooled).

The low and medium mixtures were found to be relatively close to nominal (89% and 86% respectively) while the high mixture was approximately half (48%) of the desired concentration when accounting for the baseline levels of PFAAs in the water (as determined in control samples). Otherwise when not accounting for the baseline levels of PFAAs in the system water, the summative concentrations of the mixtures were 2-fold higher than nominal for the low, 1.3-fold higher for the medium and 2/3-fold lower for the high mixture exposure regimes. Individual compositions of the PFAAs for the mixtures are summarized in Table 3.2. and varied depending on the PFAA being 62-73% for PFBA, 94-190% for PFHxA, 57-287% for PFHpA, 60-92% for PFOA, 58-118% for PFNA, 24-110% for PFOS, 0-84% for PFHxS and 42-53% for PFBS. It should be noted that although these percent differences appear high, they often represent differences in >2 ng/L.

Table 3.2. PFAA Mixture Exposures Represented by Percent of Nominal Concentration. Percent of nominal was calculated by subtracting the actual concentration from control concentrations and then dividing by the nominal concentration.

	PFBA	PFHxA	PFHpA	PFOA	PFNA	PFOS	PFHxS	PFBS
MIXLOW	62%	190%	287%	92%	118%	35%	0%	53%
MIXMED	73%	94%	74%	72%	84%	110%	84%	42%
MIXHI	65%	94%	57%	60%	58%	24%	49%	51%

Bioconcentration factors were calculated for the CTL and 3 mixtures for several of the long chain PFAAs including PFOA, PFNA, total PFOS and PFHxS while the other short PFAAs (PFBA, PFHxA, PFHpA and PFBS) were not because they were not detected in the plasma (Table 3.3).

The BCF of PFOA appeared to decrease with increases in aqueous PFOA concentration being $1.6E+02$ for the control and $7.6 E+01 - 3.6 E+01$ for the low to high mixture exposures. The BCF of PFNA was similar to PFOA being $3.1E+02$ for the control and did not appear to change with concentration, being highest for the low mixture ($5.0E+02$) and lowest for the medium mixture ($1.8E+02$). PFOS was found to be the most bioaccumulative PFAA, having a BCF of $1.1E+02$ for control and a BCF which increased with concentration being $1.7E+03$ for the high mixture exposure. Finally, the BCF of PFHxS was similar in magnitude to that of PFOA at $4.9 E+01 - 7.1E+01$ for the low to high mixture exposures but did not appear to change with concentration.

Table 3.3. Aqueous and Plasma Concentrations of PFAAs for the Mixture Exposure Groups. Brackets represent percent composition. Bioconcentration factors (**BCF**) are calculated by dividing the plasma concentration by its respective aqueous concentration.

Control (CTL)								
	PFBA	PFHxA	PFHpA	PFOA	PFNA	Total PFOS	PFHxS	PFBS
Week 1	2.2	4.9	1.9	3.2	0.7	53	9.1	2.4
Week 2-3	2.6	4.6	<LOD	1.9	0.3	25	8.6	7.5
Mean Water (ng/L)	2.4	4.7	1.9	2.5	0.4	39	8.8	4.9
Mean Plasma (ng/kg)				4.1E+02	1.3E+02	4.3E+03		
BCF (kg/L)				1.6E+02	3.1E+02	1.1E+02		
Low Mixture (MIXLOW)								
Week 1	5.1	8.2	15	17	4.3	35	6.6	3.8
Week 2-3	2.8	11	17	15	2.4	54	11	8.8
Mean Water (ng/L)	4.0	9.5E	16	16	3.4	45	8.7	6.3
Mean Plasma (ng/kg)				1.2E+03	1.7E+03	4.3E+04	4.3E+02	

BCF (kg/L)				7.6E+01	5.0E+02	9.6E+02	4.9E+01	
Medium Mixture (MIXMED)								
Week 1	6.6	8.7E	9.6	24	5.1	84	10	5.6
Week 2-3	5.5	10	9.0	24	4.1	71	16	8.4
Mean Water (ng/L)	6.1	9.4	9.3	24	4.6	77	13	7.0
Mean Plasma (ng/kg)				9.9E+02	8.5E+02	2.9E+04	9.3E+01	
BCF (kg/L)				4.1E+01	1.8E+02	3.7E+02	7.1E+00	
High Mixture (MIXHI)								
Week 1	16	21	35	83	16	84	18	15
Week 2-3	21	35	27	100	14	77	24	20
Mean Water (ng/L)	19	28	31	92	15	80	21	18
Mean Plasma (ng/kg)				3.4E+03	4.0E+03	1.4E+05	1.5E+03	
BCF (kg/L)				3.6E+01	2.7E+02	1.7E+03	7.1E+01	

Chapter 4. Discussion

The current study modeled the composition of linear PFAA species quantified in Lake Ontario after the year 2009 to study the effects of an environmentally relevant PFAA mixture on freshwater model organism *Oncorhynchus mykiss* (rainbow trout) using untargeted proteomics and Phospho-metabolomics (61). An additional set of single compound exposures were conducted at higher concentrations (25 nM PFBA, 25 nM PFBS, 25 nM PFOA or 25 nM PFOS) to gain insights on differences in biological response to PFAA congeners with different chain length and functional group. It was found that the PFAA mixtures and PFOS exposure caused the greatest change in the plasma proteome while PFOA and highest PFAA mixture caused the greatest change in the head kidney proteome. Single component exposures of rainbow trout to PFBA, PFBS and PFOA caused much lower changes to the plasma proteome while being at 125-50-fold higher concentrations than the PFAA mixtures (Table 2.1). A comparison between the mixtures and single component exposures found PFOS shared similar plasma proteomic profiles to the low and medium PFAA mixtures which suggest a similar toxicological response (Figure 3.2). Biological pathway analysis revealed the 3 treatments affected many of the same biological processes, primarily: nervous system development, lipid metabolism, DNA repair mechanisms, and muscle and cardiac system related processes (Figure 3.5). Biological pathway analysis of the head kidney proteome found that proteins related to lipid metabolism and reactive oxygen species metabolism were significantly overrepresented from rainbow trout exposed to the highest mixture and PFOA treatments (Figure 3.12). Overall, the results of the present study emphasize the need for more investigation into the risks posed by PFAA mixtures considering environmental relevance and their complex toxicokinetics and toxicodynamics.

4.1 PFAA Mixtures

The mixture exposures were 125-50-fold lower in total concentration than the single component exposures, thus it was unexpected that there were more significantly altered (p -adj<0.1) plasma proteins in the low and medium mixtures compared to the single component exposures (except for PFOS) and the high mixture exposure regime. The PFAA mixtures also exhibited an atypical concentration response where there was a decrease in the number of significantly altered proteins in the plasma from the low to high mixture exposures. Atypical dose responses are more likely in mixture exposure regimes where an increase in the number of chemical components increases the potential for interaction effects across the dose response curve (149). There are many toxicological studies investigating PFAA dose responses which have reported atypical, or biphasic responses to single compound and mixture exposure regimes (150-154). Cheng et al., reported an inverse U-shaped curve to describe vitellogenin 3 transcripts in response to zebrafish exposed to PFOS (0.1 – 100 $\mu\text{g/L}$) (154). Hu et al., 2014 consistently observed a stimulatory effect of PFAA exposures on the viability of human liver cells at low concentrations and an inhibitory one at higher concentrations (150). Additionally, longer chain lengths, or those with sulfonated functional groups were more potent (150). Binary, tertiary, and poly- PFAA mixtures caused complex toxico-dynamics with polyphasic dose response curves and strong synergism occurring in select mixtures at select concentration ranges; particularly those with higher proportions of sulfonated PFAAs (150). Rodriguez-Jorquera et al., 2019 exposed fathead minnow for 48 h to PFOS and found much higher numbers of transcripts to be altered in the blood and liver from the low PFOS treatment (0.5 $\mu\text{g/L}$; 137 and 1421) exposure relative to the high (25 $\mu\text{g/L}$; 99 and 557) (154). Additionally, a PFAS mixture exposure was found to elicit similar changes in the number of mRNA transcripts compared to the high PFOS exposure at 84

and 471 for the blood and liver respectively while being at a 25-fold lower concentration which is analogous to our own results when comparing proteomic responses between PFOS and the PFAA mixture exposures (155). Within our study, plasma proteomic responses for the PFAA mixtures suggest the components within the mixture are acting synergistically at low doses (i.e. low and medium mixtures) because the effect is greater than single compound exposures when comparing summative concentrations. However, as the mixture concentration increased from the low treatment, the synergism was abated.

The molecular mechanisms behind toxicological interactions (i.e. synergism) of mixtures include induction or suppression of xenobiotic metabolizing enzymes, toxin removal mechanisms, and changes in blood-brain-barrier (BBB) permeability (156). The most plausible mechanism for marginal decreases in toxicity at higher concentrations of PFAAs is increased elimination considering they cannot be catabolized and are known to exhibit increased elimination from fish at higher aqueous concentrations (157, 158). Based upon the measured water and plasma concentrations, we calculated the bioconcentration factor (BCF) of each PFAA for each exposure regime by dividing the concentration in rainbow trout plasma with that of the exposure water (Table 3.3). The plasma BCF for total PFOS is seen to increase from the low to high mixture exposure ($9.6E+02$ kg/L - $1.7E+03$ kg/L) whereas the BCF of PFOA and PFNA decreased (PFOA BCFs: $7.6E+02$ kg/L - $3.6E+01$ kg/L and PFNA BCFs: $5.0E+02$ - $2.7E+02$) which suggests these two-long chain PFCAs do exhibit increased elimination while PFOS exhibits the opposite trend. The bioconcentration factors calculated within our study are similar to those reported by Martin et al., 2003 exposing rainbow trout to waterborne PFAAs using flow through dosing of individual PFAAs (159). Martin et al., reported the short chain congeners to not be bioaccumulative <C8 PFCAs and <6 PFSAs while those for PFOA, PFNA, PFHxS and, PFOS exhibited BCFs of 27,

6.0E+02 and 4.3E+03 respectively (159). PFOA however, appeared to have a higher BCF in the mixtures being 76-36 for the low-high mixtures but not for the single component PFOA exposure being 18 which suggests PFOA which suggests elimination for PFOA occurs dose dependently. Thus, it is possible that the difference in toxicokinetics for the low PFOA exposure explains some of the synergism occurring in the low and medium mixture exposure regimes. It should also be noted that discrepancies between the BCFs reported by Martin et al., 2003 and our own study can be partially attributed to the differences in PFAA accumulation between whole blood and plasma. Additionally, under natural conditions the various PFAAs would have likely bioaccumulated to higher levels in the plasma, because BAFs are consistently higher than BCFs which is well reviewed by Burkhard, 2021 wherein whole body BAFs were 9.5, 6.3, 8.7, 1.8, 1.7 and, 3.5 fold higher than whole body BCFs of PFBA, PFBS, PFOA, PFNA, PFHxS and, PFOS respectively (158, 159). The trends in BCFs across the low-high mixture exposures are primarily considered to be due to renal elimination mediated by changes in levels of OATs and OATPs (55, 158, 160). Within our study, we observed significant changes to the plasma levels of several OAT proteins: Slc22a23, Slc22a18, Slc22a13 and 1 OATP protein: Slco5a; which may explain the differences in BCFs. It is however uncertain how these would affect elimination considering they can just as easily increase rates of renal resorption of PFAAs and were only detected in the plasma (161, 162). Thus, these uncertainties suggest that renal elimination could be a source of complexity within our study.

Another potential mechanism by which the mixtures exert synergism is via potentiation of receptor activity. A potentiation effect in toxicology is described as when the presence of a chemical with a non-specific effect increases the toxicity of another (156). In this case, it is possible that some PFAAs within the mixture are potentiating the toxicity of others. The argument for this would be

that the low and medium mixture exposures share similar proteomic profiles and have significantly overrepresented biological pathways as the PFOS treatment but at much lower concentrations (Figure 3.4 and 3.7). An *in vitro* study investigating the activation of Atlantic Cod Ppars (Ppara1, Ppara2, Pparb and Pparg) by PFAAs and their mixtures provided good evidence for the ability of some PFAAs to act as potentiators in the activation of these receptors. Namely, it was found that co-incubation of a PFAA with a model agonist and some binary PFAA mixtures (i.e. PFOA and PFOS) caused synergistic activation of Ppara1 and Pparb (163). The strongest potentiation effect observed was a sevenfold increase in the activity of Pparb from a co-incubation of PFDA with PPARD model agonist GW501516. Molecular dynamics simulations offered a strong argument for the mechanism behind this synergism by modeling the interaction of Ppara1 co-incubated with PFOA and PFOS. It was found that PFOS favored an alternative binding site to the endogenous ligand binding pocket which acted to further stabilize the ligand binding pocket via a conformational change occurring in an omega loop proximal to the allosteric site. The results suggest that although many PFAAs are relatively weak PPAR activators, they may be able to increase the activation of PPARs via this allosteric mechanism. Additionally, the aforementioned omega loop is known to be substantially longer in orthologous Ppar isoforms from many teleost fish species which suggests teleosts could be more sensitive to Ppar-mediated toxicity of PFAAs when compared to mammals (164-167). Within the current study, only Pparg and Ppard were significantly increased within the plasma which contradicts much of the literature, where only PPARA is reported to be activated by PFAAs. However, there is evidence to support the activation of alternative PPAR isoforms following PFOS exposures in several species including: syrian hamster, japanese medaka, fathead minnow, atlantic cod and atlantic salmon (155, 163, 168-170).

4.2 Individual PFAAs

In the present study, PFOS was 10-100-fold more bioaccumulative than PFOA while the 4 carbon PFAA congeners PFBA and PFBS did not bioaccumulate (Table 3.1). PFOA accumulated in the plasma to $1.4E+05$ ng/kg and had a BCF of $1.8E+01$ kg/L, while total PFOS accumulated approximately 100-fold higher levels with a plasma concentration of $9.1E+06$ ng/L and a BCF of $2.3E+03$ kg/L. This would explain the large differences in significantly altered plasma proteins in PFOA compared to PFOS. The 4-carbon congeners (PFBA and PFBS) were expected to cause much weaker biological effects when compared to their 8-carbon counterparts (PFOA and PFOS) largely due to their low bioaccumulative potential and reported effect concentrations being orders of magnitude higher than any long chain PFAA (61, 101, 159, 171). Our results generally support this, as PFBS caused the lowest change in the plasma proteome and no significant changes to any biological pathways. PFBS had the lowest accumulation in plasma at 0.51 ng/g and with a BCF below 1 kg/L while PFBA had a plasma concentration of 1.29 ng/L which was more than double its 4-carbon sulfonate congener PFBS, but also had a BCF below 1. BCFs do not explain why PFBA caused a stronger response than its 8-carbon congener PFOA, with 484 compared to 191 significantly altered plasma proteins, respectively. Additionally, PFBA was the only short chain congener to significantly increase Pparg, which has potential to lead to a number of changes in systemic lipid and carbohydrate metabolism. It was previously observed that the PFCAs have higher potential to activate PPARs in several studies. The mechanisms of PFBA induced toxicity are still understudied while much more is known about the effects of long chain PFAAs like PFOA and PFOS. PFBA does have either a difference in biological effect, dose response, or both when compared to PFOA. Although, it is known that PFBA causes similar effects as PFOA on thyroid hormone levels, hepatotoxicity, and lipid metabolism albeit at higher doses (172, 173), there is

evidence to suggest they also have dissimilar effects. One study evaluating developmental neurotoxicity of PFBA and PFOA (4, 40 and 400 µg/L) on zebrafish embryos found PFBA to significantly alter a greater number of genes than PFOA but were associated with different biological processes (174). PFBA was found to significantly alter the expression of the farnesoid-X-receptor (*fxr*) and liver-X-receptor (*lxr*) in a dose dependent manner which was not seen in the present study (174). Thus, it would be beneficial for future ‘Omics based studies to compare molecular changes in response to PFBA and PFOA across several concentrations.

4.3 PPARs and Lipid Metabolism

The effects of PFAAs on lipid metabolism are among the most well-established endpoints for PFAA toxicity, which is largely attributed to PFAA-induced activation of PPARA (175-178). Within the current study it was found that several PFAA treatments caused significant increases in levels of Ppard and Pparg but not Ppara (Figure 3.6). The PFAA mixtures and long chain PFAA treatments significantly increased Ppard levels while Pparg was increased in the PFBA, low mixture, medium mixture and PFOS treatments only. Activation of the two receptors is unexpected because PPARD is generally considered to not be activated by PFAAs in the literature while PPARG is known to only be weakly activated by some PFAAs (175-178). However, as discussed previously, it is likely that teleost Ppars are activated in a different way, considering the substantial differences in the omega-loop region of Ppars in teleost fish compared to mammalian PPARs (163).

In addition to elevated Ppard and pparg, proteins that are known to be markers of PPAR activation were also significantly increased, including the PPAR heterodimerization partner Rxrb along with

Lpl and Pdk2 (Figure 3.6). Proteins involved in peroxisomal fatty acid β -oxidation were significantly altered including a large, dose-dependent increase in Tysnd1 which is a protease responsible for removal of the N-terminal peroxisomal targeting signal. Abcd1 and Abcd2 are proteins specifically located in the peroxisomes which are involved in peroxisomal import of fatty acids and fatty acyl-CoAs into the peroxisomal matrix. Several additional proteins involved in more general fatty acid β -oxidation as well as cholesterol synthesis provide strong indication that PPAR signaling is active in rainbow trout via PFAA induced dual activation of Ppard and Pparg.

4.4 Oxidative Stress

An analysis of phosphorylated metabolites in the plasma found a significant increase in plasma glucose-6-phosphate (G6P) as well as a significant decrease in glucose-6-phosphate dehydrogenase (G6pd) which is an enzyme responsible for the catabolism of G6P into D-ribulose-5-phosphate and production of NADPH which is the rate limiting step in the pentose phosphate pathway (Figure 3.7). The pentose phosphate pathway is highly conserved and primarily involved in the biosynthesis of nucleotides, fatty acids and aromatic amino acids (179). Especially considering these observations are within the plasma, a relevant use of the pentose phosphate pathway is within erythrocytes which utilize the NADPH produced in the reduction of glutathione to combat oxidative stress. Glutathione is an important peptide involved in the breakdown of radicals like hydrogen peroxide via glutathione peroxidase (180). Thus, the PFOS induced PPAR signaling paired with a reduction in the capacity of erythrocytes to clear reactive oxygen species could explain some of the apoptotic and DNA damage pathways which are also being observed in the plasma proteome (Figure 3.5). Additionally, glutathione peroxidase subunit 4 (Gpx4),

glutathione S-transferase (Gstp1), glutathione synthase (Gss), and oxidative resistance 1 (Oxr1) were significantly increased in the PFOS exposure while all except Gstp1 were significantly increased in the low mixture and medium mixture exposures. Oxidative stress is a common outcome of PFAA toxicity and is likely attributed to multiple mechanisms including (1) PPAR activation and (2) mitochondrial uncoupling (181). Aptly named peroxisome proliferators, many drugs and xenobiotics which activate PPARs have been established to produce oxidative stress via the increased expression of acyl CoA oxidase enzymes. The acyl CoA oxidases (ACOX) are a family of peroxidases which catalyze the rate limiting step of peroxisomal fatty acid β -oxidation, directly produces hydrogen peroxide via the donation of electrons to molecular oxygen (182). Generally, the increased reactive oxygen species (ROS) production is managed by a concomitant increase in catalase production but there are some cases, particularly in rodents where PPAR activation leads to excessive oxidative stress and eventual tissue damage (12, 182). The second mechanism is via uncoupling of the mitochondria via induction of the mitochondrial permeability transition pore which leads to mitochondrial dysfunction and excessive ROS production (183). The results suggest that PFOS and the PFAA mixtures are causing excessive production of reactive oxygen species, resulting in proteins associated with DNA damage and apoptosis. Many markers of DNA repair and apoptosis observed to be significantly altered in the plasma including significant increases to RAD52 homologue, DNA repair protein (Rad52) which is a key protein involved in DNA double strand break repair (184). Unlike mammalian erythrocytes, fish erythrocytes are nucleated and are known to undergo apoptosis from exposure to genotoxic xenobiotics (185). Such an effect could be further investigated by performing the micronucleus assay or comet assay on fish erythrocytes (186). Rodriguez-Jorquera et al., 2019 conducted a 48h exposure of fathead minnow to PFOS and found transcripts related to DNA repair mechanisms

upregulated in the liver and erythrocytes but the pentose-phosphate pathway was only significantly altered in the liver tissue (155).

4.5 Nervous System

Another biological process among the proteins that was overrepresented in all treatment groups was nervous system development (Figure 3.5). PFAA mediated activation of PPARs can also affect proteins related to nervous system function. PPARs play many important roles in the nervous system including the regulation of energy metabolism, inflammation and oxidative stress (137). Neurons and the nervous system in general are particularly sensitive to metabolic and mitochondrial disorders due to their high metabolic demand (187). Metabolic and mitochondrial dysfunction is implicated in the etiology of many neurodegenerative diseases including hypoxic-ischemic brain injury, Alzheimer's, cerebral palsy, and amyotrophic lateral sclerosis (187, 188). PPARs generally have a neuroprotective effect on the CNS via mechanisms of insulin sensitization, mitochondrial function, and reduction in neuroinflammation (189). However, PPARs can also cause increased inflammation in mesenchymal stromal cells treated with a PPARD agonist (190). Neuronal outgrowths, myelination, and neuron differentiation require either PPARG or PPARD activation in order to occur (188, 191, 192). Previous work has demonstrated that PFOS can cause differentiation of neural stem cells (NSCs) in a PPARG dependent manner at environmentally relevant concentrations of 25 nM and 50 nM, similar to the concentration ranges used in the present study (193). Specifically, in the aforementioned study, PFOS decreased NSC proliferation and spontaneous calcium activity, neurite outgrowths and induced differentiation of NSCs into neuronal, and oligodendrocyte cell types. The effects were abated following a co-

incubation of PFOS with a PPARG antagonist (193). Although less understood, PPARD is another highly relevant target for PFAA induced neurotoxicity being relatively abundant in the vertebrate central nervous system from embryogenesis to adulthood (106, 191, 194, 195). PPARD induces differentiation of NCSs into oligodendrocytes and promotes myelination of the central nervous system (CNS) (196, 197). Thus, a pleiotropic effect from dual activation of Ppard and Pparg via PFOS and PFAA mixture exposures could be affecting the many neurological pathways observed in the present study (i.e. differentiation, neurite outgrowths and myelination).

Within the current study, ATP-binding cassette transporter A1 (Abca1) and fatty acid binding protein 6 (Fabp6) are increased with both proteins being involved in lipid transport across the BBB. Activation of PPARD can also cause increased uptake of PFAAs into the CNS via increased expression of lipid transporters at the blood-brain-barrier (BBB) (198). The CNS is a very lipid rich organ and PPARD and PPARG are key regulators of lipid transport across the BBB via expression of many relevant lipid transporters on the surface of endotheliocytes such as the ATP-binding cassette transporters (ABCs) and fatty acid binding proteins (FABPs) (198, 199). In fact, PFOS tends to be at highest concentrations in brain regions with the highest lipid content (200, 201). Although, the mechanism by which PFAAs cross the BBB is not established, it is clear that PFAAs readily cross the BBB, consistently being detected in the CNS of humans and wildlife (201). A number of mechanisms by which PFAAs cross the BBB have been proposed, including passive transport via OATs and OATPs, as well as active transport via ABC proteins and receptor mediated endocytosis of fatty acid binding proteins (201). Fatty acid binding proteins are already established to bind PFAAs and supply the CNS with lipid substrates via active transport across the BBB (198, 202). Thus, the increased expression of both Abca1 and Fabp6 could be enhancing PFAA transport across the BBB.

Another mechanism proposed for PFAA induced neurotoxicity is via effects on calcium homeostasis in neurons. PFOA and PFOS are known to increase calcium ion levels in neurons both *in vivo* and *in vitro* which has been well reviewed by Starnes et al., 2022 (122, 124, 203-206). Liu et al., 2010 found exposure of PFOS to rats significantly increased markers of calcium homeostasis perturbation including calmodulin kinase II alpha (CAMK2A) and cAMP-response element binding protein (CREB) in the CNS, which agrees with our own findings in the plasma with significant changes to Creb and Camk2 and Camk4 subunits (207, 208). In the present study, the low mixture treatment caused increases in cAMP responsive element binding protein 1 (Creb1) while all 3 treatments caused significant decreases in cAMP-response element binding protein-like 1 and 2 (Crebl1 and Crebl3) along with the low and medium mixtures causing significant decreases to Camk2a, Camk2b, Camk4 but an increase in Camk2g while PFOS increased Camk4 and decreased Camk4 only. Thus, the associated changes in Creb proteins, Camk2 and Camk4 subunits suggest neuronal calcium homeostasis is perturbed from PFOS and PFAA mixture exposure.

Additionally, PFOA and PFOS have been found to cause neuronal apoptosis from intracellular calcium overload (122, 124, 204) and intracellular storage release from effects on the 1,4,5 triphosphate receptors (IP3R) and ryanodine receptors (RYR) (122). Liao et al., also demonstrated the L-type calcium channels (CACN) to be necessary for PFOS induced neuronal calcium influx and synaptogenesis (205). We observed significant changes in many L-type calcium channels including Cacnb2, Cacna1e, Cacna1i, Cacna1d and Cacna2d4 which were generally observed to decrease while ryanodine receptor 2 (Ryr2) increased in the plasma from all 3 exposure groups. Thus, the observed changes in plasma levels of these calcium ion transporters, particularly the L-

type calcium channels further support the dysregulation of calcium homeostasis from PFOS and PFAA mixture exposure.

Within the current study, several tight junction proteins (Tjps) were found to be significantly increased in the plasma including Tjp1, Tjp2 and Tjp3, Cingulin (Cgn), cingulin like 1 (Cgnl1), coxsackievirus and adenovirus receptor (Cxadr) along with several other proteins known to comprise adherens junctions of cerebral endotheliocytes including Laminins (Lama1, Lama2, Lama3 and Lama5) and Plectin (Plec). The BBB is comprised of a continuous network of endothelial cells joined via tight and adherens junctions which serve to dynamically regulate entry into the CNS (209, 210). It is well established that PFOS disrupts the BBB as part of its neurotoxic mechanism which is well reviewed by Cao and Ng, 2021 (201). Several studies have demonstrated that PFOS disrupts tight junction integrity, reduces expression of TJPs and increases the permeability of the blood-testis-barrier and BBB in mice (211-213). One study exposing adult rats to a dose as low as PFOS 0.25 mg/kg/day caused BBB integrity changes (211) while the 2.5 mg/kg/day caused increases in proinflammatory cytokines in the cerebral cortex along with markers of tissue damage and astrocytic activation. The adverse effects on the BBB were further confirmed via transmission electron microscopy, revealing cerebral endothelial lesions, damaged tight junctions, enlarged mitochondria and swelling of myelin sheaths (211). Thus, disruption of BBB integrity could be another mode by which PFAAs affected proteins associated with nervous system related biological processes.

As was found in pathway analysis (Figure 3.5), Phosphoinositide 3-kinase (PI3K) signaling could be involved in PFOS induced BBB disruption. Induction of PI3K/AKT signaling may be related to PPARD activation as they are known to exhibit positive crosstalk, occurring several times in vascular smooth muscle cells following treatment with PPARD agonists (214-217). In the present

study, PFOS significantly altered the PI3K signaling pathway along with Protein kinase B kinases 1, 2 and 3 (Akt1, Akt2 and Akt3) within the plasma proteome. PI3k/AKT signaling in endotheliocytes is well established to increase the permeability of endothelial cells by promoting angiogenesis which involves endotheliocyte migration and reorganization of the inter and extra cellular matrices (218). An in vitro study examining the effect of PFOS on the tight junctions in human brain endothelial cells found PFOS to disrupt the BBB in a PI3K dependent manner through the use of inhibitors and a PI3K null mutant cell line (211). While the number of proteins in our study involved in PI3K/AKT signaling, DNA damage, and apoptosis were only significant in the PFOS exposure regimes, the PFAA mixtures still share many of the same protein markers occurring at environmentally realistic concentrations and compositions. Thus, the plasma results from the PFAA mixtures are most relevant because they demonstrate that neurotoxic effects of PFOS are occurring or are beginning to occur at 50 and 100 ng/L. Future work conducting brain proteomics on exposed fish could support the plasma markers of neurotoxicity observed in our study. Several techniques also exist which could be used to confirm any BBB disruption in the CNS such as the use of scanning electron microscopy on the cerebral endothelium or monitoring for methylene blue or labeled dextrans in the CNS following their intravenous injection.

4.6 PFAAs and Muscular Related Processes

In our study, the PFAA mixtures and PFOS were found to significantly alter pathways involved in heart and muscle system related processes (Figure 3.5). There are multiple epidemiology studies that associate cardiovascular diseases with PFAA levels in the blood (i.e. atherosclerosis and stroke (219)). The mechanisms by which PFAAs may exert their effects on the

muscle, heart and cardiovascular system include: metabolic changes, oxidative stress, and perturbation of calcium homeostasis (219). Just like in neurons, the changes observed in levels of plasma L-type calcium channels (Cacns) and ryanodine receptors (Ryrs) could be related to perturbed excitation contraction coupling in muscle tissue. (220, 221). L-type calcium channels have been found to be modulated by PFOS and PFOA (much lesser extent) in guinea pig ventricular myocytes, exhibiting an inhibitory effect on action potentials (222).

The second relevant mechanism by which the effects on muscle tissue is via ROS production and inflammation. A review of the literature reveals only the toxicity of PFAAs on cardiac muscle and cardiac development have been investigated. Adult mice fed 0.5 and 5 mg/kg/day PFOS exhibited increases in cardiac somatic index and several markers of cardiac damage, inflammation and apoptosis (223). The 5 mg/kg/day dose in particular caused increased serum levels of creatine kinase-isozyme-MB and troponin-T which were not observed in the present study (223). Additionally, several studies conducting fish embryonic exposures to PFOA and PFOS find adverse effects on cardiogenesis, elevated ROS production and cardiac apoptosis (224, 225). Within the current study, it is unlikely that PFAAs are causing cardiomyocyte cell death considering the lack of markers for cardiac damage in the plasma and the high doses used to elicit these effects. Although many studies exist which find environmentally relevant effects of PFAAs on cardiac development during embryogenesis, it is unlikely for these to have relevance in adults considering they involved perturbations in morphogen signaling at critical stages of cardiogenesis. PPAR activation is another relevant mode by which PFAAs could be causing changes in mature muscle tissues of rainbow trout. PPARD is highly expressed in muscle and promotes the growth, angiogenesis, and oxidative capacity of both skeletal and cardiac muscle (226, 227). PPARG is known to improve insulin sensitization of skeletal muscle as well as fatty acid uptake and

intracellular transport (226). Within our study, the 3 exposure regimes caused significant increases in Nascent polypeptide-associated complex subunit alpha (Naca) an important transcriptional regulator of muscle-specific genes involved in growth and some myosin heavy chains (Myh11, Myh7) in the plasma (228). Thus, the significant number of proteins related to muscle tissue pathways following PFAA exposure in the present study could be related to Ppard and Pparg activation. Overall, the changes in plasma proteins related to muscle and angiogenesis may not be an adverse effect; considering the beneficial effect PPAR signaling has on metabolism in these tissues, additional molecular analysis of individual tissues would help elucidate the changes seen in the plasma.

4.7 Head Kidney Proteomics

The toxicology of PFAAs on the kidney is well reviewed by Stanifer et al., 2018 (229). Analysis of the US population found PFOA was associated with development of kidney cancer (230). The study was brought about by an increase in kidney cancer associated deaths occurring in residents living in the Ohio river valley, downstream from the Parkersburg Teflon-manufacturing plant in West Virginia (231-233). Within our study, proteins from the head kidney tissue of rainbow trout were significantly altered in the PFOA and high mixture exposure regimes (Figure 3.8). The results suggest the rainbow trout head kidney is particularly sensitive to PFOA induced toxicity considering both the PFOA and high mixture treatments have the highest PFOA levels compared to the other exposure regimes. This theory is further supported by the significantly increased plasma phosphate levels caused by the PFOA treatment only (Figure 3.8). High blood phosphate is a biomarker for kidney damage in humans and there is evidence for PFOA and PFOS

to affect kidney function according to epidemiology studies (234-236). However, it was unexpected that PFOA, but not PFOS, caused changes in the kidney proteome considering both PFAAs are known to activate PPARs, produce reactive oxygen species, inflammation and tissue damage at high doses in the kidneys (229, 237, 238). There is no information on whether PFOS elicits nephrotoxicity at environmentally relevant doses while there are several lines of evidence for PFOA (163, 229). Additionally, PFCAs like PFOA are known to bioaccumulate at higher levels in the kidneys compared to PFSAAs which suggests they may be more toxic towards this organ (239).

Within our study, the high mixture and PFOA exposures caused changes to proteins primarily involved in lipid metabolism, reactive oxygen species metabolism, and immune function in head kidney tissues. Biological pathway analysis suggested that the PFOA treatment in particular caused positive regulation of interferon alpha (IFNA) production. A study exposing zebrafish for 21 days to 50-100 µg/L of PFOA also found a proinflammatory response with increases in *ifn* and interleukin-1beta (*il1b*) expression (240). In that study, the proinflammatory response was deemed to be via ROS induced tissue damage which caused toll-like receptor activation and expression of proinflammatory cytokines (240). Within our own study, increases in toll-like receptor 3 and 7 (Tlr3 and Tlr7), along with a decrease in nuclear factor kappa B subunit B1 suggest a similar mode by which PFOA is causing ROS-mediated tissue damage and further tissue damage (241). TLR3 and TLR7 are highly conserved innate immune receptors which bind double stranded RNA and double stranded DNA respectively. These two receptors could have been activated from aberrant release of oligonucleotides into the extracellular space from ROS induced tissue damage (241). This suggests that cellular damage was occurring in the head kidney tissues of rainbow trout exposed to PFOA in the present study, which was further supported by high phosphate levels in

the plasma.

4.8. Summary

Overall, the plasma protein profiles revealed the pleiotropic effects of PFAAs on many biological systems and molecular signaling pathways. The PFAA mixture exposures caused the greatest number of proteins to change, which occurred in an atypical, negative dose response. Single component exposures of 25 nM PFBA, PFBS and PFOA caused much lower effects on the plasma proteome relative to the PFAA mixtures and PFOS treatments. The PFAA mixtures and PFOS treatments shared strikingly similar effects in the plasma and appeared to activate both Ppard and Pparg while no changes in Ppara were observed. Such a difference is likely due to the differences in structure of teleost Ppar orthologs exhibiting enhanced activation by PFOS via an allosteric mechanism. A number of different biological pathways were significantly overrepresented in the low mixture, medium mixture and PFOS, associated with PPAR mediated changes in lipid metabolism, nervous system effects, PI3K/AKT signaling, oxidative stress, DNA damage and apoptosis. PFOS has been previously implicated to disrupt the BBB via a PI3K dependent mechanism which largely agrees with the changes observed in plasma endothelial junctional proteins, oxidative stress and actin filament remodeling.

In contrast, PFOA and the high mixture exposure regimes caused a number of changes to the head kidney of rainbow trout suggesting the kidney to be a particularly sensitive organ to PFOA mediated toxicity. These observations are also supported by the literature, where markers of oxidative stress and inflammation are present from PFOA exposure. Overall, the results suggest that long chain PFCAs may be more nephrotoxic while long chain PFSAAs may be more neurotoxic

which offers clues into target organ systems depending on relative composition of PFCA: PFSA for environmental mixtures.

Chapter 5. Conclusions

The current study conducted an exposure of rainbow trout to PFAAs at the composition and concentrations observed in the environment, which to our knowledge has not been done in such a way before. PFAA mixtures likely cause additive and even synergistic negative effects raising serious concern as to the risks posed by these chemicals. The current study has identified the need to establish the potential hazard posed by aberrant PPARD in vertebrate taxa other than humans and rodents. A clear relationship has been established between all structurally similar PFAAs in terms of effects on common biological pathways including nervous system development, lipid metabolism, and muscle system related processes. All of these biological systems may be connected in the pathology of PFAA toxicity.

Bibliography

1. Buck RC, Franklin J, Berger U, Conder JM, Cousins IT, de Voogt P, et al. Perfluoroalkyl and polyfluoroalkyl substances in the environment: terminology, classification, and origins. *Integr Environ Assess Manag*. 2011/07/28 ed2011. p. 513-41.
2. Organisation for Economic Cooperation and Development. Lists of PFOS, PFAS, PFOA, PFCA, Related compounds and chemicals that may degrade to pfca. 2006.
3. Kissa E. Fluorinated surfactants and repellents: CRC Press; 2001.
4. 3M Company. Phase-out plan for POSF-based products; U.S. EPA administrative record. 2000.
5. Ahrens L. Polyfluoroalkyl compounds in the aquatic environment: a review of their occurrence and fate. *J Environ Monit*. 2011;13(1):20-31.
6. Giesy JP, Kannan K. Global distribution of perfluorooctane sulfonate in wildlife. *Environmental science & technology*. 2001;35(7):1339-42.
7. Zareitalabad P, Siemens J, Hamer M, Amelung W. Perfluorooctanoic acid (PFOA) and perfluorooctanesulfonic acid (PFOS) in surface waters, sediments, soils and wastewater - A review on concentrations and distribution coefficients. *Chemosphere*. 2013;91(6):725-32.
8. Calafat AM, Wong LY, Kuklennyik Z, Reidy JA, Needham LL. Polyfluoroalkyl chemicals in the U.S. population: data from the National Health and Nutrition Examination Survey (NHANES) 2003-2004 and comparisons with NHANES 1999-2000. *Environ Health Perspect*. 2007;115(11):1596-602.

9. White SS, Fenton SE, Hines EP. Endocrine disrupting properties of perfluorooctanoic acid. *J Steroid Biochem Mol Biol*. 2011;127(1-2):16-26.
10. DeWitt JC. Toxicological effects of perfluoroalkyl and polyfluoroalkyl substances: Springer; 2015.
11. DeWitt JC, Shnyra A, Badr MZ, Loveless SE, Hoban D, Frame SR, et al. Immunotoxicity of perfluorooctanoic acid and perfluorooctane sulfonate and the role of peroxisome proliferator-activated receptor alpha. *Critical reviews in toxicology*. 2009;39(1):76-94.
12. Tan X, Xie G, Sun X, Li Q, Zhong W, Qiao P, et al. High fat diet feeding exaggerates perfluorooctanoic acid-induced liver injury in mice via modulating multiple metabolic pathways. *PLoS One*. 2013;8(4):e61409.
13. Goodrum PE, Anderson JK, Luz AL, Ansell GK. Application of a Framework for Grouping and Mixtures Toxicity Assessment of PFAS: A Closer Examination of Dose Additivity Approaches. *Toxicological Sciences*. 2020.
14. Agency for Toxic Substances and Disease Registry. Framework for Assessing Health Impacts of Multiple Chemicals and Other Stressors. 2018.
15. Health Canada. Draft objective for per- and polyfluoroalkyl substances in Canadian drinking water: Overview. 2023.
16. Goodrum PE, Anderson JK, Luz AL, Ansell GK. Application of a Framework for Grouping and Mixtures Toxicity Assessment of PFAS: A Closer Examination of Dose Additivity Approaches. *Toxicol Sci*. 2020.
17. Environment and Climate Change Canada. Environmental Sustainability Indicators: Perfluorooctane sulfonate in Fish and Water. 2019.

18. Agency for Toxic Substances & Disease Registry. Health Consultation: Per- and Polyfluoroalkyl Substances (PFAS) in the Pease Tradeport Public Water System. 2020.
19. Prevedouros K, Cousins IT, Buck RC, Korzeniowski SH. Sources, fate and transport of perfluorocarboxylates. *Environ Sci Technol*. 2006;40(1):32-44.
20. Martin JW, Asher BJ, Beesoon S, Benskin JP, Ross MS. PFOS or PreFOS? Are perfluorooctane sulfonate precursors (PreFOS) important determinants of human and environmental perfluorooctane sulfonate (PFOS) exposure? *J Environ Monit*. 2010;12(11):1979-2004.
21. Cousins IT, Goldenman G, Herzke D, Lohmann R, Miller M, Ng CA, et al. The concept of essential use for determining when uses of PFASs can be phased out. *Environmental Science: Processes & Impacts*. 2019;21(11):1803-15.
22. Suja F, Pramanik BK, Zain SM. Contamination, bioaccumulation and toxic effects of perfluorinated chemicals (PFCs) in the water environment: a review paper. *Water Sci Technol*. 2009;60(6):1533-44.
23. Liu S, Yang R, Yin N, Wang YL, Faiola F. Environmental and human relevant PFOS and PFOA doses alter human mesenchymal stem cell self-renewal, adipogenesis and osteogenesis. *Ecotoxicol Environ Saf*. 2019;169:564-72.
24. Glüge J, Scheringer M, Cousins IT, DeWitt JC, Goldenman G, Herzke D, et al. An overview of the uses of per- and polyfluoroalkyl substances (PFAS). *Environmental Science: Processes & Impacts*. 2020.
25. 3M Company. Fluorochemical Use, Distribution and Release Overview. 1999 May 1999.

26. BloombergLaw. Older PFAS That EPA Thought Obsolete Still Used, Agency Told 2020. Available from: <https://news.bloomberglaw.com/environment-and-energy/older-pfas-that-epa-thought-obsolete-still-used-agency-told>.
27. Schulz K, Silva MR, Klaper R. Distribution and effects of branched versus linear isomers of PFOA, PFOS, and PFHxS: A review of recent literature. *Science of The Total Environment*. 2020;733:139186.
28. Kim S-K, Kannan K. Perfluorinated Acids in Air, Rain, Snow, Surface Runoff, and Lakes: Relative Importance of Pathways to Contamination of Urban Lakes. *Environmental Science & Technology*. 2007;41(24):8328-34.
29. Sinclair E, Kannan K. Mass loading and fate of perfluoroalkyl surfactants in wastewater treatment plants. *Environ Sci Technol*. 2006;40(5):1408-14.
30. Ahrens L, Felizeter S, Sturm R, Xie Z, Ebinghaus R. Polyfluorinated compounds in waste water treatment plant effluents and surface waters along the River Elbe, Germany. *Marine pollution bulletin*. 2009;58(9):1326-33.
31. Xiao F, Halbach TR, Simcik MF, Gulliver JS. Input characterization of perfluoroalkyl substances in wastewater treatment plants: Source discrimination by exploratory data analysis. *Water Research*. 2012;46(9):3101-9.
32. Ahrens L, Felizeter S, Sturm R, Xie Z, Ebinghaus R. Polyfluorinated compounds in waste water treatment plant effluents and surface waters along the River Elbe, Germany. *Mar Pollut Bull*. 2009;58(9):1326-33.
33. Lin AY-C, Panchangam SC, Lo C-C. The impact of semiconductor, electronics and optoelectronic industries on downstream perfluorinated chemical contamination in Taiwanese rivers. *Environmental Pollution*. 2009;157(4):1365-72.

34. Hansen KJ, Johnson HO, Eldridge JS, Butenhoff JL, Dick LA. Quantitative characterization of trace levels of PFOS and PFOA in the Tennessee River. *Environ Sci Technol*. 2002;36(8):1681-5.
35. Appleman TD, Higgins CP, Quiñones O, Vanderford BJ, Kolstad C, Zeigler-Holady JC, et al. Treatment of poly-and perfluoroalkyl substances in US full-scale water treatment systems. *Water research*. 2014;51:246-55.
36. Busch J, Ahrens L, Sturm R, Ebinghaus R. Polyfluoroalkyl compounds in landfill leachates. *Environ Pollut*. 2010;158(5):1467-71.
37. Sepulvado JG, Blaine AC, Hundal LS, Higgins CP. Occurrence and fate of perfluorochemicals in soil following the land application of municipal biosolids. *Environmental science & technology*. 2011;45(19):8106-12.
38. Busch J, Ahrens L, Sturm R, Ebinghaus R. Polyfluoroalkyl compounds in landfill leachates. *Environmental Pollution*. 2010;158(5):1467-71.
39. Moody CA, Martin JW, Kwan WC, Muir DCG, Mabury SA. Monitoring Perfluorinated Surfactants in Biota and Surface Water Samples Following an Accidental Release of Fire-Fighting Foam into Etobicoke Creek. *Environmental Science & Technology*. 2002;36(4):545-51.
40. Liu W, Wu J, He W, Xu F. A review on perfluoroalkyl acids studies: Environmental behaviors, toxic effects, and ecological and health risks. *Ecosystem Health and Sustainability*. 2019;5(1):1-19.
41. Sunderland EM, Hu XC, Dassuncao C, Tokranov AK, Wagner CC, Allen JG. A review of the pathways of human exposure to poly-and perfluoroalkyl substances (PFASs) and present understanding of health effects. *Journal of exposure science & environmental epidemiology*. 2019;29(2):131-47.

42. Xiao F. Emerging poly- and perfluoroalkyl substances in the aquatic environment: A review of current literature. *Water Res.* 2017;124:482-95.
43. Pan Y, Zhang H, Cui Q, Sheng N, Yeung LWY, Sun Y, et al. Worldwide Distribution of Novel Perfluoroether Carboxylic and Sulfonic Acids in Surface Water. *Environmental Science & Technology.* 2018;52(14):7621-9.
44. Conder JM, Hoke RA, Wolf Wd, Russell MH, Buck RC. Are PFCAs bioaccumulative? A critical review and comparison with regulatory criteria and persistent lipophilic compounds. *Environmental science & technology.* 2008;42(4):995-1003.
45. Shi Y, Vestergren R, Nost TH, Zhou Z, Cai Y. Probing the differential tissue distribution and bioaccumulation behavior of per-and polyfluoroalkyl substances of varying chain-lengths, isomeric structures and functional groups in crucian carp. *Environmental science & technology.* 2018;52(8):4592-600.
46. Bichel HN, MacManus-Spencer LA, Luthy RG. Noncovalent interactions of long-chain perfluoroalkyl acids with serum albumin. *Environmental science & technology.* 2010;44(13):5263-9.
47. Bichel HN, MacManus-Spencer LA, Zhang C, Luthy RG. Strong associations of short-chain perfluoroalkyl acids with serum albumin and investigation of binding mechanisms. *Environmental toxicology and chemistry.* 2011;30(11):2423-30.
48. Chen YM, Guo LH. Fluorescence study on site-specific binding of perfluoroalkyl acids to human serum albumin. *Arch Toxicol.* 2009;83(3):255-61.
49. Chen Y-M, Guo L-H. Fluorescence study on site-specific binding of perfluoroalkyl acids to human serum albumin. *Archives of toxicology.* 2009;83(3):255.

50. Weiss JM, Andersson PL, Lamoree MH, Leonards PE, van Leeuwen SP, Hamers T. Competitive binding of poly- and perfluorinated compounds to the thyroid hormone transport protein transthyretin. *Toxicol Sci.* 2009;109(2):206-16.
51. Han X, Snow TA, Kemper RA, Jepson GW. Binding of perfluorooctanoic acid to rat and human plasma proteins. *Chemical research in toxicology.* 2003;16(6):775-81.
52. Sheng N, Li J, Liu H, Zhang A, Dai J. Interaction of perfluoroalkyl acids with human liver fatty acid-binding protein. *Archives of toxicology.* 2016;90(1):217-27.
53. Sheng N, Cui R, Wang J, Guo Y, Wang J, Dai J. Cytotoxicity of novel fluorinated alternatives to long-chain perfluoroalkyl substances to human liver cell line and their binding capacity to human liver fatty acid binding protein. *Archives of toxicology.* 2018;92(1):359-69.
54. Ng CA, Hungerbuehler K. Exploring the use of molecular docking to identify bioaccumulative perfluorinated alkyl acids (PFAAs). *Environmental science & technology.* 2015;49(20):12306-14.
55. Ng CA, Hungerbühler K. Bioaccumulation of perfluorinated alkyl acids: observations and models. *Environmental science & technology.* 2014;48(9):4637-48.
56. Li Y, Fletcher T, Mucs D, Scott K, Lindh CH, Tallving P, et al. Half-lives of PFOS, PFHxS and PFOA after end of exposure to contaminated drinking water. *Occup Environ Med.* 2018;75(1):46-51.
57. Genuis S, Birkholz D, Ralitsch M, Thibault N. Human detoxification of perfluorinated compounds. *Public Health.* 2010;124(7):367-75.

58. Olsen GW, Mair DC, Lange CC, Harrington LM, Church TR, Goldberg CL, et al. Per-and polyfluoroalkyl substances (PFAS) in American Red Cross adult blood donors, 2000–2015. *Environmental research*. 2017;157:87-95.
59. Jian J-M, Chen D, Han F-J, Guo Y, Zeng L, Lu X, et al. A short review on human exposure to and tissue distribution of per-and polyfluoroalkyl substances (PFASs). *Science of The Total Environment*. 2018;636:1058-69.
60. Russell MH, Waterland RL, Wong F. Calculation of chemical elimination half-life from blood with an ongoing exposure source: the example of perfluorooctanoic acid (PFOA). *Chemosphere*. 2015;129:210-6.
61. De Silva AO, Spencer C, Scott BF, Backus S, Muir DCG. Detection of a Cyclic Perfluorinated Acid, Perfluoroethylcyclohexane Sulfonate, in the Great Lakes of North America. *Environmental Science & Technology*. 2011;45(19):8060-6.
62. Wolf CJ, Takacs ML, Schmid JE, Lau C, Abbott BD. Activation of mouse and human peroxisome proliferator-activated receptor alpha by perfluoroalkyl acids of different functional groups and chain lengths. *Toxicol Sci*. 2008;106(1):162-71.
63. Bossi R, Riget FF, Dietz R, Sonne C, Fauser P, Dam M, et al. Preliminary screening of perfluorooctane sulfonate (PFOS) and other fluorochemicals in fish, birds and marine mammals from Greenland and the Faroe Islands. *Environmental Pollution*. 2005;136(2):323-9.
64. Houde M, Czub G, Small JM, Backus S, Wang X, Alaei M, et al. Fractionation and bioaccumulation of perfluorooctane sulfonate (PFOS) isomers in a Lake Ontario food web. *Environmental science & technology*. 2008;42(24):9397-403.

65. Kannan K, Tao L, Sinclair E, Pastva SD, Jude DJ, Giesy JP. Perfluorinated compounds in aquatic organisms at various trophic levels in a Great Lakes food chain. *Archives of environmental contamination and toxicology*. 2005;48(4):559-66.
66. Du D, Lu Y, Zhou Y, Li Q, Zhang M, Han G, et al. Bioaccumulation, trophic transfer and biomagnification of perfluoroalkyl acids (PFAAs) in the marine food web of the South China Sea. *Journal of Hazardous Materials*. 2021;405:124681.
67. Han Z-X, Zhang M, Lv C-X. Toxicokinetic behaviors and modes of perfluorooctane sulfonate (PFOS) and perfluorooctane acid (PFOA) on tilapia (*Oreochromis niloticus*). *African Journal of Biotechnology*. 2011;10(60):12943-50.
68. Hagens A, Vergauwen L, Benoot D, Laukens K, Knapen D. Mechanistic toxicity study of perfluorooctanoic acid in zebrafish suggests mitochondrial dysfunction to play a key role in PFOA toxicity. *Chemosphere*. 2013;91(6):844-56.
69. Lee JJ, Schultz IR. Sex differences in the uptake and disposition of perfluorooctanoic acid in fathead minnows after oral dosing. *Environ Sci Technol*. 2010;44(1):491-6.
70. Heuvel JPV, Kuslikis BI, Van Rafelghem MJ, Peterson RE. Tissue distribution, metabolism, and elimination of perfluorooctanoic acid in male and female rats. *Journal of biochemical toxicology*. 1991;6(2):83-92.
71. Kudo N, Suzuki E, Katakura M, Ohmori K, Noshiro R, Kawashima Y. Comparison of the elimination between perfluorinated fatty acids with different carbon chain length in rats. *Chemico-biological interactions*. 2001;134(2):203-16.
72. Han X, Nabb DL, Russell MH, Kennedy GL, Rickard RW. Renal Elimination of Perfluorocarboxylates (PFCAs). *Chemical Research in Toxicology*. 2012;25(1):35-46.

73. Han X, Nabb DL, Russell MH, Kennedy GL, Rickard RW. Renal elimination of perfluorocarboxylates (PFCAs). *Chemical research in toxicology*. 2011;25(1):35-46.
74. Kudo N, Katakura M, Sato Y, Kawashima Y. Sex hormone-regulated renal transport of perfluorooctanoic acid. *Chem Biol Interact*. 2002;139(3):301-16.
75. Andersen ME, Butenhoff JL, Chang S-C, Farrar DG, Kennedy Jr GL, Lau C, et al. Perfluoroalkyl acids and related chemistries—toxicokinetics and modes of action. *Toxicological sciences*. 2008;102(1):3-14.
76. Andersen ME, Clewell HJ, 3rd, Tan YM, Butenhoff JL, Olsen GW. Pharmacokinetic modeling of saturable, renal resorption of perfluoroalkylacids in monkeys--probing the determinants of long plasma half-lives. *Toxicology*. 2006;227(1-2):156-64.
77. Vidal A, Lafay F, Daniele G, Vulliet E, Rochard E, Garric J, et al. Does water temperature influence the distribution and elimination of perfluorinated substances in rainbow trout (*Oncorhynchus mykiss*)? *Environmental Science and Pollution Research*. 2019;26:16355-65.
78. Consoer DM, Hoffman AD, Fitzsimmons PN, Kosian PA, Nichols JW. Toxicokinetics of perfluorooctane sulfonate in rainbow trout (*Oncorhynchus mykiss*). *Environ Toxicol Chem*. 2016;35(3):717-27.
79. Consoer DM, Hoffman AD, Fitzsimmons PN, Kosian PA, Nichols JW. Toxicokinetics of perfluorooctanoate (PFOA) in rainbow trout (*Oncorhynchus mykiss*). *Aquat Toxicol*. 2014;156:65-73.
80. Bjork JA, Lau C, Chang SC, Butenhoff JL, Wallace KB. Perfluorooctane sulfonate-induced changes in fetal rat liver gene expression. *Toxicology*. 2008;251(1-3):8-20.

81. Bjork JA, Wallace KB. Structure-activity relationships and human relevance for perfluoroalkyl acid-induced transcriptional activation of peroxisome proliferation in liver cell cultures. *Toxicol Sci.* 2009;111(1):89-99.
82. Kennedy GL, Butenhoff JL, Olsen GW, O'Connor JC, Seacat AM, Perkins RG, et al. The Toxicology of Perfluorooctanoate. *Critical Reviews in Toxicology.* 2010;34(4):351-84.
83. Biegel LB, Hurtt ME, Frame SR, O'Connor JC, Cook JC. Mechanisms of extrahepatic tumor induction by peroxisome proliferators in male CD rats. *Toxicol Sci.* 2001;60(1):44-55.
84. Haugom B, Spydevold O. The mechanism underlying the hypolipemic effect of perfluorooctanoic acid (PFOA), perfluorooctane sulphonic acid (PFOSA) and clofibrilic acid. *Biochim Biophys Acta.* 1992;1128(1):65-72.
85. Xie Y, Yang Q, Nelson BD, DePierre JW. Characterization of the adipose tissue atrophy induced by peroxisome proliferators in mice. *Lipids.* 2002;37(2):139-46.
86. Xie Y, Yang Q, Nelson BD, DePierre JW. The relationship between liver peroxisome proliferation and adipose tissue atrophy induced by peroxisome proliferator exposure and withdrawal in mice. *Biochem Pharmacol.* 2003;66(5):749-56.
87. Dong H, Lu G, Yan Z, Liu J, Ji Y. Molecular and phenotypic responses of male crucian carp (*Carassius auratus*) exposed to perfluorooctanoic acid. *Sci Total Environ.* 2019;653:1395-406.
88. Wei Y, Shi X, Zhang H, Wang J, Zhou B, Dai J. Combined effects of polyfluorinated and perfluorinated compounds on primary cultured hepatocytes from rare minnow (*Gobiocypris rarus*) using toxicogenomic analysis. *Aquat Toxicol.* 2009;95(1):27-36.

89. Wang L, Wang Y, Liang Y, Li J, Liu Y, Zhang J, et al. Specific accumulation of lipid droplets in hepatocyte nuclei of PFOA-exposed BALB/c mice. *Sci Rep.* 2013;3:2174.
90. Wang L, Wang Y, Liang Y, Li J, Liu Y, Zhang J, et al. PFOS induced lipid metabolism disturbances in BALB/c mice through inhibition of low density lipoproteins excretion. *Sci Rep.* 2014;4:4582.
91. Guruge KS, Yeung LW, Yamanaka N, Miyazaki S, Lam PK, Giesy JP, et al. Gene expression profiles in rat liver treated with perfluorooctanoic acid (PFOA). *Toxicol Sci.* 2006;89(1):93-107.
92. Hu W, Jones PD, Celius T, Giesy JP. Identification of genes responsive to PFOS using gene expression profiling. *Environ Toxicol Pharmacol.* 2005;19(1):57-70.
93. Hu W, Jones PD, Decoen W, Newsted JL, Giesy JP. Comparison of gene expression methods to identify genes responsive to perfluorooctane sulfonic acid. *Environ Toxicol Pharmacol.* 2005;19(1):153-60.
94. Rosen MB, Schmid JR, Corton JC, Zehr RD, Das KP, Abbott BD, et al. Gene Expression Profiling in Wild-Type and PPAR α -Null Mice Exposed to Perfluorooctane Sulfonate Reveals PPAR α -Independent Effects. *PPAR research.* 2010;2010:794739.
95. Rosen MB, Abbott BD, Wolf DC, Corton JC, Wood CR, Schmid JE, et al. Gene profiling in the livers of wild-type and PPAR α -null mice exposed to perfluorooctanoic acid. *Toxicol Pathol.* 2008;36(4):592-607.
96. Rosen MB, Lee JS, Ren H, Vallanat B, Liu J, Waalkes MP, et al. Toxicogenomic dissection of the perfluorooctanoic acid transcript profile in mouse liver: evidence for the involvement of nuclear receptors PPAR alpha and CAR. *Toxicol Sci.* 2008;103(1):46-56.

97. Wu X, Xie G, Xu X, Wu W, Yang B. Adverse bioeffect of perfluorooctanoic acid on liver metabolic function in mice. *Environ Sci Pollut Res Int*. 2018;25(5):4787-93.
98. Wei Y, Chan LL, Wang D, Zhang H, Wang J, Dai J. Proteomic analysis of hepatic protein profiles in rare minnow (*Gobiocypris rarus*) exposed to perfluorooctanoic acid. *J Proteome Res*. 2008;7(4):1729-39.
99. Wei Y, Liu Y, Wang J, Tao Y, Dai J. Toxicogenomic analysis of the hepatic effects of perfluorooctanoic acid on rare minnows (*Gobiocypris rarus*). *Toxicol Appl Pharmacol*. 2008;226(3):285-97.
100. Oshida K, Vasani N, Thomas RS, Applegate D, Rosen M, Abbott B, et al. Identification of modulators of the nuclear receptor peroxisome proliferator-activated receptor alpha (PPARalpha) in a mouse liver gene expression compendium. *PLoS One*. 2015;10(2):e0112655.
101. Wolf CJ, Schmid JE, Lau C, Abbott BD. Activation of mouse and human peroxisome proliferator-activated receptor-alpha (PPARalpha) by perfluoroalkyl acids (PFAAs): further investigation of C4-C12 compounds. *Reprod Toxicol*. 2012;33(4):546-51.
102. Ren H, Vallanat B, Nelson DM, Yeung LWY, Guruge KS, Lam PKS, et al. Evidence for the involvement of xenobiotic-responsive nuclear receptors in transcriptional effects upon perfluoroalkyl acid exposure in diverse species. *Reprod Toxicol*. 2009;27(3-4):266-77.
103. Den Broeder MJ, Kopylova VA, Kamminga LM, Legler J. Zebrafish as a Model to Study the Role of Peroxisome Proliferating-Activated Receptors in Adipogenesis and Obesity. *PPAR Res*. 2015;2015:358029.
104. Desvergne B, Wahli W. Peroxisome proliferator-activated receptors: nuclear control of metabolism. *Endocr Rev*. 1999;20(5):649-88.

105. Kersten S, Stienstra R. The role and regulation of the peroxisome proliferator activated receptor alpha in human liver. *Biochimie*. 2017;136:75-84.
106. Braissant O, Fougère F, Scotto C, Dauca M, Wahli W. Differential expression of peroxisome proliferator-activated receptors (PPARs): tissue distribution of PPAR-alpha, -beta, and -gamma in the adult rat. *Endocrinology*. 1996;137(1):354-66.
107. Vamecq J, Dessein AF, Fontaine M, Briand G, Porchet N, Latruffe N, et al. Mitochondrial dysfunction and lipid homeostasis. *Curr Drug Metab*. 2012;13(10):1388-400.
108. Burgoon L. Inhibition of fatty acid beta oxidation leading to nonalcoholic steatohepatitis (NASH) 2019 [Available from: <https://aopwiki.org/aops/213>].
109. Keller BJ, Marsman DS, Popp JA, Thurman RG. Several nongenotoxic carcinogens uncouple mitochondrial oxidative phosphorylation. *Biochim Biophys Acta*. 1992;1102(2):237-44.
110. Langley AE. Effects of perfluoro-n-decanoic acid on the respiratory activity of isolated rat liver mitochondria. *J Toxicol Environ Health*. 1990;29(3):329-36.
111. Mashayekhi V, Tehrani KH, Hashemzaei M, Tabrizian K, Shahraki J, Hosseini MJ. Mechanistic approach for the toxic effects of perfluorooctanoic acid on isolated rat liver and brain mitochondria. *Hum Exp Toxicol*. 2015;34(10):985-96.
112. Walters MW, Bjork JA, Wallace KB. Perfluorooctanoic acid stimulated mitochondrial biogenesis and gene transcription in rats. *Toxicology*. 2009;264(1-2):10-5.
113. Wang Y, Wang L, Chang W, Zhang Y, Zhang Y, Liu W. Neurotoxic effects of perfluoroalkyl acids: Neurobehavioral deficit and its molecular mechanism. *Toxicology Letters*. 2019;305:65-72.

114. Long Y, Wang Y, Ji G, Yan L, Hu F, Gu A. Neurotoxicity of perfluorooctane sulfonate to hippocampal cells in adult mice. *PloS one*. 2013;8(1):e54176.
115. Fuentes S, Colomina MT, Vicens P, Franco-Pons N, Domingo JL. Concurrent exposure to perfluorooctane sulfonate and restraint stress during pregnancy in mice: effects on postnatal development and behavior of the offspring. *Toxicological Sciences*. 2007;98(2):589-98.
116. Luebker DJ, Case MT, York RG, Moore JA, Hansen KJ, Butenhoff JL. Two-generation reproduction and cross-foster studies of perfluorooctanesulfonate (PFOS) in rats. *Toxicology*. 2005;215(1-2):126-48.
117. Wang Y, Liu W, Zhang Q, Zhao H, Quan X. Effects of developmental perfluorooctane sulfonate exposure on spatial learning and memory ability of rats and mechanism associated with synaptic plasticity. *Food and Chemical Toxicology*. 2015;76:70-6.
118. Jantzen CE, Annunziato KM, Cooper KR. Behavioral, morphometric, and gene expression effects in adult zebrafish (*Danio rerio*) embryonically exposed to PFOA, PFOS, and PFNA. *Aquatic toxicology (Amsterdam, Netherlands)*. 2016;180:123-30.
119. Jantzen CE, Annunziato KA, Bugel SM, Cooper KR. PFOS, PFNA, and PFOA sub-lethal exposure to embryonic zebrafish have different toxicity profiles in terms of morphometrics, behavior and gene expression. *Aquatic Toxicology*. 2016;175:160-70.
120. Harada KH, Ishii TM, Takatsuka K, Koizumi A, Ohmori H. Effects of perfluorooctane sulfonate on action potentials and currents in cultured rat cerebellar Purkinje cells. *Biochemical and biophysical research communications*. 2006;351(1):240-5.
121. Liao C-y, Cui L, Zhou Q-f, Duan S-m, Jiang G-b. Effects of perfluorooctane sulfonate on ion channels and glutamate-activated current in cultured rat hippocampal neurons. *Environmental Toxicology and Pharmacology*. 2009;27(3):338-44.

122. Liu X, Jin Y, Liu W, Wang F, Hao S. Possible mechanism of perfluorooctane sulfonate and perfluorooctanoate on the release of calcium ion from calcium stores in primary cultures of rat hippocampal neurons. *Toxicology in vitro*. 2011;25(7):1294-301.
123. Zhang Q, Zhao H, Liu W, Zhang Z, Qin H, Luo F, et al. Developmental perfluorooctane sulfonate exposure results in tau hyperphosphorylation and β -amyloid aggregation in adults rats: Incidence for link to Alzheimer's disease. *Toxicology*. 2016;347-349:40-6.
124. Wang Y, Zhao H, Zhang Q, Liu W, Quan X. Perfluorooctane sulfonate induces apoptosis of hippocampal neurons in rat offspring associated with calcium overload. *Toxicology Research*. 2015;4(4):931-8.
125. Grandjean P, Andersen EW, Budtz-Jørgensen E, Nielsen F, Mølbak K, Weihe P, et al. Serum vaccine antibody concentrations in children exposed to perfluorinated compounds. *JAMA*. 2012;307(4):391-7.
126. Fenton SE, Ducatman A, Boobis A, DeWitt JC, Lau C, Ng C, et al. Per-and Polyfluoroalkyl Substance Toxicity and Human Health Review: Current State of Knowledge and Strategies for Informing Future Research. *Environmental Toxicology and Chemistry*. 2020.
127. Looker C, Luster MI, Calafat AM, Johnson VJ, Burleson GR, Burleson FG, et al. Influenza Vaccine Response in Adults Exposed to Perfluorooctanoate and Perfluorooctanesulfonate. *Toxicological Sciences*. 2014;138(1):76-88.
128. Abraham K, Mielke H, Fromme H, Völkel W, Menzel J, Peiser M, et al. Internal exposure to perfluoroalkyl substances (PFASs) and biological markers in 101 healthy 1-year-old children: associations between levels of perfluorooctanoic acid (PFOA) and vaccine response. *Archives of toxicology*. 2020;94(6):2131-47.

129. Granum B, Haug LS, Namork E, Stølevik SB, Thomsen C, Aaberge IS, et al. Pre-natal exposure to perfluoroalkyl substances may be associated with altered vaccine antibody levels and immune-related health outcomes in early childhood. *J Immunotoxicol.* 2013;10(4):373-9.
130. Stein CR, McGovern KJ, Pajak AM, Maglione PJ, Wolff MS. Perfluoroalkyl and polyfluoroalkyl substances and indicators of immune function in children aged 12-19 y: National Health and Nutrition Examination Survey. *Pediatr Res.* 2016;79(2):348-57.
131. Qazi MR, Hassan M, Nelson BD, DePierre JW, Abedi-Valugerdi M. Both sub-acute, moderate-dose and short-term, low-dose dietary exposure of mice to perfluorooctane sulfonate exacerbates concanavalin A-induced hepatitis. *Toxicol Lett.* 2013;217(1):67-74.
132. Qazi MR, Nelson BD, Depierre JW, Abedi-Valugerdi M. 28-Day dietary exposure of mice to a low total dose (7 mg/kg) of perfluorooctanesulfonate (PFOS) alters neither the cellular compositions of the thymus and spleen nor humoral immune responses: does the route of administration play a pivotal role in PFOS-induced immunotoxicity? *Toxicology.* 2010;267(1-3):132-9.
133. DeWitt JC, Peden-Adams MM, Keller JM, Germolec DR. Immunotoxicity of Perfluorinated Compounds: Recent Developments. *Toxicologic Pathology.* 2011;40(2):300-11.
134. Yang Q, Xie Y, Depierre JW. Effects of peroxisome proliferators on the thymus and spleen of mice. *Clin Exp Immunol.* 2000;122(2):219-26.
135. Qazi MR, Nelson BD, DePierre JW, Abedi-Valugerdi M. High-dose dietary exposure of mice to perfluorooctanoate or perfluorooctane sulfonate exerts toxic effects on myeloid and B-lymphoid cells in the bone marrow and these effects are partially dependent on reduced food consumption. *Food Chem Toxicol.* 2012;50(9):2955-63.

136. Pascual G, Glass CK. Nuclear receptors versus inflammation: mechanisms of transrepression. *Trends Endocrinol Metab.* 2006;17(8):321-7.
137. Zolezzi JM, Santos MJ, Bastías-Candia S, Pinto C, Godoy JA, Inestrosa NC. PPARs in the central nervous system: roles in neurodegeneration and neuroinflammation. *Biol Rev Camb Philos Soc.* 2017;92(4):2046-69.
138. Yang Q, Xie Y, Alexson SE, Nelson BD, DePierre JW. Involvement of the peroxisome proliferator-activated receptor alpha in the immunomodulation caused by peroxisome proliferators in mice. *Biochem Pharmacol.* 2002;63(10):1893-900.
139. Ward JM, Peters JM, Perella CM, Gonzalez FJ. Receptor and nonreceptor-mediated organ-specific toxicity of di (2-ethylhexyl) phthalate (DEHP) in peroxisome proliferator-activated receptor α -null mice. *Toxicologic pathology.* 1998;26(2):240-6.
140. Cunard R, DiCampli D, Archer DC, Stevenson JL, Ricote M, Glass CK, et al. WY14, 643, a PPAR α ligand, has profound effects on immune responses in vivo. *The Journal of Immunology.* 2002;169(12):6806-12.
141. Zhang H, Fang W, Wang D, Gao N, Ding Y, Chen C. The role of interleukin family in perfluorooctanoic acid (PFOA)-induced immunotoxicity. *Journal of Hazardous Materials.* 2014;280:552-60.
142. Sprague JB. The ABCs of Pollutant Bioassay Using Fish. In: Cairns J, Dickson KL, editors. West Conshohocken, PA: ASTM International; 1973. p. 6-30.
143. Fulton TW. Rate of growth of sea fishes. [Edinburgh]: [Neill & Co.]; 1902.
144. Simmons DB, Bols NC, Duncker BP, McMaster M, Miller J, Sherry JP. Proteomic profiles of white sucker (*Catostomus commersonii*) sampled from within the Thunder Bay Area of Concern

reveal up-regulation of proteins associated with tumor formation and exposure to environmental estrogens. *Environ Sci Technol*. 2012;46(3):1886-94.

145. Schilling B, Rardin MJ, MacLean BX, Zawadzka AM, Frewen BE, Cusack MP, et al. Platform-independent and label-free quantitation of proteomic data using MS1 extracted ion chromatograms in skyline: application to protein acetylation and phosphorylation. *Mol Cell Proteomics*. 2012;11(5):202-14.

146. Packa V, Maedler S, Howell T, Bostan V, Diep N, Tooley R, et al. Unbiased Measurement of Phosphate and Phosphorus Speciation in Surface Waters. *Environmental science & technology*. 2018;53(2):820-8.

147. Chawade A, Alexandersson E, Levander F. Normalyzer: A Tool for Rapid Evaluation of Normalization Methods for Omics Data Sets. *Journal of Proteome Research*. 2014;13(6):3114-20.

148. Willforss J, Chawade A, Levander F. NormalyzerDE: Online Tool for Improved Normalization of Omics Expression Data and High-Sensitivity Differential Expression Analysis. *Journal of Proteome Research*. 2019;18(2):732-40.

149. Bart S, Short S, Jager T, Eagles EJ, Robinson A, Badder C, et al. How to analyse and account for interactions in mixture toxicity with toxicokinetic-toxicodynamic models. *Science of The Total Environment*. 2022;843:157048.

150. Hu J, Li J, Wang J, Zhang A, Dai J. Synergistic effects of perfluoroalkyl acids mixtures with J-shaped concentration-responses on viability of a human liver cell line. *Chemosphere*. 2014;96:81-8.

151. Zhang L, Niu J, Li Y, Wang Y, Sun D. Evaluating the sub-lethal toxicity of PFOS and PFOA using rotifer *Brachionus calyciflorus*. *Environ Pollut*. 2013;180:34-40.

152. Mulkiwicz E, Jastorff B, Składanowski AC, Kleszczyński K, Stepnowski P. Evaluation of the acute toxicity of perfluorinated carboxylic acids using eukaryotic cell lines, bacteria and enzymatic assays. *Environ Toxicol Pharmacol*. 2007;23(3):279-85.
153. Cheng Y, Cui Y, Chen H-m, Xie W-p. Thyroid disruption effects of environmental level perfluorooctane sulfonates (PFOS) in *Xenopus laevis*. *Ecotoxicology*. 2011;20(8):2069-78.
154. Cheng Y, Cui Y, Dang ZC, Xie WP, Li HS, Yin HH, et al. [Effects of perfluorooctane sulfonate (PFOS) exposure on vitellogenin mRNA level in zebrafish (*Brachydanio rerio*)]. *Huan Jing Ke Xue*. 2012;33(6):1865-70.
155. Rodriguez-Jorquera IA, Colli-Dula RC, Kroll K, Jayasinghe BS, Parachu Marco MV, Silva-Sanchez C, et al. Blood Transcriptomics Analysis of Fish Exposed to Perfluoro Alkyls Substances: Assessment of a Non-Lethal Sampling Technique for Advancing Aquatic Toxicology Research. *Environ Sci Technol*. 2019;53(3):1441-52.
156. Binderup M-L, Dalgaard M, Dragsted LO, Hossaini A, Ladefoged O, Lam HR, et al. Combined Actions and Interactions of Chemicals in Mixtures: The Toxicological Effects of Exposure to Mixtures of Industrial and Environmental Chemicals. 2003.
157. Han J, Gu W, Barrett H, Yang D, Tang S, Sun J, et al. A Roadmap to the Structure-Related Metabolism Pathways of Per- and Polyfluoroalkyl Substances in the Early Life Stages of Zebrafish (*Danio rerio*). *Environmental Health Perspectives*. 2021;129(7):077004.
158. Burkhard LP. Evaluation of Published Bioconcentration Factor (BCF) and Bioaccumulation Factor (BAF) Data for Per- and Polyfluoroalkyl Substances Across Aquatic Species. *Environmental Toxicology and Chemistry*. 2021;40(6):1530-43.

159. Martin JW, Mabury SA, Solomon KR, Muir DC. Bioconcentration and tissue distribution of perfluorinated acids in rainbow trout (*Oncorhynchus mykiss*). *Environmental Toxicology and Chemistry: An International Journal*. 2003;22(1):196-204.
160. Ankley GT, Cureton P, Hoke RA, Houde M, Kumar A, Kurias J, et al. Assessing the Ecological Risks of Per- and Polyfluoroalkyl Substances: Current State-of-the Science and a Proposed Path Forward. *Environmental Toxicology and Chemistry*. 2021;40(3):564-605.
161. Pizzurro DM, Seeley M, Kerper LE, Beck BD. Interspecies differences in perfluoroalkyl substances (PFAS) toxicokinetics and application to health-based criteria. *Regulatory Toxicology and Pharmacology*. 2019;106:239-50.
162. Kudo N, Kawashima Y. Toxicity and toxicokinetics of perfluorooctanoic acid in humans and animals. *The Journal of toxicological sciences*. 2003;28(2):49-57.
163. Söderstrøm S, Lille-Langøy R, Yadetie F, Rauch M, Milinski A, Dejaegere A, et al. Agonistic and potentiating effects of perfluoroalkyl substances (PFAS) on the Atlantic cod (*Gadus morhua*) peroxisome proliferator-activated receptors (Ppars). *Environment International*. 2022;163:107203.
164. You C, Jiang D, Zhang Q, Xie D, Wang S, Dong Y, et al. Cloning and expression characterization of peroxisome proliferator-activated receptors (PPARs) with their agonists, dietary lipids, and ambient salinity in rabbitfish *Siganus canaliculatus*. *Comp Biochem Physiol B Biochem Mol Biol*. 2017;206:54-64.
165. Boukouvala E, Antonopoulou E, Favre-Krey L, Diez A, Bautista JM, Leaver MJ, et al. Molecular characterization of three peroxisome proliferator-activated receptors from the sea bass (*Dicentrarchus labrax*). *Lipids*. 2004;39(11):1085-92.

166. Raingard D, Bilbao E, Sáez-Morquecho C, de Cerio OD, Orbea A, Cancio I, et al. Cloning and transcription of nuclear receptors and other toxicologically relevant genes, and exposure biomarkers in European hake (*Merluccius merluccius*) after the Prestige oil spill. *Mar Genomics*. 2009;2(3-4):201-13.
167. Kondo H, Misaki R, Gelman L, Watabe S. Ligand-dependent transcriptional activities of four torafugu pufferfish *Takifugu rubripes* peroxisome proliferator-activated receptors. *General and Comparative Endocrinology*. 2007;154(1):120-7.
168. Fang C, Wu X, Huang Q, Liao Y, Liu L, Qiu L, et al. PFOS elicits transcriptional responses of the ER, AHR and PPAR pathways in *Oryzias melastigma* in a stage-specific manner. *Aquat Toxicol*. 2012;106-107:9-19.
169. Jacquet N, Maire MA, Landkocz Y, Vasseur P. Carcinogenic potency of perfluorooctane sulfonate (PFOS) on Syrian hamster embryo (SHE) cells. *Archives of Toxicology*. 2012;86(2):305-14.
170. Arukwe A, Mortensen AS. Lipid peroxidation and oxidative stress responses of salmon fed a diet containing perfluorooctane sulfonic- or perfluorooctane carboxylic acids. *Comp Biochem Physiol C Toxicol Pharmacol*. 2011;154(4):288-95.
171. Cousins IT, DeWitt JC, Glüge J, Goldenman G, Herzke D, Lohmann R, et al. Strategies for grouping per-and polyfluoroalkyl substances (PFAS) to protect human and environmental health. *Environmental Science: Processes & Impacts*. 2020;22(7):1444-60.
172. Butenhoff JL, Bjork JA, Chang S-C, Ehresman DJ, Parker GA, Das K, et al. Toxicological evaluation of ammonium perfluorobutyrate in rats: Twenty-eight-day and ninety-day oral gavage studies. *Reproductive Toxicology*. 2012;33(4):513-30.

173. Valsecchi S, Conti D, Crebelli R, Polesello S, Rusconi M, Mazzoni M, et al. Deriving environmental quality standards for perfluorooctanoic acid (PFOA) and related short chain perfluorinated alkyl acids. *Journal of Hazardous Materials*. 2017;323:84-98.
174. Wasel O, Thompson KM, Freeman JL. Assessment of unique behavioral, morphological, and molecular alterations in the comparative developmental toxicity profiles of PFOA, PFHxA, and PFBA using the zebrafish model system. *Environment International*. 2022;170:107642.
175. Takacs ML, Abbott BD. Activation of mouse and human peroxisome proliferator-activated receptors (alpha, beta/delta, gamma) by perfluorooctanoic acid and perfluorooctane sulfonate. *Toxicol Sci*. 2007;95(1):108-17.
176. Buhrke T, Kibellus A, Lampen A. In vitro toxicological characterization of perfluorinated carboxylic acids with different carbon chain lengths. *Toxicology Letters*. 2013;218(2):97-104.
177. Rosen MB, Das KP, Wood CR, Wolf CJ, Abbott BD, Lau C. Evaluation of perfluoroalkyl acid activity using primary mouse and human hepatocytes. *Toxicology*. 2013;308:129-37.
178. Bangma J, Szilagyi J, Blake BE, Plazas C, Kepper S, Fenton SE, et al. An assessment of serum-dependent impacts on intracellular accumulation and genomic response of per- and polyfluoroalkyl substances in a placental trophoblast model. *Environ Toxicol*. 2020;35(12):1395-405.
179. Ge T, Yang J, Zhou S, Wang Y, Li Y, Tong X. The Role of the Pentose Phosphate Pathway in Diabetes and Cancer. *Frontiers in Endocrinology*. 2020;11.
180. Wamelink MM, Struys EA, Jakobs C. The biochemistry, metabolism and inherited defects of the pentose phosphate pathway: a review. *Journal of Inherited Metabolic Disease: Official Journal of the Society for the Study of Inborn Errors of Metabolism*. 2008;31(6):703-17.

181. Wielsøe M, Long M, Ghisari M, Bonfeld-Jørgensen EC. Perfluoroalkylated substances (PFAS) affect oxidative stress biomarkers in vitro. *Chemosphere*. 2015;129:239-45.
182. Schönfeld P, Dymkowska D, Wojtczak L. Acyl-CoA-induced generation of reactive oxygen species in mitochondrial preparations is due to the presence of peroxisomes. *Free Radical Biology and Medicine*. 2009;47(5):503-9.
183. Brand MD, Nicholls DG. Assessing mitochondrial dysfunction in cells. *Biochemical Journal*. 2011;435(2):297-312.
184. Rossi MJ, DiDomenico SF, Patel M, Mazin AV. RAD52: Paradigm of Synthetic Lethality and New Developments. *Frontiers in Genetics*. 2021;12.
185. Witeska M. Erythrocytes in teleost fishes: a review. *Zoology and Ecology*. 2013;23(4):275-81.
186. Al-Sabti K, Metcalfe CD. Fish micronuclei for assessing genotoxicity in water. *Mutation Research/Genetic Toxicology*. 1995;343(2-3):121-35.
187. Muddapu VR, Dharshini SAP, Chakravarthy VS, Gromiha MM. Neurodegenerative Diseases – Is Metabolic Deficiency the Root Cause? *Frontiers in Neuroscience*. 2020;14.
188. Chiang MC, Cheng YC, Chen HM, Liang YJ, Yen CH. Rosiglitazone promotes neurite outgrowth and mitochondrial function in N2A cells via PPARgamma pathway. *Mitochondrion*. 2014;14(1):7-17.
189. Bordet R, Ouk T, Petrault O, Gele P, Gautier S, Laprais M, et al. PPAR: a new pharmacological target for neuroprotection in stroke and neurodegenerative diseases. *Biochemical Society Transactions*. 2006;34(6):1341-6.

190. Bernardo ME, Fibbe WE. Mesenchymal stromal cells: sensors and switchers of inflammation. *Cell Stem Cell*. 2013;13(4):392-402.
191. D'Angelo M, Antonosante A, Castelli V, Catanesi M, Moorthy N, Iannotta D, et al. PPARs and Energy Metabolism Adaptation during Neurogenesis and Neuronal Maturation. *Int J Mol Sci*. 2018;19(7):1869.
192. Kanakasabai S, Pestereva E, Chearwae W, Gupta SK, Ansari S, Bright JJ. PPAR γ agonists promote oligodendrocyte differentiation of neural stem cells by modulating stemness and differentiation genes. *PLoS One*. 2012;7(11):e50500.
193. Wan Ibrahim WN, Tofighi R, Onishchenko N, Rebellato P, Bose R, Uhlén P, et al. Perfluorooctane sulfonate induces neuronal and oligodendrocytic differentiation in neural stem cells and alters the expression of PPAR γ in vitro and in vivo. *Toxicol Appl Pharmacol*. 2013;269(1):51-60.
194. Peters JM, Lee SS, Li W, Ward JM, Gavrilova O, Everett C, et al. Growth, adipose, brain, and skin alterations resulting from targeted disruption of the mouse peroxisome proliferator-activated receptor beta(delta). *Mol Cell Biol*. 2000;20(14):5119-28.
195. Moreno S, Farioli-Vecchioli S, Ceru M. Immunolocalization of peroxisome proliferator-activated receptors and retinoid X receptors in the adult rat CNS. *Neuroscience*. 2004;123(1):131-45.
196. Almad A, McTigue DM. Chronic expression of PPAR-delta by oligodendrocyte lineage cells in the injured rat spinal cord. *J Comp Neurol*. 2010;518(6):785-99.
197. Braissant O, Wahli W. Differential expression of peroxisome proliferator-activated receptor- α , - β , and - γ during rat embryonic development. *Endocrinology*. 1998;139(6):2748-54.

198. Pifferi F, Laurent B, Plourde M. Lipid Transport and Metabolism at the Blood-Brain Interface: Implications in Health and Disease. *Front Physiol.* 2021;12:645646.
199. Locher KP. Review. Structure and mechanism of ATP-binding cassette transporters. *Philos Trans R Soc Lond B Biol Sci.* 2009;364(1514):239-45.
200. Greaves AK, Letcher RJ, Sonne C, Dietz R. Brain region distribution and patterns of bioaccumulative perfluoroalkyl carboxylates and sulfonates in East Greenland polar bears (*Ursus maritimus*). *Environmental Toxicology and Chemistry.* 2013;32(3):713-22.
201. Cao Y, Ng C. Absorption, distribution, and toxicity of per- and polyfluoroalkyl substances (PFAS) in the brain: a review. *Environmental Science: Processes & Impacts.* 2021;23(11):1623-40.
202. Liu Y, Colby JK, Zuo X, Jaoude J, Wei D, Shureiqi I. The Role of PPAR- δ in Metabolism, Inflammation, and Cancer: Many Characters of a Critical Transcription Factor. *Int J Mol Sci.* 2018;19(11).
203. Dusza HM, Cenijn PH, Kamstra JH, Westerink RHS, Leonards PEG, Hamers T. Effects of environmental pollutants on calcium release and uptake by rat cortical microsomes. *NeuroToxicology.* 2018;69:266-77.
204. Fang X, Wu C, Li H, Yuan W, Wang X. Elevation of intracellular calcium and oxidative stress is involved in perfluorononanoic acid-induced neurotoxicity. *Toxicology and Industrial Health.* 2018;34(3):139-45.
205. Liao C-y, Li X-y, Wu B, Duan S, Jiang G-b. Acute Enhancement of Synaptic Transmission and Chronic Inhibition of Synaptogenesis Induced by Perfluorooctane Sulfonate through Mediation of Voltage-Dependent Calcium Channel. *Environmental Science & Technology.* 2008;42(14):5335-41.

206. Starnes HM, Rock KD, Jackson TW, Belcher SM. A Critical Review and Meta-Analysis of Impacts of Per- and Polyfluorinated Substances on the Brain and Behavior. *Frontiers in Toxicology*. 2022;4.
207. Liu X, Liu W, Jin Y, Yu W, Wang F, Liu L. Effect of gestational and lactational exposure to perfluorooctanesulfonate on calcium-dependent signaling molecules gene expression in rats' hippocampus. *Arch Toxicol*. 2010;84(1):71-9.
208. Liu X, Liu W, Jin Y, Yu W, Liu L, Yu H. Effects of subchronic perfluorooctane sulfonate exposure of rats on calcium-dependent signaling molecules in the brain tissue. *Arch Toxicol*. 2010;84(6):471-9.
209. Haseloff RF, Dithmer S, Winkler L, Wolburg H, Blasig IE. Transmembrane proteins of the tight junctions at the blood–brain barrier: Structural and functional aspects. *Seminars in Cell & Developmental Biology*. 2015;38:16-25.
210. Sweeney MD, Zhao Z, Montagne A, Nelson AR, Zlokovic BV. Blood-brain barrier: from physiology to disease and back. *Physiological reviews*. 2018.
211. Yu Y, Wang C, Zhang X, Zhu J, Wang L, Ji M, et al. Perfluorooctane sulfonate disrupts the blood brain barrier through the crosstalk between endothelial cells and astrocytes in mice. *Environ Pollut*. 2020;256:113429.
212. Qiu L, Zhang X, Zhang X, Zhang Y, Gu J, Chen M, et al. Sertoli Cell Is a Potential Target for Perfluorooctane Sulfonate–Induced Reproductive Dysfunction in Male Mice. *Toxicological Sciences*. 2013;135(1):229-40.
213. Wang X, Li B, Zhao WD, Liu YJ, Shang DS, Fang WG, et al. Perfluorooctane sulfonate triggers tight junction "opening" in brain endothelial cells via phosphatidylinositol 3-kinase. *Biochem Biophys Res Commun*. 2011;410(2):258-63.

214. Hayashi Ki, Takahashi M, Kimura K, Nishida W, Saga H, Sobue K. Changes in the balance of phosphoinositide 3-kinase/protein kinase B (Akt) and the mitogen-activated protein kinases (ERK/p38MAPK) determine a phenotype of visceral and vascular smooth muscle cells. *The Journal of cell biology*. 1999;145(4):727-40.
215. Zhang H, Jiang L, Guo Z, Zhong J, Wu J, He J, et al. PPAR β/δ , a Novel Regulator for Vascular Smooth Muscle Cells Phenotypic Modulation and Vascular Remodeling after Subarachnoid Hemorrhage in Rats. *Scientific Reports*. 2017;7(1):45234.
216. Rossi F, Bertone C, Petricca S, Santiemma V. Adrenomedullin antagonizes angiotensin II-stimulated proliferation of human aortic smooth muscle cells. *Peptides*. 2006;27(11):2935-41.
217. Li J, Xuan W, Yan R, Tropak MB, Jean-St-Michel E, Liang W, et al. Remote preconditioning provides potent cardioprotection via PI3K/Akt activation and is associated with nuclear accumulation of β -catenin. *Clinical science*. 2011;120(10):451-62.
218. Tse JC, Kalluri R. Mechanisms of metastasis: epithelial-to-mesenchymal transition and contribution of tumor microenvironment. *Journal of cellular biochemistry*. 2007;101(4):816-29.
219. Meneguzzi A, Fava C, Castelli M, Minuz P. Exposure to Perfluoroalkyl Chemicals and Cardiovascular Disease: Experimental and Epidemiological Evidence. *Front Endocrinol (Lausanne)*. 2021;12:706352.
220. Rossi D, Pierantozzi E, Amadsun DO, Buonocore S, Rubino EM, Sorrentino V. The Sarcoplasmic Reticulum of Skeletal Muscle Cells: A Labyrinth of Membrane Contact Sites. *Biomolecules*. 2022;12(4).
221. Shiels HA, Sitsapesan R. Is there something fishy about the regulation of the ryanodine receptor in the fish heart? *Experimental Physiology*. 2015;100(12):1412-20.

222. Harada K, Xu F, Ono K, Iijima T, Koizumi A. Effects of PFOS and PFOA on L-type Ca²⁺ currents in guinea-pig ventricular myocytes. *Biochem Biophys Res Commun*. 2005;329(2):487-94.
223. Xu D, Li L, Tang L, Guo M, Yang J. Perfluorooctane sulfonate induces heart toxicity involving cardiac apoptosis and inflammation in rats. *Experimental and Therapeutic Medicine*. 2022;23(1):1-9.
224. Cheng W, Yu Z, Feng L, Wang Y. Perfluorooctane sulfonate (PFOS) induced embryotoxicity and disruption of cardiogenesis. *Toxicol In Vitro*. 2013;27(5):1503-12.
225. Liu X, Liu S, Qiu W, Magnuson JT, Liu Z, Yang G, et al. Cardiotoxicity of PFOA, PFOS, and PFOSA in Early Life Stage Zebrafish: Molecular Changes to Behavioral-level Response. *Sustainable Horizons*. 2022;3:100027.
226. Manickam R, Duszka K, Wahli W. PPARs and Microbiota in Skeletal Muscle Health and Wasting. *Int J Mol Sci*. 2020;21(21).
227. Fan W, Waizenegger W, Lin CS, Sorrentino V, He M-X, Wall CE, et al. PPAR δ Promotes Running Endurance by Preserving Glucose. *Cell metabolism*. 2017;25(5):1186-93.e4.
228. Rospert S, Dubaquié Y, Gautschi M. Nascent-polypeptide-associated complex. *Cellular and Molecular Life Sciences CMLS*. 2002;59:1632-9.
229. Stanifer JW, Stapleton HM, Souma T, Wittmer A, Zhao X, Boulware LE. Perfluorinated Chemicals as Emerging Environmental Threats to Kidney Health. A Scoping Review. 2018;13(10):1479-92.

230. Shearer JJ, Callahan CL, Calafat AM, Huang W-Y, Jones RR, Sabbiseti VS, et al. Serum Concentrations of Per- and Polyfluoroalkyl Substances and Risk of Renal Cell Carcinoma. *JNCI: Journal of the National Cancer Institute*. 2021;113(5):580-7.
231. Vieira VM, Hoffman K, Shin H-M, Weinberg JM, Webster TF, Fletcher T. Perfluorooctanoic acid exposure and cancer outcomes in a contaminated community: a geographic analysis. *Environmental health perspectives*. 2013;121(3):318-23.
232. Steenland K, Woskie S. Cohort mortality study of workers exposed to perfluorooctanoic acid. *American journal of epidemiology*. 2012;176(10):909-17.
233. Barry V, Winquist A, Steenland K. Perfluorooctanoic acid (PFOA) exposures and incident cancers among adults living near a chemical plant. *Environmental health perspectives*. 2013;121(11-12):1313-8.
234. Shankar A, Xiao J, Ducatman A. Perfluoroalkyl chemicals and chronic kidney disease in US adults. *American journal of epidemiology*. 2011;174(8):893-900.
235. Vearrier D, Jacobs D, Greenberg MI. Serum perfluorooctanoic acid concentration is associated with clinical renal disease but not clinical cardiovascular disease. *Clin Toxicol (Phila)*. 2013;51:326.
236. Kataria A, Trachtman H, Malaga-Diequez L, Trasande L. Association between perfluoroalkyl acids and kidney function in a cross-sectional study of adolescents. *Environmental Health*. 2015;14(1):1-13.
237. Chou H-C, Wen L-L, Chang C-C, Lin C-Y, Jin L, Juan S-H. From the Cover: l-Carnitine via PPAR γ - and Sirt1-Dependent Mechanisms Attenuates Epithelial-Mesenchymal Transition and Renal Fibrosis Caused by Perfluorooctanesulfonate. *Toxicological Sciences*. 2017;160(2):217-29.

238. Cui L, Zhou Q-f, Liao C-y, Fu J-j, Jiang G-b. Studies on the Toxicological Effects of PFOA and PFOS on Rats Using Histological Observation and Chemical Analysis. *Archives of Environmental Contamination and Toxicology*. 2009;56(2):338-49.
239. Pérez F, Nadal M, Navarro-Ortega A, Fàbrega F, Domingo JL, Barceló D, et al. Accumulation of perfluoroalkyl substances in human tissues. *Environment international*. 2013;59:354-62.
240. Zhang H, Shen L, Fang W, Zhang X, Zhong Y. Perfluorooctanoic acid-induced immunotoxicity via NF-kappa B pathway in zebrafish (*Danio rerio*) kidney. *Fish & Shellfish Immunology*. 2021;113:9-19.
241. Duan D, Zhang S, Li X, Guo H, Chen M, Zhang Y, et al. Activation of the TLR/MyD88/NF-κB Signal Pathway Contributes to Changes in IL-4 and IL-12 Production in Piglet Lymphocytes Infected with Porcine Circovirus Type 2 In Vitro. *PLOS ONE*. 2014;9(5):e97653.